UNIVERSITY OF KWAZULU-NATAL

VAPOUR-LIQUID EQUILIBRIUM STUDIES AT LOW PRESSURE USING A STATIC-CELL CLUSTER

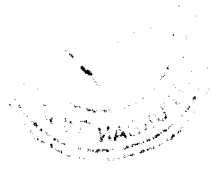

by

ILDEPHONSE HABYALIMANA

Durban
2006

The work presented in this thesis was performed at Howard College Campus, University of KwaZulu-Natal, from February 2003 to December 2004 under supervision of Professor D. Ramjugernath and Professor J.D. Raal.

I hereby declare that this thesis, unless specifically indicated to the contrary in the text, is my own work and has not been submitted for degree at any other University or Institution.

Ildephonse Habyalimana

As supervisor of this candidate, I approve this thesis for submission

Professor D. Ramjugernath

Professor J.D. Raal

ACKNOWLEDGEMENTS

I am grateful to acknowledge the following people for the wonderful contribution made to this work:

- My supervisors, Professor D. Ramjugernath and Professor J.D Raal for their immense support during two years of this project. I learnt a lot from them.

- Thanks to my wife Elisabeth for her encouragement and support during my studies.

- Prathieka, Allen and Mukhokheli for their appreciated contribution.

- My collegues in the Thermodynamics Research Unit: Minal, Warren, Myriam,Tyrone, Natasha,Prashant, Scott for their ideas.

- The workshop and IT staff for their help, in particular Les Henwood for his help in sorting out the leaks presented in manifold.

- Glassblower, Peter Siegling for constructing 4 static-cells cluster used in this project.

- The National Research Foundation (NRF), for financial support.

TABLE OF CONTENTS

ABSTRACT

Phase equilibrium data are vital in process design for chemical industries. Development of new equipment needs knowledge of thermodynamics and phase equilibrium relationships and reliable vapour liquid equilibrium (VLE) data can even make existing equipment work more efficiently. Physical and thermodynamic properties are a key tool in different operations unit, such as distillation, extraction, absorption, diffusion, etc.

In this project, a static method has been developed for gathering VLE data. The equipment used is a modification of the Raal design (Raal and Mühlbauer [1998]). The new design of the static cell involves the implementation of a water jacket around the equilibrium cell for the circulation of hot water. A thread fitting has been made on the top of each condenser for connecting/ disconnecting in case of cleaning the assembly without damaging the isolating valves. A draft tube-magnetic stirring mechanism produces internal vapour liquid recirculation through the condensers. This has significantly reduced the experimental time taken for the degassing and equilibration procedures. The main advantage of equipment developed is that in the same amount of time multiple measurements can be made using a 4-cell cluster. The static cell apparatus provides P-x data at constant temperature.

Vapour pressure data for two pure components (cyclohexane+ethanol) and their binary system were measured in order to test this new cell. Further work included the measurement of binary VLE for mixtures of 1-hexene +N-methyl-2-pyrrolidone (NMP) and water+NMP at different temperatures. As these components play an important role in separating mixtures as solvents, their activity coefficients at infinite dilution were calculated using the Maher and Smith (1979) techniques. The non-ideality of system has been taken in account by using second Virial coefficients, which were calculated by the method of Hayden and O' Connell (1975). Thereafter computation of vapour composition from the P-T-x data was undertaken using relevant techniques such as Barker's Method. More models (such as Wilson, NRTL) for fitting the measured data were used in this work.

- Cyclohexane + ethanol at 35°C, 50°C
- 1-Hexene + N-methyl-2-pyrrolidone at 40°C, 50°C, 60°C
- Water + N-methyl-2-pyrrolidone at 40°C, 50°C, 60°C

The measurements of vapour pressures for the first system which was used for testing the operating procedure and measuring capacity of the new static cell cluster and its data show a reasonable agreement with the published data [Joseph et al. (2001)].

During this work the manifold has presented problems of leaking which was responsible of lower precision in the dilute region. Despite this, the new design presents advantages over other design discussed in this work, such as a significant reduction of experimental time taken for degassing the solutions to half an hour. The normal degassing method (which is applied to various static cells) was lengthy freezing-evacuation-thawing cycles. Seven to nine cycles were required, with about 1 hour per cycle [Maher and Smith (1979)]. And also, the time taken for equilibration procedures for each cell is 30 minutes due to the draft tube- magnetic stirring assembly. This is very important since the equilibration time for many static cells is much longer as indicated by Maher and Smith (1979).

LIST OF FIGURES

LISTS OF TABLES

NOMENCLATURE

A	Constant in Antoine equation
B	Constant in Antoine equation
B_{ii}	Second Virial coefficient of pure component I (cm^3/mol)
B_{ij}	Second Virial coefficient corresponding to the pairs interactions of unlike molecules (cm^3/mol)
C	Constant in Antoine equation
f_i^v	Vapour phase fugacity (kPa)
f_i^l	Liquid phase fugacity (kPa)
$\hat{f}_i$	Fugacity of component I in solution (kPa)
g_{ii}	NRTL activity coefficient equation parameter (J/mol)
G^E	Excess Gibbs free energy of mixing (J/mol)
V^E	Excess volume of mixing (m^3)
G_{ij}	NRTL parameter
L	Liquid phase
P	Pressure (kPa)
P_D	Deviation pressure (kPa)
R	Universal gas constant (8.314 J/mol.K)
T	Temperature (K)
T_c	Critical temperature (K)
T_r	Reduced temperature (K)
V_i^L	Liquid molar volume of component *i* (cm^3/mol)
x_i	Liquid mole fraction of component *i*
y_i	Vapour mole fraction of component *i*
Z	Compressibility factor
Pcalc	Calculated Pressure ((kPa)
Pexp	Experimental Pressure (kPa)
ΔP	Pressure residuals (kPa)
ycalc	Calculated vapour composition
yexp	Experimental vapour composition

Δy Vapour composition residuals

Greek letters

β_2 Term in equation

δ_{12} Term in equation

ε_i^{∞} Term in equation

γ_i Liquid activity coefficient

γ_i^{∞} Infinite dilution activity coefficient

μ_i Chemical potential of component I

μ_r Reduced dipole moment (debye)

ϕ Fugacity coefficient

$\hat{\phi}_i$ Fugacity coefficient of component i in solution

$\hat{\phi}_i^{sat}$ Saturated fugacity coefficient of component

λ Wilson equation fitted parameter

ω Acentric factor

Superscripts

E Excess property

l Liquid phase

sat Saturated

v Vapour phase

$\wedge$ in solution property

CHAPTER 1

INTRODUCTION

Many chemical compounds are similar in their physical properties and it is difficult to separate them by conventional distillation. The way of dealing with this matter is to add to the system a third/additional component (called an entrainer), which alters the behaviour of the mixture and improves the separability of the components. In this process called extractive distillation, the solvent added to the mixture increases the relative volatility of the components and the separation of two chemicals becomes easier. The introduction of a suitable solvent, which has a higher affinity for one component than the other, changes the molecular interactions between the original species. The selectivity of a solvent is very important for separation, since a higher selectivity leads to a larger relative volatility. One of the most useful entrainers is N-methyl-2-pyrrolidone (NMP).

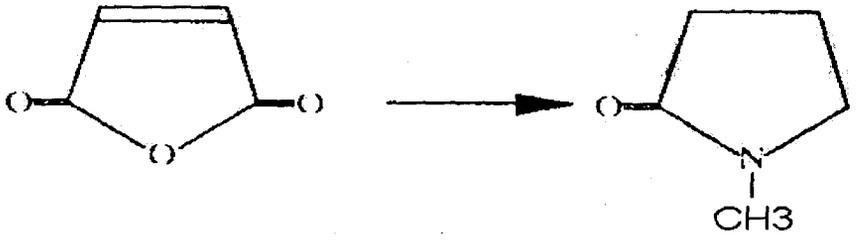

Maleic anhydride N-Methyl-2-pyrrolidone

Figure 1-1: Production of NMP from maleic anhydride

The reaction of maleic anhydride to produce NMP is complicated. It is a colorless liquid and has a boiling point of (204°C) and a low melting point (-24.4°C). NMP is powerful polar solvent and dissolves most organic and inorganic compounds. This wide range of solvent ability offers NMP the use in industry in recovery or separation processes for certain components. For instance, NMP dissolves a large

number of resins, waxes, agricultural and pharmaceutical chemicals, inorganic salts, carbohydrates and certain gases [Digby et al. (1971)].

It contains a nitrogen atom and has strong polarity and is completely miscible with water. The selectivity and capacity of NMP depends on the water content [Fischer and Gmehling (1996)]. Equilibrium data of water in NMP is very important for optimizing the removal of water in NMP by distillation processes. The role played by NMP and other chemicals in separation of mixtures cannot be implemented without the knowledge of their physical properties. These properties are the cornerstone of VLE data. They are essential in process development. A successful design of chemical plant, which involves the choice of unit operations as well as the size of equipment cannot be done without reliable physical properties.

Recirculating stills have long been employed for gathering equilibrium data which are essential for design of separation equipment. They can provide complete P-T-x- y data sets. However, for binary systems a partial set of any of the three variables is sufficient since the fourth can be calculated through the use of the Gibbs-Duhem equation. The greatest source of error in most VLE measurement is usually the sampling and analysis of the vapour phase which is eliminated in favour of calculating it. Recirculating stills are not in a position to take advantage of this since, in their normal mode of operation, they produce isobaric data. For isobaric data, the Gibbs-Duhem equation contains an excess enthalpy term that is not easily evaluated because the data are not available. The isothermal form of the Gibbs-Duhem equation presents no such problems and maintains a high degree of rigour for low pressure computations. Static cells, which operate isothermally, are therefore well suited to produce VLE data with subsequent data reduction. Thus, it was reasoned that accurate measurement of pressure as a function of composition at constant temperature is adequate and the vapour phase composition is then calculated.

An objective of this work has been to modify the Raal static cell cluster (Raal and Mühlbauer [1998]) by the introduction of various changes in order to improve its performance. The weaknesses of the old design were highlighted on basis of observation that no detailed study or thesis was carried out using this assembly. Only one isothermal data set was reported in book of Raal and Mühlbauer (1998). The implementation of water jacket around the equilibrium cell produced significant improvement. In this work, the author has introduced a modified static cell cluster to gather VLE data. This was used to study the following systems: Cyclohexane + ethanol; 1-hexene +NMP and water + NMP.

CHAPTER 2

SURVEY OF EXPERIMENTAL APPARATUS

Accurate vapour-liquid equilibrium data are very important for the design of separation equipment. Consequently scientists and engineers always seek to develop reliable methods to measure VLE.

Recirculating stills (Figure 2-1) have long been used for gathering VLE data. For each experiment, this method provides one data point set, consisting for a binary system of measured values of P, T, x_1 and y_1. It is known that the greatest source of error in most VLE measurements is usually the sampling and analysis of the vapour phase.

However, for a binary mixture a set of any three variables is sufficient since the fourth one can be calculated using the Gibbs-Duhem equation. Therefore, the introduction of experimental error into the data by sampling the vapour phase can be eliminated in favour of its calculation. Recirculation methods are not in a position to take advantage of this because; they produce isobaric data in their normal mode of operation. The Gibbs-Duhem equation contains an excess enthalpy term that is not easy to evaluate due to lack of this data, whereas its isothermal form does not present such problems since at low pressures $V^E/RT \cong 0$. With no necessity of sampling the vapour phase, static methods are suitable for accurate measurement of pressure as a function of composition at constant temperature.

Thus, the objective of this chapter is to review some approaches for measuring P,T,x data which have been developed by several authors and their application. More details about static apparatus can be encountered in the book of Raal and Mühlbauer (1998).

2.1 Dynamic Equilibrium Still

In the dynamic equilibrium still (Figure 2-1) the heat applied in the still pot is induced continuously to produce the boiling of the liquid phase. The vapours produced are directed upwards in a vertical tube into a disengaging chamber. In this chamber, the phases are assumed to be in equilibrium. Evolved vapours are separated from the liquid phase, and continually drained into a receiver where it condenses. Note that a sample can be withdrawn from the receiver for analysis. The condensed vapour returns to the still by gravity flow and mixes with the boiling liquid. The composition of the liquid phase and the vapour condensate change with time until steady values are reached.

During this process, the pressure is controlled in the chamber and the temperature is measured. One data point set (x_1, y_1, T and P) is produced in each experiment of a binary system. The dynamic still produces a state of dynamic equilibrium, which may be assumed to be close to the true thermodynamic equilibrium. Abbott (1986), Hala et al. (1967) and Malanowski (1982 a) presented reviews of still design and circulation methods respectively. In their works, they analysed the principles of operation and the relative strengths and weaknesses of various designs.

Some problems that could occur in the dynamic still are:

- superheating of the boiling liquid;
- partial condensation of the vapour in the disengaging chamber (vapour composition);
- entrainment of liquid in the condenser ; and
- evaporation of samples before analysis.

All the problems mentioned above form obstacles to the collection of accurate data. Measurements are generally made either isobarically, or isothermally. In the first case, the pressure is controlled at a constant value and the temperature is measured. In the second case, the temperature is controlled and the pressure is measured. Generally, data from circulating stills are isobaric, although they can run isothermically (see eg. Joseph at al. (2001). In these cases, either (x_1, y_1, P) or (x_1, y_1, T) form complete data sets.

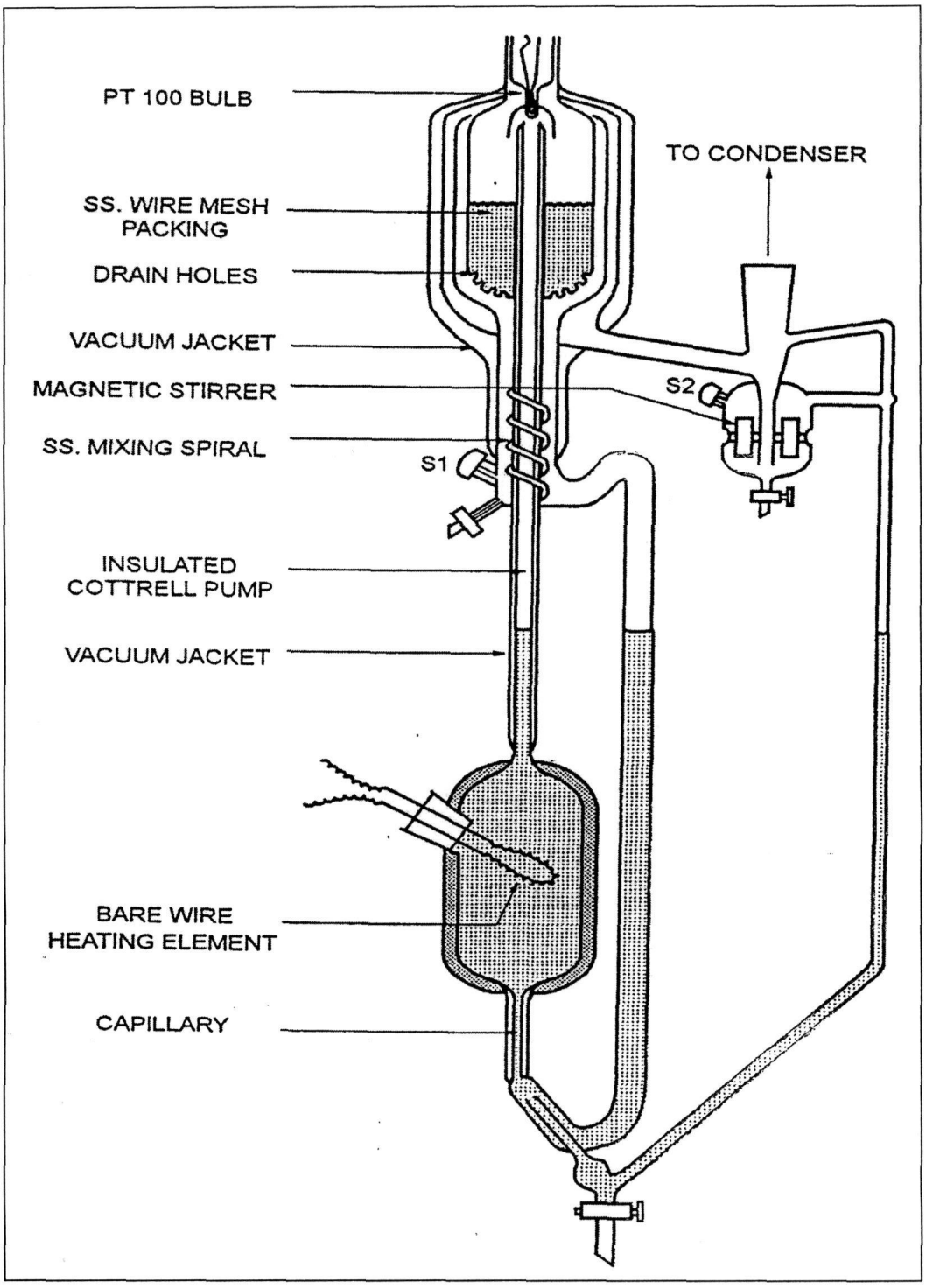

Figure 2-1: Dynamic VLE still of Raal and Mühlbauer (1998)

2.2 Static apparatus

It is equipment in which a static equilibrium is obtained. In this apparatus, a liquid mixture is charged to a previously evacuated cell placed in a constant- temperature water bath. A stirring mechanism is used for bringing liquid and vapour phases to equilibrium. The static cell provides isothermal data whereas dynamic stills, in general, produce isobaric data. The vapour composition is difficult to measure because at low pressures, since the amount of vapour is very small and its sampling would disturb the equilibrium. Thus, in many cases of static equilibrium cells, the vapour is not sampled for analysis. Inoue et al.(1975) proposed a design to allow for vapour sampling by connecting larger flasks in the vapour space to increase the vapour hold up.

Isothermal data measurement presents an advantage in view of the fact that activity coefficients which represent VLE are more sensitive to temperature than to pressure and the constants in different equations of correlation are obtained from isothermal data.

One of the major problems with static cells is the necessity for complete degassing of the system. In case a small amount of gases dissolved in the charged liquids is not completely removed it can render the vapour pressure measurement erroneous.

The accurate measurement of the vapour composition is often difficult and expensive and it requires a lot of time for get one P-x data point. Given a set of equilibrium x- P data at constant T, vapour compositions can be computed using different correlations and data reduction models. This process will save time and effort. The thermodynamic consistency testing cannot be done, since the Gibbs-Duhem equation has been applied in the computation.

In addition to the dynamic still problems mentioned in section 2.1, the following types of systems present problems with recirculating stills and are best handled with static equilibrium cells:

- systems forming multiple liquid phases,
- viscous systems,
- systems containing a very non-volatile component and
- systems of very high relative volatility.

Vapour Liquid Equilibria as represented by activity coefficients are generally more sensitive to temperature than to pressure and the temperature dependence of constants in correlating equations is more readily determined from isothermal data. The isothermal form of the Gibbs_Duhem equation presents no problems since at low pressures $V^E/RT \cong 0$. From the points mentioned above, the static method has been chosen for handling the systems

(1-hexene + NMP and water + NMP) used in this work as they contain NMP which is a non-volatile component.

Another advantage of static method over dynamic method:

If an equilibrium cell is charged initially with known masses of the species, then the liquid phase compositions are given by material balance equations. The only measurements required are pressure and temperature. This eliminates the need for complicated sample withdrawal for analysis. In this way the issue of sample analysis and instrument calibration for equilibrium sample analysis is replaced by an accurate computational method.

2.2.1 Experimental apparatus of Gibbs and Van Ness (1972)

This is a static equilibrium cell equipped with volumetric metering of degassed liquid from piston injectors. Before filling the piston injectors, the two liquids were thoroughly degassed by refluxing, cooling and evacuation in a special flask. This step was repeated several times. Once the first pure liquid is metered into the glass equilibrium cell whose capacity is about $100\,cm^3$, they proceed to undertake vapour pressure measurements.

The equilibrium cell was immersed in a water bath controlled by a thermostat and the contents where agitated by a magnetic stirrer. The ethanol /n-heptane system data showed excellent agreement with those obtained by Van Ness et al.(1965) and with those of Raal et al.(1998). The use of this apparatus generated accurate data.

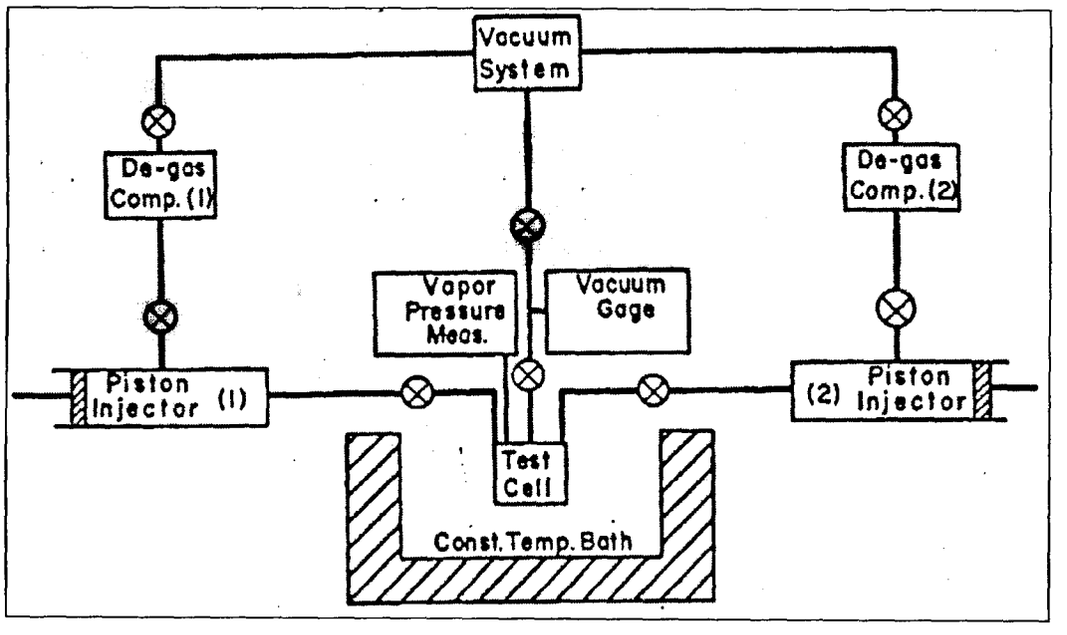

Figure 2-2: Schematic diagram of equipment of Gibbs and Van Ness (1972)

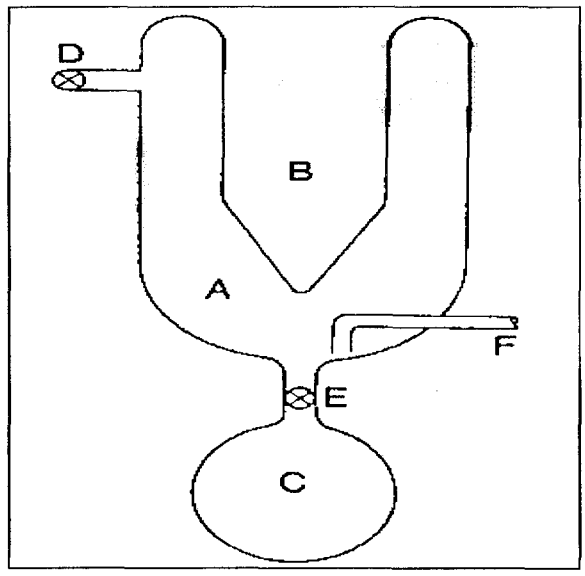

Figure 2-3: Degassing apparatus of Gibbs and Van Ness (1972)

A, reflux chamber; B, cold finger; C liquid-storage bulb; D, vacuum stopcock; E Teflon needle valve; F, port to piston-injector.

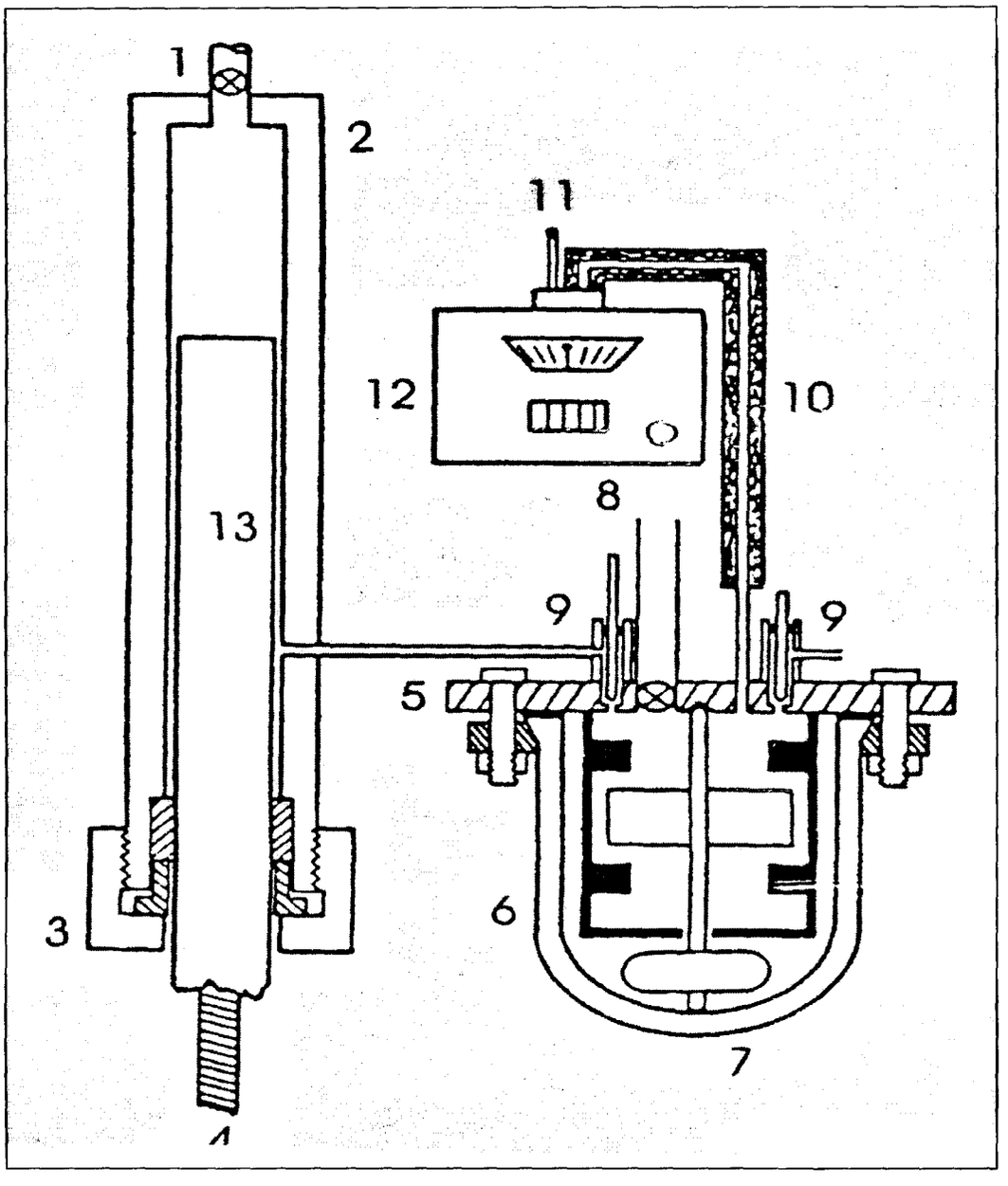

Figure 2-4: Gibbs and Van Ness (1972) static VLE apparatus.

1, line to degassing vessel; 2, piston injector body; 3, packing nut; 4, lead screw; 5, cell cover;6, glass cup; 7, Teflon-coated magnet; 8, port to vacuum system; 9, needle valves; 10, heated line; 11, line to reference vacuum; 12, pressure gauge; 13, piston.

2.2.2 Experimental apparatus of Hermsen and Prausnitz (1962)

This static equilibrium cell is highly accurate (Hermsen and Prausnitz [1962]). The equilibrium cell has an interior volume of 20 cm^3 and it is constructed from Hastelloy C with Pyrex glass windows. In the figure below, the cell is not shown in detail. The difference between this assembly and that of Gibbs and Van Ness is the connection of liquid metering pumps, which serve for introducing components into the equilibrium cell.

Once the process of degassing the pure liquids in the degassing stills which are connected to the equilibrium cell is finished, they are charged into the equilibrium cell.

Vapour pressures were measured using an isoteniscope connected in series with a mercury manometer. The highly purified liquids had measured vapour pressures, which were in very good agreement with published values in the literature. The above two static equilibrium cells produce P-x data, and the vapour composition is obtained by computation applying the Gibbs-Duhem equation as is the cases of many static cells.

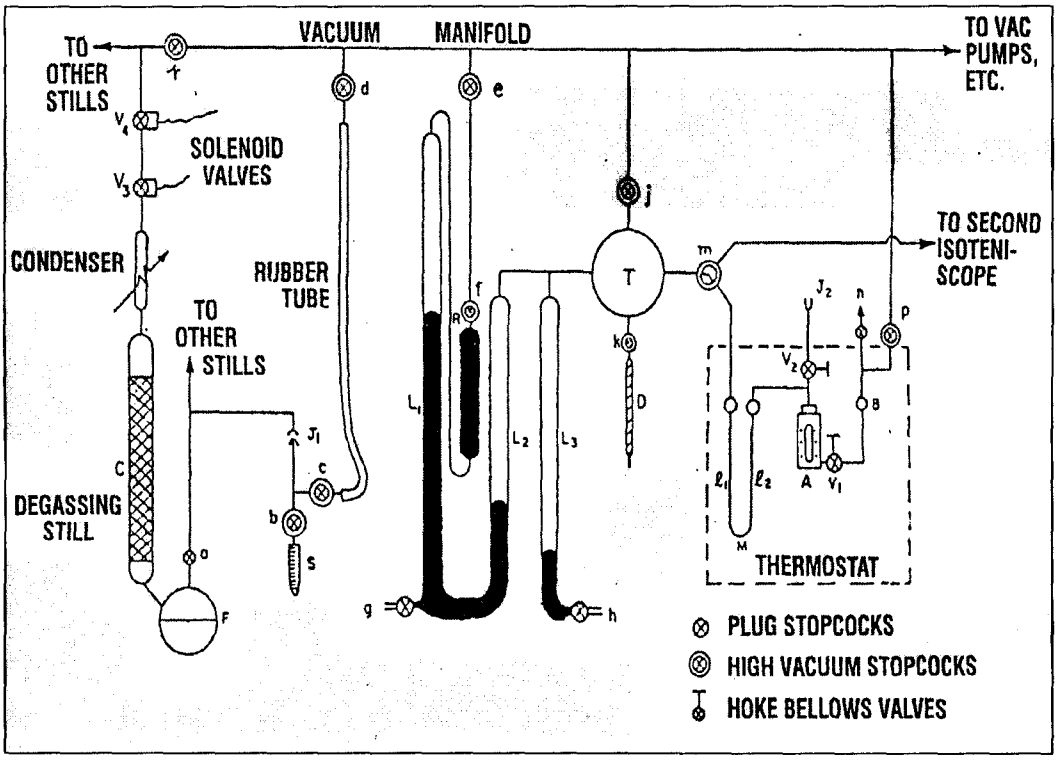

Figure 2-5: Hermsen and Prausnitz (1962) static cell assembly.

2.2.3 Experimental apparatus of Maher and Smith (1979)

At the selected temperature, both the above-mentioned apparatus types produce only a single pair of data points (P-x-y) and the process is very slow. For increasing the rate of data production, Maher and Smith (1979) designed and constructed a multi-cell apparatus with 15 small cells connected by Bellows valves mounted in a ring to a common low-volume manifold. The use of Bellows valves eliminates leaks, which are a common problem in static equilibrium cells.

Fifteen cells of approximately $25\,cm^3$ each are charged two with pure-components and 13 with intermediate binary solutions. The cells are loaded by adding the desired amounts of liquid to each cell and weighted after each addition. The contents of the cell were degassed by successive freezing-evacuation-thawing cycles. This process is very long as seven to nine cycles were required and each cycle lasted one hour. Note that the degassing technique could not remove water, which must therefore be eliminated by other means.

After degassing, the manifold with the attached cells is immersed in a temperature-controlled bath and connected to a pressure transducer. No means of mechanical stirring was used for agitating the equilibrium cells contents and this may explain the long times taken to obtain equilibrium (one day). This apparatus has been used for many years and many VLE data sets have been collected. For more information, the reader is referred to Raal and Mühlbauer (1998) and Maher and Smith (1979).

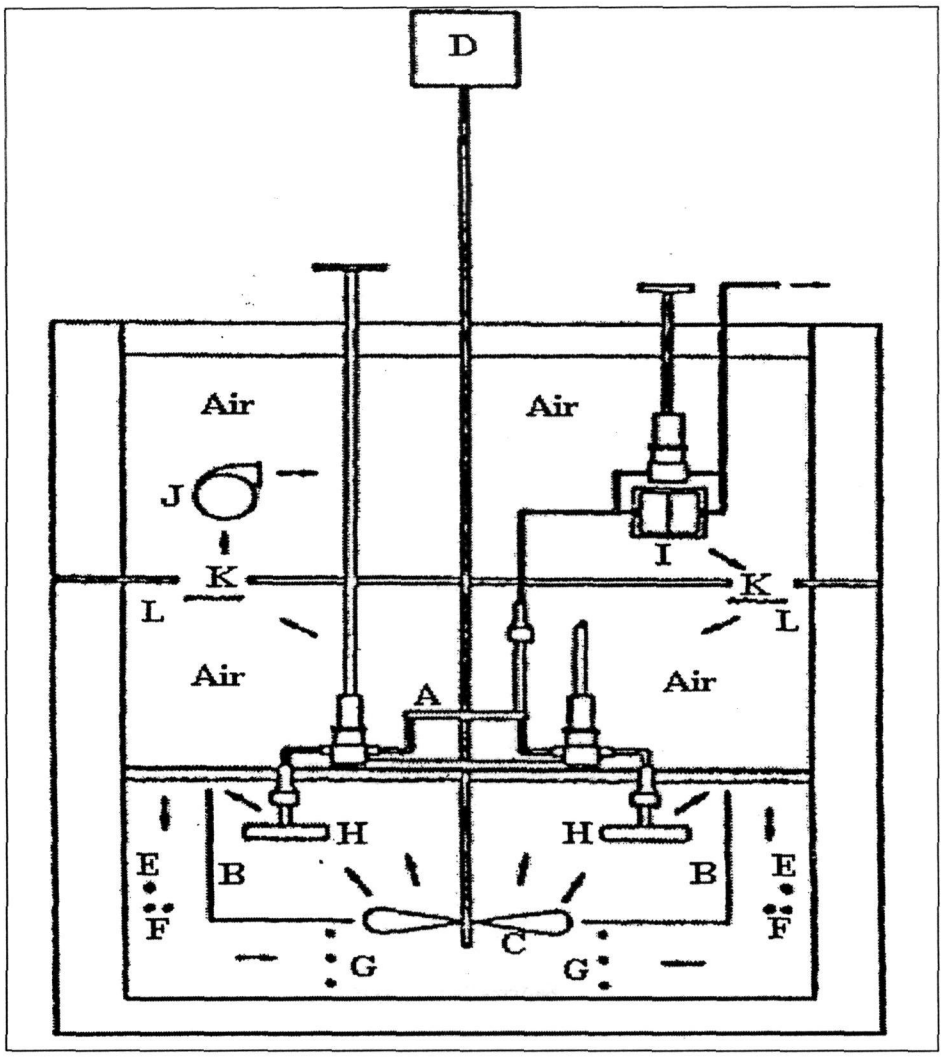

Figure 2-6: Apparatus of Maher and Smith (1979)

A, manifold assembly; B, baffle tank; C, impeller; D, impeller motor; E, auxiliary heater; F, auxiliary cooling coils; G, control heater; H, cells; I; nulling transducer; J, air bath blower; K, opening for airflow; L, air bath heaters.

2.2.4 Static cell of Kolbe and Gmehling (1985)

This apparatus, in its mode of operation uses Gibbs and Van Ness's (1972) principles. This static cell can work up to 150°C and pressures between 100 mbar and 10 bars. As shown in Figure 2-7, the pure degassed liquids are contained in vessels, A and B. These vessels are glass flasks closed by a Teflon valve (Rotaflo) with volumes of 500 ml.

Exactly known amounts of pure-substances are introduced into the equilibrium cell using the dosage equipment. The equilibrium cell is immersed in a thermostated bath and equilibrium temperature is measured using a Hewlett-Packard 2801 A quartz thermometer. The vapour

pressure in the cell is determined using a pressure balance. A differential pressure indicator is used for separating vapour and the pressure balance by means of a membrane. The objective is to avoid contact and also to keep the vapour volume as small as possible.

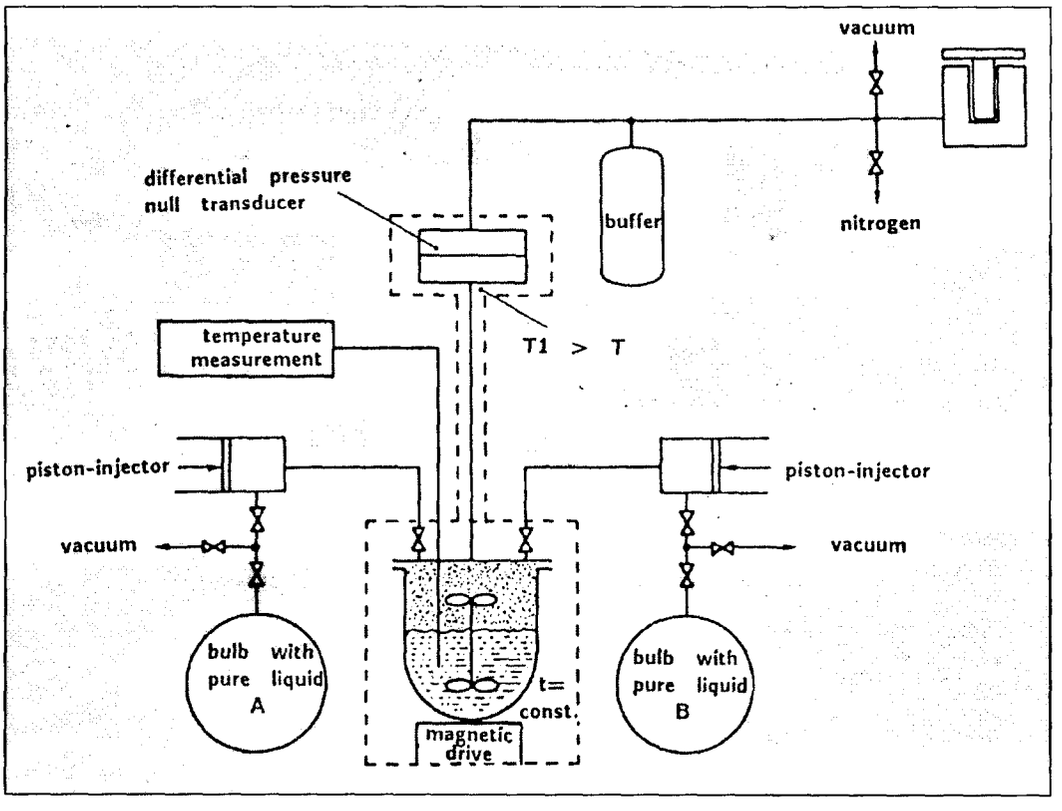

Figure 2-7: Kolbe and Gmehling (1985) static cell apparatus

2.2.5 Fischer and Gmehling static cell (1994)

During degassing and purification, this unit is degassed for 5h by vacuum rectification, which is the Van Ness and Abbot (1978) procedure. During rectification, the reboiler is maintained at constant temperature (depending on the system) and volatile gases were removed through a capillary at the top of the column. The completion of degassing is recognised by the metallic clicking sound in the reboiler. This procedure presents a disadvantage of enriching less volatile impuritities in the degassed liquid in the reboiler if there is no further separation. Therefore, a new

procedure of degassing was employed Figure 2-8. This apparatus presents a Vigreux column of 60 cm, which has got approximately five theoretical stages. Chemical reactions can occur before degassing in this unit and the desired compound to be separated by distillation after degassing.

This static cell seems to be a modification of that of Kolbe and Gmehling (1985). In its mode of operation, the equilibrium cell is maintained at constant-temperature in a bath by a thermostat. The liquid composition is determined by amounts of liquid injected into the equilibrium cell using piston injectors.

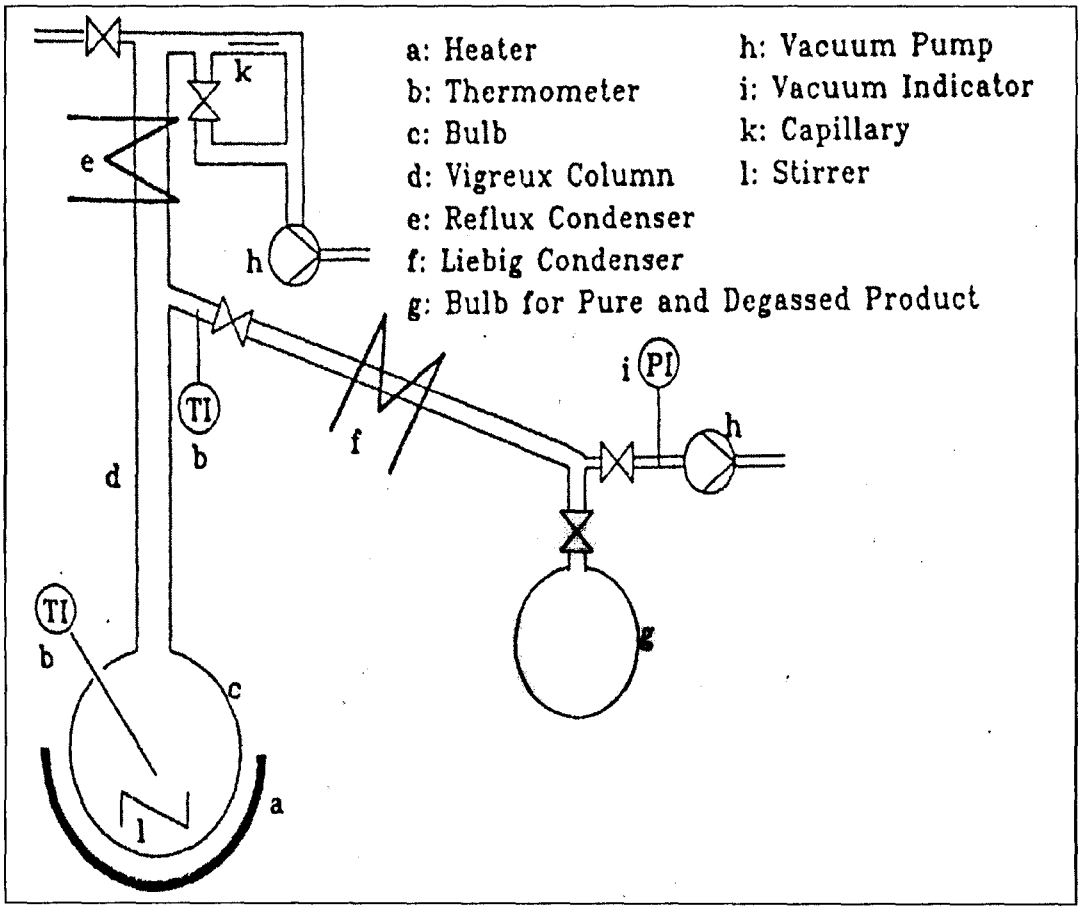

Figure 2-8: Fischer and Gmehling (1994) purification and degassing apparatus

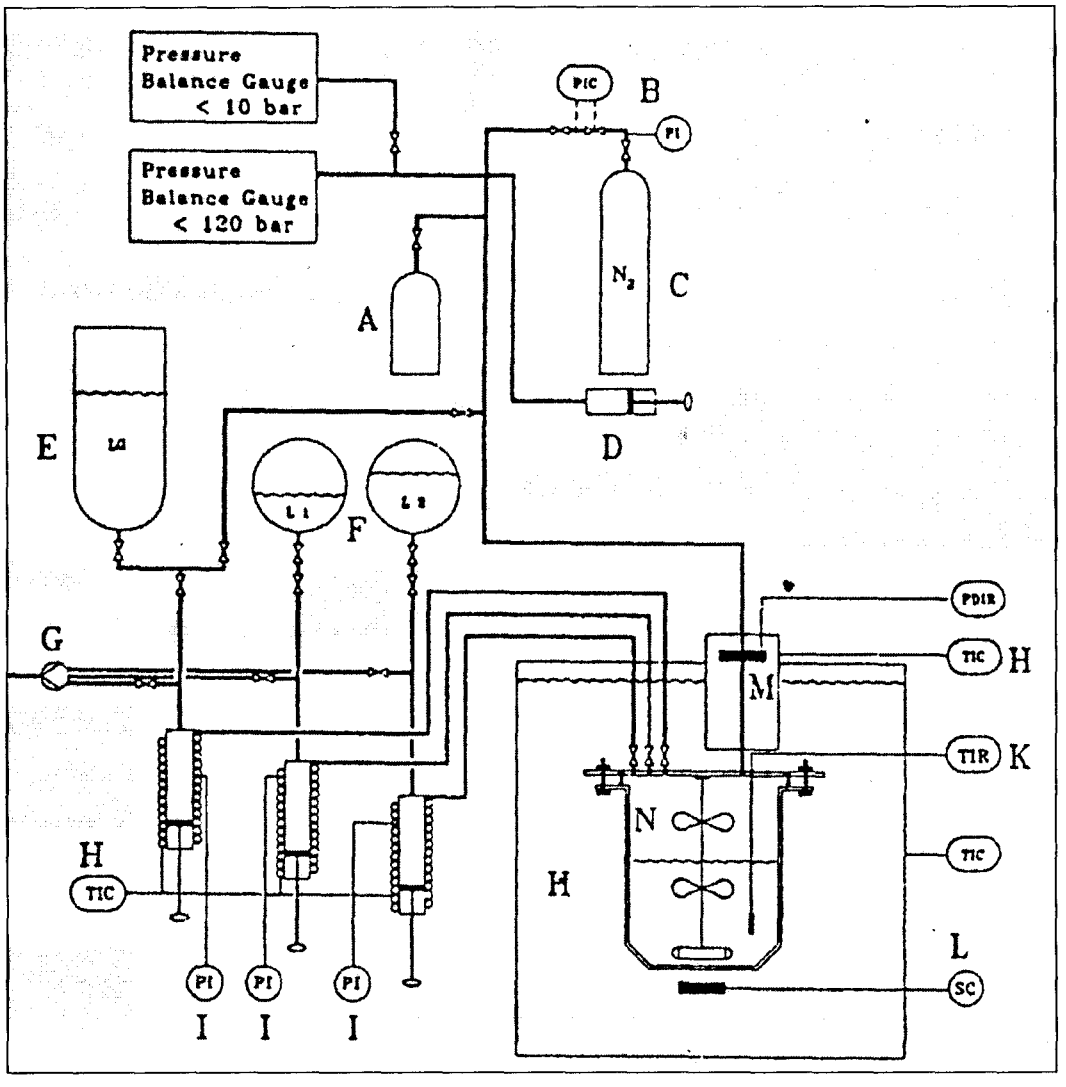

Figure 2-9: Fischer and Gmehling (1994) static cell.

a, buffer volume; b, pressure regulator; c, nitrogen flask; d, variable volume; e, container for liquid gas; f, container for degassed liquids; g, vacuum pump; h, constant temperature bath; l, bourdon pressure Gauge; k, quartz thermometer; l, rotating magnetic field; m, differential pressure Null indicator; n, equilibrium cell.

2.3 Semimicro techniques

This category of apparatus may overlap with static methods. They differ in size.

2.3.1 Experimental apparatus of Wichterle and Hala (1963) and Wichterle and Boublikova (1969)

Wichterle and Hala (1963) proposed a very rapid and moderately accurate method for measuring VLE in a semimicro static cell. The apparatus is made from glass and consists essentially of a small conical flask connected to a glass stopcock. The entire assembly is imbedded in a glass vessel, which facilitates the circulation of water. The stopcock is connected to a carrier gas supply and to a GC. In its mode of operation, the equilibrium cell is fed with a liquid mixture of known composition and is magnetically stirred, the pressure is not measured and there is no degassing.

In 1969, this static micro cell was redesigned; the simple stopcock has been replaced by an eight-way stopcock in which a larger amount of vapour was trapped in the front portion of the stopcock. The new design was used to produce data for the system n-hexane/toluene, which were in good agreement with the published data. For more information the reader is referred to Raal and Mühlbauer (1998).

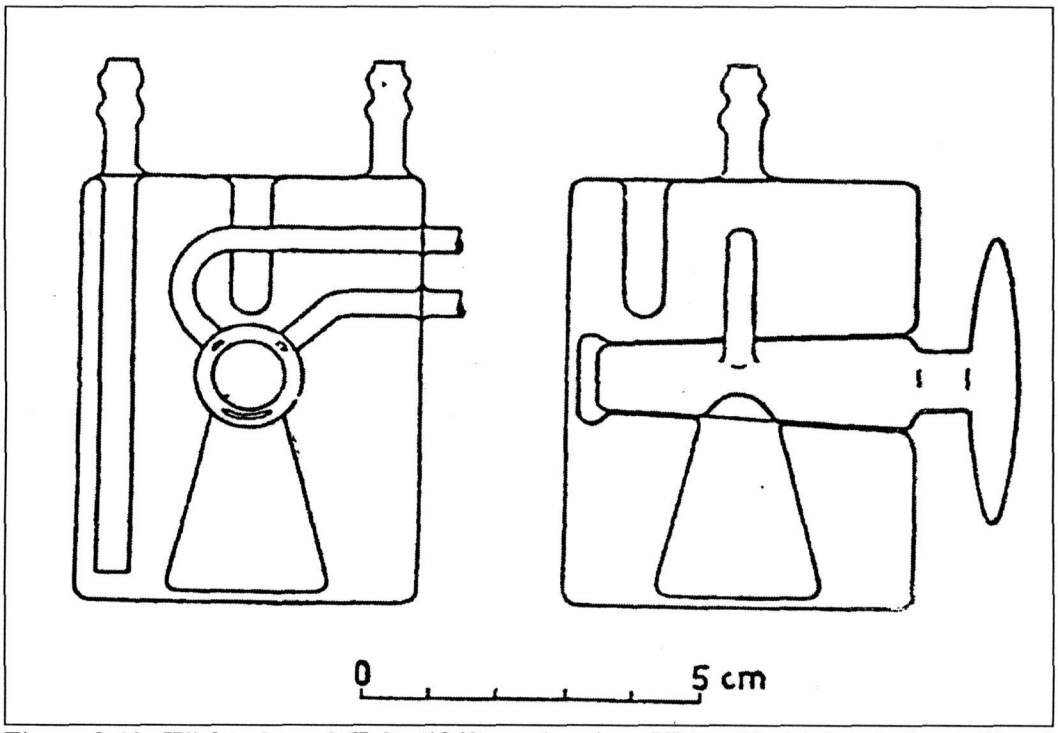

Figure 2-10: Wichterle and Hala (1963) static micro VLE cell: (a) front view without cock plug; (b) complete view

2.3.2 Raal and Mühlbauer (1998) cell

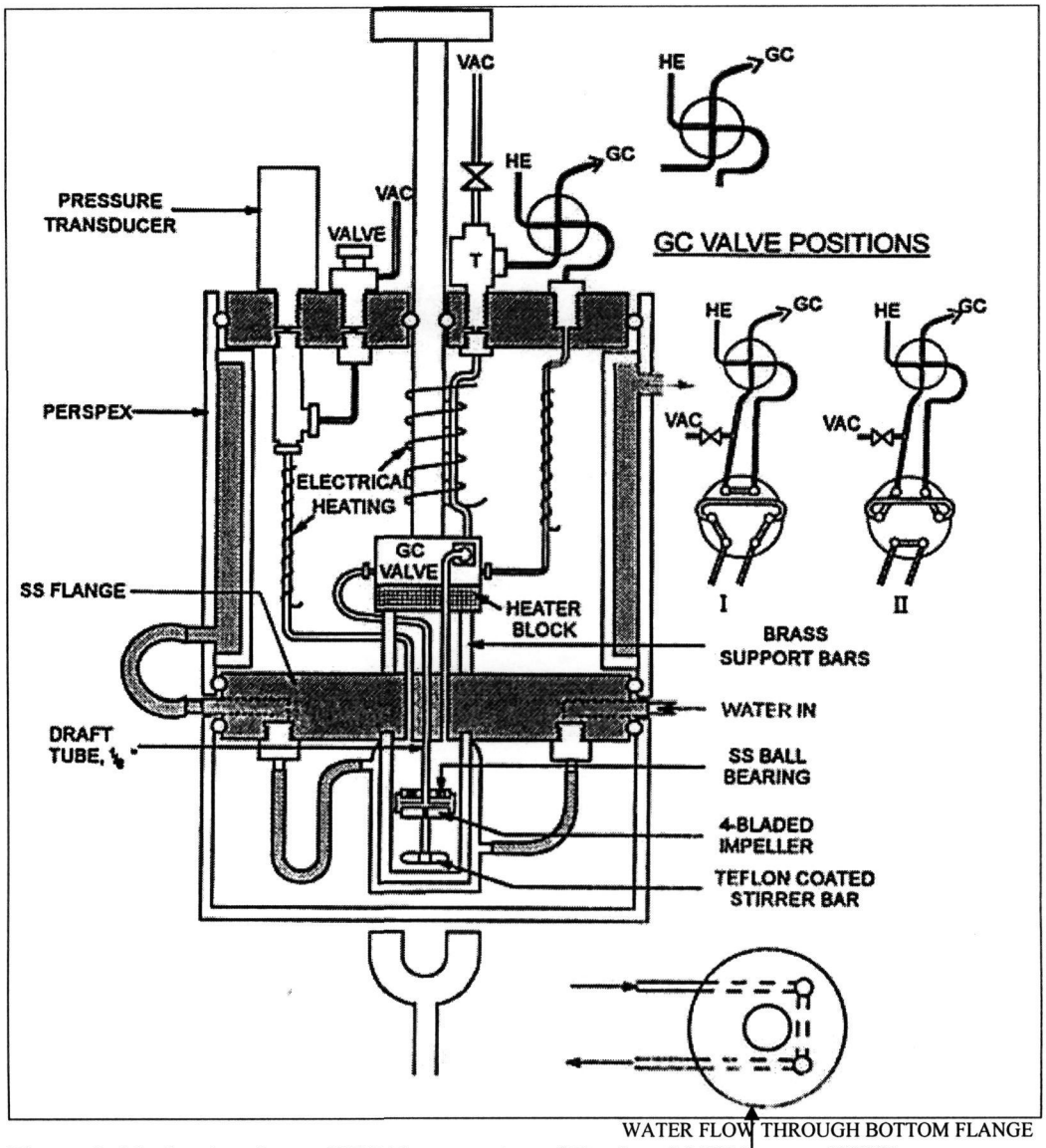

Figure 2-11: Static microcell VLE apparatus of Raal and Mühlbauer (1998)

This apparatus is more robust and versatile. Some of the features of the Wichterle design have been incorporated in this equipment. The equilibrium cell is made from Pyrex tube whose ID is ± 18 mm and is surrounded by a water jacket. The equilibrium cell has an interior draft tube which ends with an impeller whose role is to induce a circulating vapour flow through a 1/16-in six-port GC sampling valve.

Initially in its design, the draft tube with a flanged bottom was extended to just above the surface of the liquid with the idea that the cavitations created by the magnetic rotation in the liquid surface would draw vapour through the draft tube. This arrangement however failed,

with no apparent circulation. In the new design, a small impeller was located in the vapour space just below the bottom of the draft tube. The impeller was fixed to the magnetic stirring bar and this improved the vapour circulation through the draft tube.

This apparatus is characterised by sampling the vapour phase to a GC through the flow connections for analysis, without disturbing the equilibrium in the equilibrium cell.

This semimicro static cell has various connections, which cannot be discussed here. For more details the reader is referred to Raal and Mühlbauer (1998).

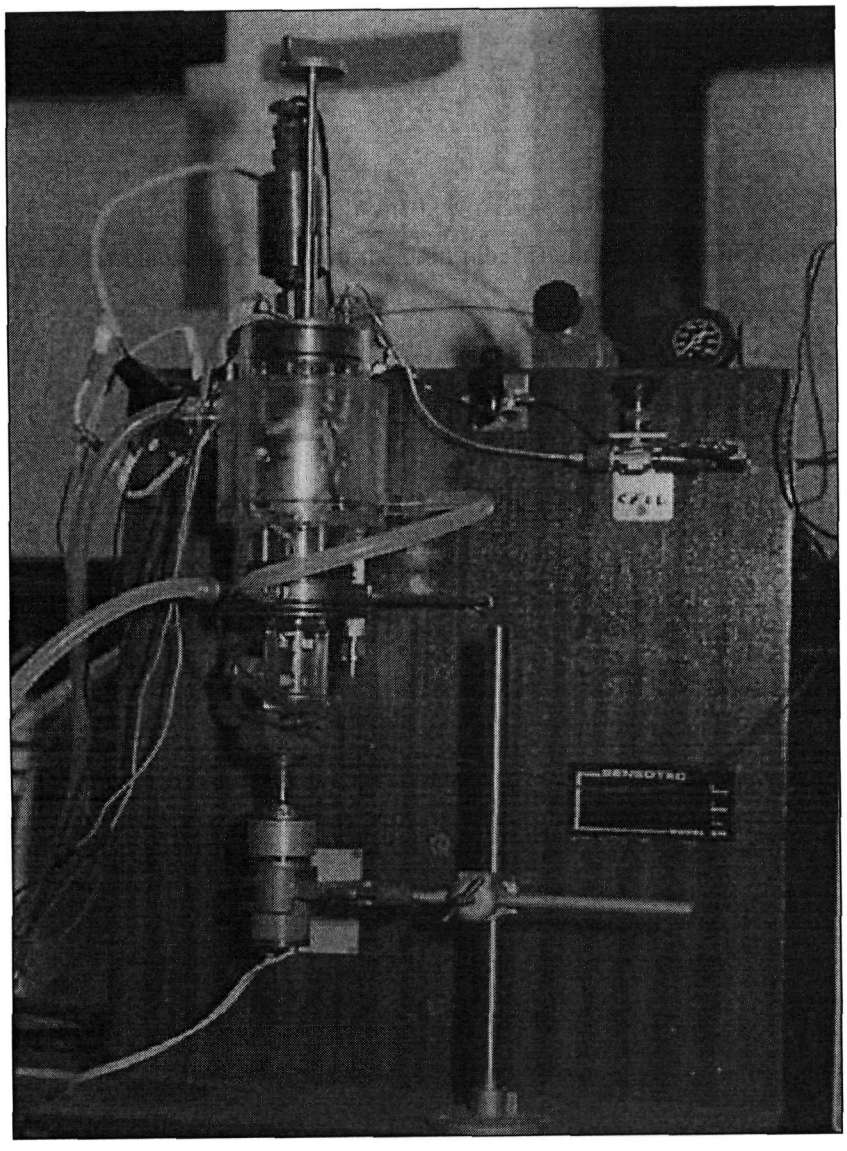

Figure 2-12: (a) Photograph of the static microcell apparatus of Raal and Mühlbauer (1998)

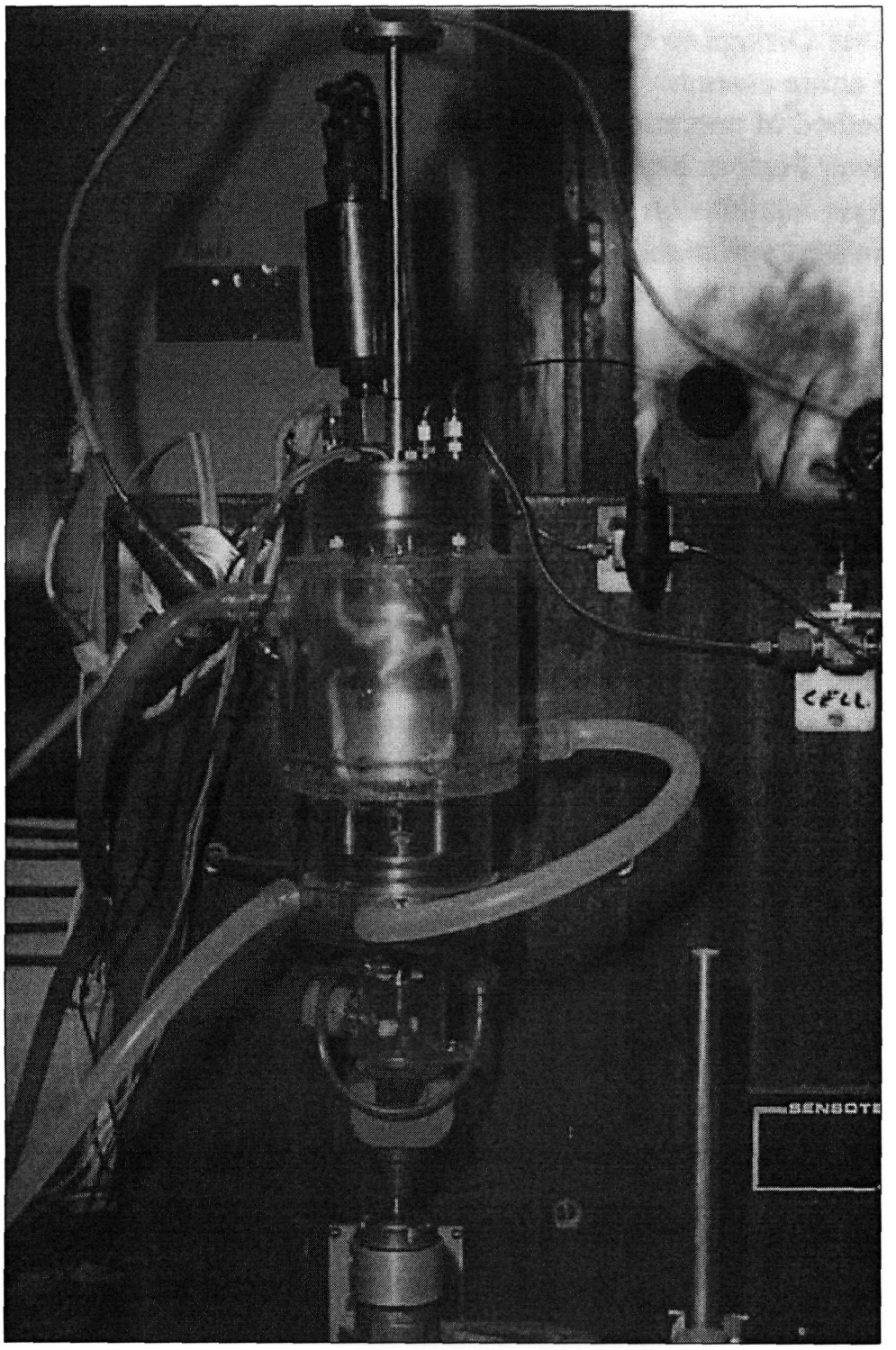

Figure 2-13: (b) Close-up of microcell apparatus of Raal and Mühlbauer (1998)

2.4 Use of a degassing condenser

The procedure used for degassing liquids mixtures without appreciable alteration in composition is to attach a degassing condenser directly to the equilibrium cells. Davidson et al.(1967) used this method with a three-flask assembly. The magnetic stirrer induces a gentle boiling of the flask contents and dissolved gases are removed. Refrigerated coolant was used in the condenser to avoid loss of the more volatile components. After 10 minutes of boiling, the flasks were placed in a dry ice/acetone mixture and opened to vacuum. To obtain equilibrium, the entire assembly including mercury manometers is immersed in a constant temperature bath.

This principle of degassing using a condenser is attractive because it saves time and can eliminate the time spent in freezing-thawing cycles.

CHAPTER 3

THERMODYNAMIC FUNDAMENTALS OF LOW PRESSURE VAPOUR-LIQUID EQUILIBRIUM

The concept of equilibrium is important to thermodynamics and is closely tied to the definitions of properties and states. It depends on several variables, such as pressure, temperature and on the chemical nature and the concentrations of species present in mixtures.

The objective of this chapter is to give some definitions and basic relations related to solution thermodynamics. For instance fugacity, activity coefficients and different models for data reduction are presented. The knowledge of these relations will help to develop methods, which are used to analyse VLE data quickly and accurately. The application of phase equilibria in separation process design needs better understanding of ideal and non-ideal solutions and the mathematical relations utilised for modelling the gathered VLE data. This requires multicomponent properties, which are very difficult to measure. Thus a thermodynamic framework of theory can be used for predicting and correlating multicomponent systems. Many relevant works about thermodynamic fundamentals of low pressure vapour-liquid equilibrium have been presented by several authors, such as Walas (1985), Smith et al.(1987) and Van Ness and Michael Abbott (1987).

In this chapter different correlations for analysing VLE data have been presented and the following methods were chosen to be used in this work:

- The Hayden and O'Connell method was chosen to describe vapour phase deviations from ideality of the mixtures where the cross-coefficient B_{12} for the binary systems and the second virial coefficients for each of the pure components were calculated.
- The Barker's Method for calculating vapour phase composition and
- The Wilson and the NRTL methods for fitting the activity coefficients versus liquid composition.

These methods were selected because they have been used largely by various authors (DECHEMA vapour-liquid data collection, Walas (1985)) for handling VLE data.

3.1 Fugacity and activity coefficients

A system is said to be in thermodynamic equilibrium when the macroscopic properties describing the state of system do not change in time or in other words in a binary phase PVT system, phase equilibrium is established when there is no driving force for the transport of chemical species from one phase to another.

The chemical potential and fugacity are criteria for measuring the equilibrium.

$$\mu_i = \mu_i^1 = \mu_i^2 \tag{3.1}$$

$$\hat{f}_i = \hat{f}_i^1 = \hat{f}_i^2 \tag{3.2}$$

The chemical potential, u_i and fugacity, f_i in a multicomponent system are identical in all phases at physical equilibrium.

Chemical potential is an entity which cannot be expressed as an absolute quantity and its numerical values are very difficult to relate to other understood physical quantities.

Thus, chemical potential is not used for calculations of phase equilibria.

Instead of chemical potential, fugacity invented by G.N Lewis in 1901, is employed as a substitute. The partial fugacity of species i in a mixture, according to Sandler(1994) is a pseudo-pressure, defined in terms of the chemical potential by

$$\hat{f}_i = c\exp(\frac{\mu_i}{RT}) \tag{3.3}$$

where c is a temperature dependent constant .

Regardless of the value of c, it is shown by Prausnitz, Lichtenthaler, and Azevedro (1986) that

$$\mu_i^1 = \mu_i^2 = \mu_i^3 = ...\mu_i^N \tag{3.4}$$

can be replaced with

$$\hat{f}_i^1 = \hat{f}_i^2 = \hat{f}_i^3 = ...\hat{f}_i^N \tag{3.5}$$

Then, at equilibrium, a given species has the same partial fugacity in each existing phase. This criterion, together with equality of phase temperatures and pressures,

$$T^1 = T^2 = T^3 = ... \tag{3.6}$$

and

$$P^1 = P^2 = P^3 = ...P^N \tag{3.7}$$

constitute the required conditions for phase equilibria.

The partial fugacity of a pure component is the pure component fugacity, f_i. In the case of pure ideal gas, where $P_i = y_i P$, fugacity and pressure have a close relationship, then their ratio for a pure substance can be defined as follow.

$$\phi_i = \frac{f_i}{P} \tag{3.8}$$

where ϕ_i is the pure species fugacity coefficient ,which has a value of 1.0 for an ideal gas.

For a mixture, partial fugacity coefficients are defined by

$$\hat{\phi}_{iv} \equiv \frac{\hat{f}_{iv}}{y_i P} \tag{3.9}$$

$$\hat{\phi}_{il} = \frac{\hat{f}_{il}}{x_i P} \tag{3.10}$$

As the behaviour of ideal gas is approached, $\hat{\phi}_{iv} \to 1.0$ and $\hat{\phi}_{il} \to P_i^{sat}/P$,

where P_i^{sat} is the saturated vapour pressure.

Eq(3.9) and Eq(3.10) represent deviations to fugacity due to pressure and composition.

3.2 Properties of ideal gases

An ideal mixture in the context of vapour-liquid equilibrium is one that obeys Raoult's Law. This model assumes that the vapour phase is an ideal gas and the liquid phase is an ideal solution. In its application, the partial pressure of a pure component in the vapour phase is equal to its mole fraction in the liquid multiplied by its vapour pressure at the system temperature.

$$y_i P = x_i P^{sat} \tag{3.11}$$

An ideal gas is a special case of a general mixture but is one with significant practical utility. Physically, a gas satisfies the ideal gas relation when the gas molecules are treated as independent of one another. A mixture of ideal gases also satisfies this molecular independence idealisation. The mixture properties are simply mole or mass weighted averages of the individual pure substance properties. Since an ideal gas implies molecular independence, the final volume is the sum of the volumes occupied by each gas

independently. The relation is demonstrated by the equation of state for a binary mixture of ideal gases and is called the Amagat-Leduc law of additive volumes.

Each component is described by

$$P_A V_A = n_A R T_A \tag{3.12a}$$

and

$$P_B V_B = n_B R T_B \tag{3.12b}$$

and the mixture is given as

$$P_C V_C = n_C R T_C \tag{3.12c}$$

where $n_C = n_A + n_B$ (3.13)

$$m_C = m_A + m_B \tag{3.14}$$

$$V_C = V_A + V_B \tag{3.15}$$

For constant temperature, constant pressure of mixing, $T_A = T_B = T_C$ and $P_A = P_B = P_C$.

Thus, $V_A = \dfrac{n_A R T_A}{P_A} = \dfrac{n_A R T_C}{P_C}$ (3.16a)

and

$$V_B = \frac{n_B R T_B}{P_B} = \frac{n_B R T_C}{P_C} \tag{3.16b}$$

The sum of the volumes gives

$$V_A + V_B = (n_A + n_B)\frac{R T_C}{P_C} \tag{3.17}$$

as we know $n_A + n_B = n_C$, then $V_A + V_B = V_C$, and the mixture relation in Eq (3.12a) is satisfied.

The mixture volume is the sum of individual gas volumes. This development could also be viewed as proof that the mixture is an ideal gas when the individual ideal gases are combined. Also eliminating RT_C / P_C from Eqs (3.16) and (3.12) yields the general relation,

$$\frac{V_i}{V} = \frac{n_i}{n} = y_i \tag{3.18}$$

A multi component mixture of two or more ideal gases is given as

$$V = \sum_i V_i = \sum_i y_i V \tag{3.19}$$

where V_i is named **the partial volume** of component i.

According to Howell et al.(1992), the partial volume is the pure component volume that would result at the mixture temperature and pressure if that component were separated from the mixture. An alternative view for a mixture of ideal gases considers the mixing of two gases which are initially at different pressures but occupy equivalent volumes at the same temperature. Physically, the pressure exerted on a plane within an ideal gas results, from the change in momentum of the independent molecules in random motion. Thus, the pressure contribution from mixing two ideal gases, which have independent molecules, should be the sum of the individual gas pressure contributions (with volumes and temperatures equal). This is called Dalton's law of additive pressures.

The **ideal gas equation of state** for the components and mixtures is given in Eq. (3.12). For a constant temperature and equal volume mixing,

$T_A = T_B = T_C$ and $V_A = V_B = V_C$. Then,

$$P_A = \frac{n_A RT_A}{V_A} = \frac{n_A RT_C}{V_C} \tag{3.20a}$$

and

$$P_B = \frac{n_B RT_B}{V_B} = \frac{n_B RT_C}{V_C} \tag{3.20b}$$

Thus, the sum of the pressure is as follow

$$P_A + P_B = (n_A + n_B)\frac{RT_C}{V_C} \tag{3.21}$$

where $n_A + n_B = n_C$ and $P_A + P_B = P_C$ so the mixture relation in Eq.(3.12) is satisfied. When RT_C/V_C is eliminated from Eq.(3.20) with Eq.(3.12) the general relation is produced .

$$\frac{P_i}{P} = \frac{n_i}{n} = y_i \tag{3.22}$$

where P_i is called the **partial pressure** of component i.

The partial pressure of component i is the pressure that would be exerted by the component at the mixture temperature and volume if it were separated from the mixture. A general multi component mixture of ideal gases yields

$$P = \sum_i P_i = \sum_i y_i P \tag{3.23}$$

The above relation, which was stated as the Amagat-Leduc law and Dalton's law, yield identical information. Modification of these statements of ideal gases is available for real gas properties and will be described latter.

3.3 Partial Molal Properties

In general, a mixture extensive property M can be expressed as a function of the two intensive properties T and P and the number of moles of the individual components $n_A, n_B, n_C, \ldots$as M= M(T,P, $n_A, n_B, n_C, \ldots.$)

$$dM = (\frac{\partial M}{\partial T})_{T,n_A,n_B,\ldots} dT + (\frac{\partial M}{\partial P})_{T,n_A,n_B,\ldots} dP + (\frac{\partial M}{\partial n_A})_{T,P,n_B,n_C,\ldots} dn_A + (\frac{\partial M}{\partial n_B})_{T,P,n_A,n_C,\ldots} dn_B + \ldots \tag{3.24}$$

$$\overline{M}_A = \overline{M}_{T,P,n_B,n_C,\ldots} = (\frac{\partial M}{\partial n_B})_{T,P,n_B,n_C,\ldots} \tag{3.25}$$

$$\overline{M}_B = \overline{M}_{T,P,n_A,n_n,\ldots} = (\frac{\partial M}{\partial n_B})_{T,P,n_A,n_C,\ldots} \tag{3.26}$$

$$\overline{M}_C = etc$$

$\overline{M}_i$ is the **partial molar property** of species i in solution , and may stand for the partial molar internal energy $\overline{U}_i$, the partial molar enthalpy $\overline{H}_i$, the partial molar entropy $\overline{S}_i$, the partial molar Gibbs energy $\overline{G}_i$, etc.

This function represents the change of total property nM due to addition at constant T and P of a differential amount of species i to a finite amount of solution.

3.4 The Gibbs –Duhem Relation

It is assumed that the Gibbs function is dependent on temperature, pressure and the concentrations of the various chemical species present in the system. Thus, independent

variables are T, P, n_i. Before further considering the relationships between phases, it is advantageous to develop some of the equations relating variables within a given phase. The equation for the change of free energy for a closed system is:

dG= -SdT +VdP, **(3.37a)**

That implies that, at constant mass, system free energy is a function of temperature and pressure only. For an open system it also depends on the number of moles of each component. Thus the functional relationship is

G= f (T, P, $N_1, N_2,...$)

Writing in differential form

$$dG=(\frac{\partial G}{\partial T})_{P,N_j} dT + (\frac{\partial G}{\partial P})_{T,N_j} dP + \sum_i (\frac{\partial G}{\partial N_i})_{T,P,N_{j\neq 1}} dN_i \ldots \quad \textbf{(3.37b)}$$

It is evident from an examination of Eq. (3.37) that

$$(\frac{\partial G}{\partial T})_{P,N_j} = -S \text{ and } (\frac{\partial G}{\partial P})_{T,N_j} = V,... \quad \textbf{(3.38)}$$

and note that $(\frac{\partial G}{\partial N_i})_{T,P,N_{j\neq i}}$ is defined as **the partial molar Gibbs functions** $\overline{G}$.

Commonly the partial molar Gibbs function is called the electrochemical potential, or simply the chemical potential , and is given the symbol $\overline{\mu}$ and defined as

$$(\frac{\partial G}{\partial n_i})_{T,P,N_{j\neq i}} \equiv \overline{\mu}_i \quad \textbf{(3.39)}$$

The chemical potential is the driving potential for the mass transfer of components.

$\overline{\mu}$ is an intensive property that depends on the relative amounts of each species present in the mixture .

Applying the substitution in Eq. (3.37b)

$$dG= - SdT +VdP + \sum \mu_i dN_i \ldots \quad \textbf{(3.40)}$$

is the equation describing the change in free energy in a system of variable mass.

If a system is made starting from zero mass at constant temperature and pressure,

$$dG = \sum_i \mu_i dN_i \tag{3.41}$$

Starting from zero mass, the initial free energy is zero; thus the integral equation becomes

$$\int_0^G dG = G = \sum_i \int_0^{N_i} \mu_i dN_i \tag{3.42}$$

passing through different steps ,we obtain

$$dG = \sum_i \mu_i dN_i + \sum_i N_i d\mu_i = -SdT + VdP + \sum_i \mu_i dN_i, \tag{3.43}$$

which gives

$$\sum_i N_i d\mu_i = -SdT + VdP \tag{3.44}$$

If a specification of constant temperature and pressure is applied, the equations become

$$\sum_i N_i d\mu_i = 0 \tag{3.45}$$

$$\sum_i x_i d\mu_i = 0 \tag{3.46}$$

Eq.(3.46) is known as the **Gibbs-Duhem equation** .

Eq.(3.45) and (3.46) are often used to test experimental data for thermodynamic consistency.

3.5 Non-ideal systems

Non-ideal behaviour can be described using two approaches: The activity coefficients for the liquid phase and the equation of state approach for the vapour phase. These are two fundamentally different methods used for representing phase equilibrium data. They are employed to correlate or predict vapour –liquid equilibrium.

3.5.1 Activity coefficients approach

Activity coefficients are measures of deviations from ideal distributions of components between equilibrium phases.

At equilibrium of two phases; we have

$$\hat{f}_i^v = \hat{f}_i^l \quad (i = 1, 2, \ldots, N) \tag{3.47}$$

Let the fugacities in above the equation be replaced by fugacity coefficients, defined by

$$\hat{\phi}_i = \hat{f}_i / x_i P$$

Letting y_i representing a vapour-phase mole fraction, the following equation can be written as:

$$\hat{f}_i^v = \hat{\phi}_i^v P_i = \hat{\phi}_i^v y_i P \tag{3.48a}$$

Similarly, representing a liquid-phase mole fraction by x_i, we have

$$\hat{f}_i^l = \hat{\phi}_i^l x_i P \tag{3.38b}$$

and if the liquid-phase fugacities in Eq. (3.47) are eliminated in favour of activity coefficients, the following expression is obtained

$$\gamma_i = \hat{f}_i^l / x_i f_i^l \tag{3.49a}$$

Thus, it can be written as:

$$\hat{f}_i^l = \gamma_i x_i f_i^l \tag{3.49b}$$

such that

$$y_i \hat{\phi}_i P = x_i \gamma_i f_i$$

Introducing G.N Lewis equation relating excess Gibbs Energy and fugacity,

dG= RTdln f, **(3.50a)**

relating above equation to the Eq. (3.37a), we get

d G_i= V_i dP- S_i dT= RTd ln f_i **(3.50b)**

At constant T,

$$\text{d ln } f_i = \frac{V_i^l}{RT} \text{dP}$$

Integration from P_i^{sat} to P gives the following relationship:

$$\hat{f}_i^l = P_i^{sat} \phi_i^{sat} \exp\left[\int_{P_i^{sat}}^{P} \frac{V_i^L}{RT} dP\right] \tag{3.50c}$$

$\hat{\phi}_i$ refers to vapour phase and γ_i and f_i are liquid phase properties.

The general expression for VLE is

$$\hat{\phi}_i^v y_i P = \gamma_i x_i P_i^{sat} \phi_i^{sat} \exp\left[\int_{P_i^{sat}}^{P} \frac{V_i^L}{RT} dP\right] \tag{3.51a}$$

Since V_i, the liquid-phase molar volume, is a very weak function of the P at temperatures well below T_c [Smith et al. (1987)], an approximation is obtained when V_i is assumed constant at the value for saturated liquid, V_i^l :

$$\hat{\phi}_i y_i P = \gamma_i x_i P_i^{sat} \phi_i^{sat} \exp[-\frac{V_i^L (P - P_i^{sat})}{RT}] \qquad \textbf{(3.51b)}$$

After substitution for the pure component fugacity [Equation (3.50)], the following equation is obtained,

$$y_i \Phi_i P = x_i \gamma_i P_i^{sat} \qquad \textbf{(3.52a)}$$

where,

$$\Phi_i = \frac{\hat{\phi}_i^v}{\phi_i^{sat}} \exp[-\frac{V_i^l (P - P_i^{sat})}{RT}] \qquad \textbf{(3.52b)}$$

Equation (3.52a) is called the **gamma/phi** formulation of VLE. It reduces to the Raoult's law when $\Phi_i = \gamma_i = 1$, and to modified Raoult's law when $\Phi_i = 1$.

According to Smith and Van Ness (1987), at low pressure, Φ_i is usually of the order of unity, and is identically unity under assumptions that the vapour phase is an ideal gas and the fugacities of liquids are independent of pressure.

The exponential is called the **Poynting factor.** At low to moderate pressures, its omission introduces negligible errors, and the Equation (3.52b) is often simplified:

$$\Phi_i = \frac{\hat{\phi}_i}{\phi_i^{sat}}$$

3.5.2Evaluation of the fugacity coefficients

Calculation of the fugacity coefficients requires knowledge of the P-T-x behaviour of the system. Activity coefficients for a pure liquid is unity and those of a component in a mixture approach unity tangentially as the concentration of that component approaches 100% and generally have maximum values at infinite dilution. This information is obtained from an equation of state. The general expression to determine the fugacity coefficient is

$$\ln \phi_i = \int_o^P \frac{(\hat{Z}_i - 1)}{P} dP, \qquad \textbf{(3.53)}$$

applying the exponential we obtain

$$\hat{\phi}_i^{sat} = \exp\left(\int_0^P (\bar{Z}-1)\frac{dP}{P}\right) \qquad \text{(const.T,y)} \qquad \textbf{(3.54)}$$

and

$$\phi_i^{sat} = \exp\left(\int_0^{P_i} (Z_i-1)\frac{dP}{P}\right) \qquad \text{(const T)} \qquad \textbf{(3.55)}$$

3.5.3 Virial equation of state

Virial equations of state are infinite power series expressions of the compressibility Z as a function either the density or pressure and are used for handling vapour phase non-idealities at low pressure. The pressure series may be written as:

$$Z=\frac{PV}{RT} = 1 + B'P + C'P^2 + \ldots \qquad \textbf{(3.56a)}$$

$$= 1 + \frac{BP}{RT} + \frac{(C-B^2)}{RT^2}P^2 + \ldots \qquad \textbf{(3.56b)}$$

where B is the **second Virial coefficient**, C the third viral coefficient and so on ; they depend on temperature and composition only. Since very little is known about the third virial coefficient C and beyond, this equation of state is applied mainly in its two-parameter form:

$$Z = 1 + B'P = 1 + \frac{BP}{RT} \qquad \textbf{(3.57)}$$

When this expression is rearranged in the volume –explicit form it becomes

$$V=\frac{RT}{P} + B\ldots \qquad \textbf{(3.58)}$$

According to Prausnitz et al.(1980), this equation of state [Eq.(3.57)] is particularly useful for describing the vapour phase .Application of an infinite series to practical calculations is of course impossible, and truncations of the Virial equations to two or three terms are employed . The degree of truncation is determined not only by the temperature and pressure

but also by the availability of correlations or data for the Virial coefficients. Usually the values of B and C are available. The composition dependencies are given by

$$B_{mixture}=\sum\sum y_i y_i Bij \quad \textbf{(3.59)}$$

Where B_{ii} is the second virial coefficient of component i and B_{ij} is a cross second Virial coefficient, y_i, y_j are mole fractions for a gas mixture, with indices i and j identifying species.

The coefficient B_{ij} characterizes a bimolecular interaction between molecules i and j, and therefore $B_{ij}=B_{ji}$.

Experiments values are compiled by Dymond & Simith (1980) and Cholinski et al.(1986).

$$\ln\hat{\phi}_i^v = B_{ii} + \frac{1}{2}\sum\sum y_k y_l (2\delta_{kl} - \delta_{kl}) \quad \textbf{(3.60)}$$

and

$$\ln\phi_i^{sat} = \frac{B_{ii}P_i^{sat}}{RT} \quad \textbf{(3.61)}$$

where $\delta_{kl} = 2B_{kl} - B_{kk} - B_{ll}$ **(3.62)**

B_{ii} stands for Virial coefficients of pairs of like molecules and B_{ji} represents the cross-Virial coefficient which corresponds to the pairs interactions of unlike molecules .

As we have seen above, the fugacity coefficients of any component in the vapour phase can be calculated if the second Virial coefficient of the pure components and the cross second Virial coefficients are available.

The truncated Virial equation is only applicable to gases at low to moderate pressures. The fugacity correction expression becomes

$$\Phi_i = \exp\{\frac{(B_{ii}+V_i^L)(P-P_i^{sat})}{RT} + (\frac{P}{RT})\frac{1}{2}\sum\sum y_j y_k (2\delta_{ji} - \delta_{jk})\} \quad \textbf{(3.63)}$$

3.5.4 Second virial coefficient correlations

Various generalized methods for predicting second Virial coefficients are available, such as that of Black (1958). Tsonopoulos (1974) developed an empirical correlation, which is an extension of Pitzer-Curl (1957) to the following polar compounds, which have not been

taken in account by Pitzer Curl: ketones, aldehydes, acetonitrile, ethers, alcohols, phenol, and water.

3.5.4.1 The Hayden and –O'Connell correlation

The Hayden and O'Connell (1975) method is widely used for predicting pure-component and cross second Virial coefficients for simple and complex systems, and it has the advantage of handling organic acid dimerization.

In its application to pure components, this method requires the following parameters for each component: critical temperature T_c, and pressure P_c, Thompson's mean radius of gyration R_d or the parachor and dipole moment, and, if appropriate, a parameter to describe chemical association. This parameter has dependence only on the type of group such as hydroxyl, amine, ester, carboxylic acid, etc. These parameters mentioned above are available in Prausnitz et al. (1980) for large number of compounds.

Reid et al.(1980) developed methods which can be used for predicting the critical properties of compounds not available in literature. In those methods it has been shown that the various kinds of intermolecular forces contribute to the second Virial coefficient in different ways.

The Virial equation of state relates the compressibility factor to the independent intensive variables of composition, temperature, and pressure or density.

According to the Hayden and O'Connell (1974) method, the Virial coefficient is assumed to be a contribution of the bound, metastable bound and free pairs, which can be summarized as follows:

$$B_{total} = B_{free(pairs)} + B_{metastable(bound)} + B_{bound} + B_{chem} \qquad \textbf{(3.64)}$$

B_{free} is the contribution due to relatively free molecules in other words, molecules in which intermolecular forces are weak. B_{bound} is the contribution related to bounded or dimerized molecules; in these molecules chemical forces are significant.

The correlation for B_{free}, for nonpolar substances, the acentric factor or critical compressibility factor should not be employed because they are affected by the polarity and complexing interactions as well. The mean radius of gyration used by Thompson and Braun (1968) is assumed to be the most applicable. For polar substances with large dipole moments ω>1.45, the critical properties are affected by polarity and the device of angle averaging was introduced for determining the effect of polarity.

Mixing rules have been used for calculating cross coefficient and solvation effects.

For more details about the formulation of the Hayden and O'Connell method the reader is referred to the Hayden and O'Connell (1974) paper. This correlation has been used in this work for calculating the second Virial coefficients (Appendix C). This correlation was chosen because many authors employ it for fitting VLE data and it takes in account many chemicals properties (Eq.3.64).

3.5.4.2. The Tsonopoulos (1974) correlation

This empirical correlation of second Virial coefficients is used for polar and non-polar systems and is formulated as follows:

$$\frac{BP_c}{RT_c} = f^0 + \omega f^1 + \frac{a}{T_r^6} - \frac{b}{T_r^8} \tag{3.65}$$

$$f^0 = 0.1445 - \frac{0.330}{T_r} - \frac{0.1385}{T_r^2} - \frac{0.0121}{T_r^3} - \frac{0.000607}{T_r^8} \tag{3.66}$$

$$f^1 = 0.0637 + \frac{0.331}{T_r^2} - \frac{0.423}{T_r^3} - \frac{0.008}{T_r^8} \tag{3.67}$$

The values of a and b are dependent on the type of interaction under consideration:

- Polar molecules in which no hydrogen bonding occurs, and b are given by the following expressions:

$$a = -2.140 * 10^{-4} \mu_r - 4.308 * 10^{-21} \mu_r^8 \tag{3.68}$$

where:

$$\mu_r = \frac{10^5 \mu . P_c}{T_c^2} \tag{3.69}$$

$$b = 0 \tag{3.70}$$

- Nonpolar molecules, for example, inert gases and hydrocarbons where hydrogen bonding does not occur, are characterised by a zero dipole moment.

$$a = 0.0878 \tag{3.71}$$

$$b = 9.08 * 10^{-3} + 6.957 * 10^{-4} \mu_r \tag{3.72}$$

Another correlation of the B_{ii} for polar systems, which is similar to Tsonopoulos, is that proposed by Black (1958).

3.5.5 Infinite dilution activity coefficients

Usually, a molecule exhibits its highest degree of non-ideality when it is completely surrounded by unlike molecules. The product of vapour pressure and activity coefficient is a measure of the escaping tendency of the molecule. It is very difficult to extrapolate the activity coefficient from finite concentration to infinite dilution.

The measurement and use of infinite dilution activity coefficients has considerable importance in design of distillation equipment. Data in this region are usually the least accurate and the error in P-T-x data goes to infinity, as infinite dilution is approached. Therefore, they need good data in the region to design and to simulate. Experimental activity coefficients at infinite dilution are particularly useful for calculating the parameters needed in an expression for the excess Gibbs energy.

In a binary system, γ_1^{∞} and γ_2^{∞}, can be used to evaluate two constants in any expression for G^E. For instance, in the Van Laar equation

$$G^E = Ax_1x_2\left(x_1\frac{A}{B}+x_2\right)^{-1} \tag{3.73}$$

$$RT\,ln\gamma_1 = A\left(1+\frac{A}{B}\frac{x_1}{x_2}\right)^{-2} \tag{3.74}$$

$$RT\,ln\gamma_2 = B\left(1+\frac{B}{A}\frac{x_2}{x_1}\right)^{-2} \tag{3.75}$$

At the endpoints, as $x_1 \to 0$ or as $x_2 \to 0$ Equations (3.74) and (3.75) become $RT\,ln\gamma_1^{\infty} = A$ and

$$RT\,ln\gamma_2^{\infty} = B. \tag{3.76}$$

Calculation of parameters from γ^{∞} data is relatively simple for two-parameter equations for excess Gibbs energy. Schreiber and Eckert (1971) have shown that the vapour-liquid equilibrium over the entire range of composition can be predicted if reliable values of γ_1^{∞} and γ_2^{∞} are available. Pierotti, Deal and Derr (1959) have presented a correlation, which can be

used to predict γ^{∞} for water, hydrocarbons, and typical organic components, e.g esters, aldehydes, alcohols, ketones, nitriles, in the temperature range of 25 to 100 °C .

Experimentally, infinite dilution activity coefficients can be determined in different ways: differential ebulliometry, differential static apparatus, gas chromatographic methods and inert gas stripping. More details for these methods are found in Raal and Mühlbauer (1998).

3.5.5.1Evaluation of infinite dilution activity coefficients

As has been pointed out by Maher and Smith (1979) in their paper, infinite dilution activity coefficients are difficult to measure directly (particularly the isothermal values), and the simple extrapolation of the binary γ_i curves to the endpoints seldom gives accurate values.

In their work they determined γ_1^{∞} and γ_2^{∞} values when total pressure VLE data were being reduced by the Mixon-Gumowski-Carpenter method [Mixon et al.(1965)].

Some comments on the topic of extrapolation of γ_i to infinite dilution are given by Alessi et al. (1991), who defined the infinitely dilute region as being reached when a molecule of type 1 has no contact with other type 1 molecules and interacts only with type 2 molecules (in a binary mixture).

Gautreaux and Coates (1955) presented an equation used to calculate the γ_i^{∞} values from isothermal data. A convenient form with correction for vapour-phase non-ideality by the truncated virial EOS is given by Pividal and Sandler (1988).

$$\gamma_1^{\infty} = \frac{\varepsilon_1^{\infty} P_2^{sat}}{P_1^{sat}} \left[1 - \beta \frac{d \ln P_2^{sat}}{dT} \left(\frac{\partial T}{\partial x_1} \right)_P^{x_1 \to 0} \right] \tag{3.77}$$

where:

$$\varepsilon_1^{\infty} = \exp\left[\frac{(B_{11} - V_1^L)(P_2^{sat} - P_1^{sat}) + \delta_{12} P_2^{sat}}{RT} \right] \tag{3.78}$$

$$\beta = 1 + P_2^{sat} \left(\frac{B_{22} - V_2^L}{RT} \right) \tag{3.79}$$

$$\delta_{12} = 2B_{12} - B_{11} - B_{22} \tag{3.80}$$

The B_{ii} and B_{ij} are second Virial coefficients for like and unlike species respectively, the P_i^{sat} are pure component vapour pressures and V_i^L is the liquid molar volume.
A convenient low-pressure simplification is given by:

$$\varepsilon_1 = 1 = \beta \tag{3.81}$$

Infinite dilution activity coefficients are difficult to measure directly (particularly for isothermal values) [Maher and Smith (1979)], and the simple extrapolation of the binary γ_i curves to the endpoints seldom gives accurate values. According to them, the P versus x_1 plot can be converted to the "deviation pressure" P_D versus x_1 defining P_D as follows:

$$P_D = P - P_2^{sat} - \left(P_1^{sat} - P_2^{sat}\right)x_1 \tag{3.82}$$

Differentiating the above equation when x_1 tends to zero ($x_1 \to 0$), the useful limiting properties are obtained

$$\left(\frac{P_D}{x_1 x_2}\right)_{x_1 \to 0} = \left(\frac{\partial P / \partial x_1}{1 - 2x_1}\right)_{x_1 \to 0} = \left(\frac{\partial P}{\partial x_1}\right)_{x_1 = 0}, \tag{3.83}$$

$$\left(\frac{P_D}{x_1 x_2}\right)_{x_2 \to 0} = \left(\frac{\partial P_D}{\partial x_2}\right)_{x_2 = 0} = -\left(\frac{\partial P_D}{\partial x_1}\right)_{x_1 = 0}. \tag{3.84}$$

Therefore,

$$\left(\frac{\partial P}{\partial x_1}\right)_{x_1 = 0} = \left(\frac{P_D}{x_1 x_2}\right)_{x_1 = 0} + P_1^{sat} - P_2^{sat}, \tag{3.85}$$

$$\left(\frac{\partial P}{\partial x_1}\right)_{x_1 = 1} = -\left(\frac{P_D}{x_1 x_2}\right)_{x_1 = 1} + P_1^{sat} - P_2^{sat}. \tag{3.86}$$

The $\left(P_D / x_1 x_2\right)$ vs x_1 plot will determine the extrapolation of the endpoint slopes; i.e.

$$\left(\frac{\partial P_D}{\partial x_1}\right)_{x_1 = 0}^{\infty} = \gamma_1^{\infty} \tag{3.87}$$

and

$$\left(\frac{\partial P_D}{\partial x_1}\right)_{x_1 = 1}^{\infty} = \gamma_2^{\infty}. \tag{3.88}$$

If the slope of (P_D/x_1x_2) vs. x_1 is not linear, (x_1x_2/P_D) can be plotted and if linear will allow reliable extrapolations at both endpoints.

3.5.6 Different models for activity coefficients

Many equations have been proposed for correlating activity coefficients with composition and temperature. Different models of activity coefficients are widely used and the superiority of one method over others is not always clear. The most comprehensive comparison of five of the models is made in the DECHEMA vapour-liquid data collection (1979). In this data compilation the best fit of experimental data by these formulas is identified in every case.
From the statistical analysis done in the DECHEMA, the Wilson equation comes out the best, and the Van Laar and UNIQUAC come as the worst; but there are some differences for particular classes of substances, and the NRTL (Non Random-Two Liquid) equation for instance comes out the best for aqueous systems. These equations have two parameters each, except the symmetrical Margules equation, which has one parameter, and the NRTL, which has three. Four of these models can be used for multi component mixtures. Activity coefficients γ_i are generally calculated by differentiation of the excess Gibbs free energy G^E but in practice the process is reversed and G^E is evaluated from knowledge of activity coefficients. In addition to various references mentioned for each equation, Wallas (1985) and Raal and Mühlbauer (1998) are recommended for more details about these models.

3.5.6.1 The Margules equation

The Margules equation is the oldest. It was formulated in 1895 and is one of the simplest expressions for the molar excess Gibbs free energy. Margules' work was before fugacity and activity coefficients were introduced.
For a binary system:

$$\frac{G^E}{RT} = x_1x_2(A_{21}x_1 + A_{12}x_2) \tag{3.89}$$

where A_{12} and A_{21} are binary parameters dependent on temperature, but not on the composition. The Margules activity coefficients in a binary mixture are given by

$$\ln\gamma_1 = [A_{12} + 2(A_{21} - A_{12})x_1]x_2^2 \quad (3.90)$$

$$\ln\gamma_2 = [A_{21} + 2(A_{12} - A_{21})x_2]x_1^2 \quad (3.91)$$

A_{12} and A_{21} are generally obtained by fitting VLE data. Note that the value of activity coefficients of each component correctly tends to one as the mole fraction of the component goes to one.

The Margules equation works well for binary systems in which the two components are very similar in size, shape and chemical nature.

3.5.6.2 The Wilson equation

This model of solution behaviour was introduced by G.M.Wilson in 1964, and as for the Margules equation contains two adjustable parameters for a binary system (Λ_{12} and Λ_{21}) which are related to the pure component liquid molar volumes (v_i). This method is based on the assumption that, around each molecule, there is a local composition that is different from the bulk composition.

For a binary system, Wilson excess Gibbs energy has the following form:

$$\frac{G^E}{RT} = -x_1 \ln(x_1 + \Lambda_{12}x_2) - x_2 \ln(x_2 + \Lambda_{21}x_1) \quad (3.92)$$

where

Λ_{12} and Λ_{21} are parameters specific to the binary pair.

These parameters are defined in terms of the molar liquid volume v_i of the pure component i, and energies of interaction λ_{ij} between the molecules i and j as follows

$$\Lambda_{ij} \equiv \frac{v_j}{v_i}\exp[-\frac{\lambda_{ij} - \lambda_{ii}}{RT}] \quad (3.93)$$

The expressions for the liquid activity coefficients are:

$$\ln\gamma_1 = -\ln(x_1 + \Lambda_{12}x_2) + x_2(\frac{\Lambda_{12}}{x_1 + \Lambda_{21}x_2} - \frac{\Lambda_{21}}{x_2 + \Lambda_{21}x_1}) \quad (3.94)$$

$$\ln \gamma_2 = -\ln(x_2 + \Lambda_{21}x_1) + x_1\left(\frac{\Lambda_{21}}{x_2 + \Lambda_{21}x_1} - \frac{\Lambda_{12}}{x_1 + \Lambda_{12}x_2}\right) \quad \textbf{(3.95)}$$

The Wilson equation has two parameters ($\lambda_{12} - \lambda_{11}$) and ($\lambda_{21} - \lambda_{22}$) which characterise the molecular interactions between the components and are solvable only numerically when experimental activity coefficients are known. For a given number of measurements, finding the most reliable value of parameters is the problem. According to Walas (1985), the Wilson equation cannot handle liquid-liquid immiscibility.

3.5.6.3 The NRTL equation

The NRTL equation is also based on a local composition model for the excess Gibbs free energy.

This model has a third parameter and, according to Walas (1985), Marina and Tassios (1973) found that this parameter α_{12} when set equal to -1 gives excellent representation for both miscible and partially immiscible binaries.

Renon & Prausnitz (1968) published a model in which they showed that this parameter is strictly an empirical factor not clearly related to any mechanism for the range of numerical values found experimentally. The NRTL expression for the excess Gibbs energy is as follows:

$$\frac{G^E}{RT} = x_1x_2\left[\frac{\tau_{21}G_{21}}{x_1 + x_2G_{21}} + \frac{\tau_{12}G_{12}}{x_2 + x_1G_{12}}\right] \quad \textbf{(3.96)}$$

where $\tau_{12} = (g_{12} - g_{22})/RT$, **(3.97)**

$$\tau_{21} = (g_{12} - g_{11})/RT \ , \quad \textbf{(3.98)}$$

$$G_{12} = \exp(-\alpha_{12}\tau_{12}) \ , \quad \textbf{(3.99)}$$

$$G_{21} = \exp(-\alpha_{12}\tau_{21}) \ . \quad \textbf{(3.100)}$$

The activity coefficients are obtained by differentiation as

$$\ln\gamma_1 = x_2^2[\tau_{21}(\frac{G_{21}}{x_1 + x_2 G_{21}})^2 + (\frac{\tau_{12}G_{12}}{(x_2 + x_1 G_{21})^2})] \quad \textbf{(3.101)}$$

$$\ln\gamma_2 = x_1^2[\tau_{12}(\frac{G_{12}}{x_2 + x_1 G_{12}})^2 + (\frac{\tau_{21}G_{21}}{(x_1 + x_2 G_{21})^2})] \quad \textbf{(3.102)}$$

Where g_{11} and g_{22} are the Gibbs energy parameters of the pure substances and the assumption is made that $g_{12} = g_{21}$. These equations have three adjustable parameters: $(g_{12} - g_{22})$, $(g_{21} - g_{11})$ and $\alpha_{12}(\alpha_{12} = \alpha_{21})$. Renon et al. (1971) found that α_{12}, Δg_{12}, and Δg_{21} are linear function of the temperature. A major advantage of the NRTL model is its ability to represent highly non-ideal systems. The NRTL model is superior to Margules and Van Laar models in that its multicomponent equations can be expressed entirely in terms of binary parameters.

3.5.6.4 The Van Laar equation

The Van Laar model was proposed in 1910 and its development is based on the Van der Waals EOS. According to Walas[1985] this equation is regarded as purely empirical because the fit of activity coefficient data with Van der Waals equation is poor.

According to Van Ness et al (1982), the Margules and the Van Laar equations are a special case of a general treatment based on rational functions, i.e., on equations for $G^E/x_1 x_2 RT$ given by ratios of polynomials. They have the advantage of providing a great flexibility in the fitting of VLE data for binary systems. The equations of the activity coefficients are

$$\ln\gamma_1 = A[\frac{Bx_2}{Ax_1 + Bx_2}]^2 , \quad \textbf{(3.103)}$$

$$\ln\gamma_2 = B[\frac{Ax_1}{Ax_1 + Bx_2}]^2 . \quad \textbf{(3.104)}$$

The parameters can be calculated from a single set of activity coefficient data with

$$A = \ln\gamma_1^{\infty} = \ln\gamma_1[1 + \frac{x_2 \ln\gamma_2}{x_1 \ln\gamma_1}]^2 \quad \textbf{(3.105)}$$

$$B = \ln \gamma_1^{\infty} = \ln \gamma_2 [1 + \frac{x_1 \ln \gamma_1}{x_2 \ln \gamma_2}]^2 \quad \textbf{(3.106)}$$

Van Laar's equations have a disadvantage in that they cannot represent extrema of activity coefficients.

3.5.6.5 The Modified Wilson or T-K Wilson equation

Various modifications of the Wilson equation have been undertaken by different authors. Hiranuma(1974,1975) developed quite a complicated equation based on a theoretical third parameter and others like Schulte et al.(1980) and Nagata et al.(1975) did the continuation of the work.

Tsuboka and Katayama (1975) proposed a successful modification.

The excess Gibbs energy of T-K Wilson equation is as follows:

$$\frac{G^E}{RT} = x_1 \ln[\frac{x_1 + V_{12}x_2}{x_1 + \Lambda_{12}x_2}] + x_2 \ln[\frac{x_2 + V_{21}x_1}{\Lambda_{21}x_1 + x_2}]. \quad \textbf{(3.107)}$$

The expressions of activity coefficients for a binary system becomes

$$\ln \gamma_1 = \ln[\frac{x_1 + V_{12}x_2}{x_1 + \Lambda_{12}x_2}] + (\beta - \beta_v)x_2 \quad \textbf{(3.108)}$$

$$\ln \gamma_2 = \ln[\frac{x_2 + V_{21}x_1}{x_2 + \Lambda_{21}x_1}] + (\beta - \beta_v)x_1 \quad \textbf{(3.109)}$$

where

$$\beta_v = \frac{V_{12}}{x_1 + V_{12}x_2} - \frac{V_{21}}{V_{21}x_1 + x_2}, \quad \textbf{(3.110)}$$

$$\beta = \frac{\Lambda_{12}}{x_1 + \Lambda_{12}x_2} - \frac{\Lambda_{21}}{\Lambda_{21}x_1 + x_2}, \quad \textbf{(3.111)}$$

$$V_{12} = V_2 / V_1, \quad \textbf{(3.112)}$$

$$V_{21} = V_1/V_2 \ , \tag{3.113}$$

V_i are the molal volume

V_{12} and V_{21} are the ratios of the molal volume.

The values of parameters Λ_{12} and Λ_{21} are given in Wilson equation.

The T-K-Wilson equation is applicable to liquid-liquid equilibria, whereas the Wilson is not [Walas (1985)].

3.5.6.6 The UNIQUAC (Universal Quasi-Chemical) equation

This model is based on the concept of local compositions adopted by Abrams and Prausnitz(1975). They proposed that the excess Gibbs energy is a sum of two parts:

1.The configurational or combinatorial part which accounts for the size and shape of the molecules.

2.The residual part accounts for energetic interactions between molecules.

$$G^E = G^E(combinatorial) + G^E(residual) \tag{3.114}$$

$$\frac{G^E(combinatorial)}{RT} = x_1 \ln\frac{\Phi_1}{x_1} + x_2 \ln\frac{\Phi_2}{x_2} + \frac{z}{2}(q_1 x_1 \ln\frac{\theta_1}{\Phi_1} + q_2 x_2 \ln\frac{\theta_2}{\Phi_2}) \tag{3.115}$$

$$\frac{G^E(residual)}{RT} = -q_1 x_1 \ln(\theta_1 + \theta_2 \tau_{21}) - q_2 x_2 \ln(\theta_2 + \theta_1 \tau_{12}) \tag{3.116}$$

where

$$\Phi_i = \frac{x_i r_i}{\sum_j x_j r_j} \tag{3.117}$$

$$\theta_i = \frac{x_i q_i}{\sum_j x_j q_j} \tag{3.118}$$

$$\tau_{ji} = \exp(-\frac{a_{ji}}{RT}) \tag{3.119}$$

z is a co-ordination number ,usually taken as equal to 10, Φ_i stands for volume fractions, and θ_i

are surface area fractions for component i . r_i and q_i are parameters of volume and surface area respectively. Their values can be found from pure molecular structure and are compiled in the DECHEMA data book (1979). These factors may also be obtained from group contributions by Reid et al. (1977), and Fredenslund et al.(1977).

This model is characterised by its wide range of applicability such as:

-Multicomponent mixtures,

-Liquid-Liquid equilibria and

-Molecules whose sizes are widely different are very well represented by this model.

The disadvantages of this equation are based in its algebraical complexity.

The activity coefficients for binary system have the following expressions

$$\ln\gamma_1 = \ln\frac{\Phi_1}{x_1} + (\frac{z}{2})q_1 \ln\frac{\theta_1}{\Phi_1} + \Phi_2(l_1 - \frac{r_1}{r_2}l_2) - q_1\ln(\theta_1 + \theta_2\tau_{21}) + \theta_2 q_1(\frac{\tau_{21}}{\theta_1 + \theta_2\tau_{21}} - \frac{\tau_{12}}{\theta_2 + \theta_1\tau_{12}}) \tag{3.120}$$

$$\ln\gamma_2 = \ln\frac{\Phi_2}{x_2} + (\frac{z}{2})q_2 \ln\frac{\theta_2}{\Phi_2} + \Phi_1(l_2 - \frac{r_2}{r_1}l_1) - q_2\ln(\theta_2 + \theta_1\tau_{12}) + \theta_1 q_2(\frac{\tau_{12}}{\theta_2 + \theta_1\tau_{12}} - \frac{\tau_{21}}{\theta_1 + \theta_2\tau_{21}}) \tag{3.121}$$

where

$$l_i = (\frac{z}{2})(r_i - q_i) - (r_i - 1) \tag{3.122}$$

According to Anderson and Prausnitz (1978), the UNIQUAC equation is applicable to multicomponent systems without the introduction of any parameters beyond those required to describe the constituent of binary systems.

3.6 Data reduction

Methods of data reduction can be divided largely into two groups: model-based methods and model-free method.

Model –based methods: In this method, an analytical form of the Gibbs free energy is assumed with its dependence on liquid phase composition and temperature; and model –free methods do not require such prior assumption.

Several methods have been used for the calculation of component behaviour from gross mixture behaviour.

Ljunglin and Van Ness (1962) have suggested the classification of these two methods into two categories, direct and indirect methods.

3.6.1 The Direct Method

It consists of calculation of vapour compositions by integrating a first order differential equation derived from the Gibbs–Duhem equation relating phase compositions at equilibrium.

A convenient form of the general equation relating pressure, temperature and fugacities for any binary liquid, is the starting point for the derivation of the general coexistence equation.

$$\frac{V}{RT}dP+\frac{(H^{*}-H)}{RT^{2}}dT=x_{1}d\ln\bar{f}_{1}-x_{2}d\ln\bar{f}_{2} \qquad \textbf{(3.123)}$$

The derivation of this equation is very long and it will not be developed here. The entire derivation of this coexistence equation can be found in the Ljunglin and Van Ness (1962) paper. Only the final result is shown below:

$$\varphi dP-\Omega dT=(y_{1}-x_{1})d\ln\frac{\gamma_{1}^{v}}{\gamma_{2}^{V}}+\frac{y_{1}-x_{1}}{y_{1}(1-y_{1})}dy_{1} \qquad \textbf{(3.124)}$$

$$\varphi=\frac{\Delta V^{V}+x_{1}V_{1}^{V}+x_{2}V_{2}^{V}-V^{L}}{RT} \qquad \textbf{(3.125)}$$

$$\Omega=\frac{(\Delta H^{V}+x_{1}H_{1}^{V}+x_{2}H_{2}^{V}-H^{L})}{RT^{2}} \qquad \textbf{(3.126)}$$

In the above equations, the susperscripts L and V represent liquid phase and vapour phase respectively. ΔV^V and ΔH^V stand for the volume change per mole and heat of mixing per mole in the vapour phase respectively. γ_i^V is the vapour phase activity coefficients.

According to Raal and Mühlbauer (1998), for a binary system, this equation can be evaluated at constant temperature or at constant pressure and either Ω and φ has to be evaluated.

The use of the Virial EOS truncated to two terms for evaluating φ and the vapour phase activity coefficients is convenient.

$$Z(=PV/RT) = 1 + BP/RT, \tag{3.127}$$

giving

$$\ln\frac{\gamma_1^V}{\gamma_2^V} = \frac{PS}{RT}(1-2y_1) \tag{3.128}$$

and

$$\varphi = \frac{y_1 y_2 \delta - V^L + x_1 B_{11} + x_2 B_{22}}{RT} + \frac{1}{P} \tag{3.129}$$

with $\delta = 2B_{12} - B_{11} - B_{22}$ (3.130)

The Equation (3.124) becomes

$$\frac{dy_1}{dP} = \frac{dy_1}{dx_1}\Big/\frac{dP}{dx_1} = \frac{\varphi - (1-2y_1)(y_1 - x_1)(\delta/RT)}{[(y_1 - x_1)/y_1(1-y_1)] - (y_1 - x_1)(2P\delta/RT)} \tag{3.131}$$

Assuming that the vapour phase is an ideal gas and that the molar volume of the liquid phase is negligible compared to that of the vapour:

$$\frac{dy_1}{d\ln P} = \frac{y_1(1-y_1)}{y_1 - x_1} \tag{3.132}$$

The Equation (3.131) can be integrated either by a marching procedure or by a relaxation technique.

Stating values for numerical integration using a Runge–Kutta procedure can be obtained from this equation and by application of L'Hopital's rule by Van Ness (1970).

At constant pressure the Eqs. (3.131) and (3.132) become

$$-\Omega\frac{dT}{dy_1} = (y_1 - x_1)\frac{d\ln(\gamma_1^V/\gamma_2^V)}{dy_1} + \frac{y_1 - x_1}{y_1(1-y_1)} \tag{3.133a}$$

$$-\Omega\frac{dT}{dy_1} = \frac{y_1 - x_1}{y_1(1-y_1)} \tag{3.133b}$$

where $(\gamma_1^V = 1.0)$ and Ω can be evaluated with little loss in accuracy from

$$-\Omega = \frac{H^E - x_1L_1 - x_2L_2}{RT} \tag{3.134}$$

Raal and Brouckaert (1992) integrated the Equation (3.133b) using a fourth order Runge-Kutta method. In this procedure it has been found that the P-x data are fitted to analytical expression so that pressures can be generated at appropriate liquid composition. According to Raal and Mühlbauer (1998) others polynomials have been used, but many others have been advocated, such as Tchebichef polynomials, cubic spline fits, orthogonal polynomials. Similar procedures have been used by several authors such as Scatchard and Raymond (1938), Mixon et al.(1965).

3.6.2 The indirect method

This method has received greatest attention in recent years because it involves the Gibbs-Duhem equation for calculating the liquid activity coefficients. Vapour phase composition is then deduced from different expressions of activity coefficients. One of the indirect methods employed frequently is that of Mixon et al. (1965). It is based on the expression for total pressure,

$$P = \frac{\sum x_i\gamma_i P_i^{sat}}{\Phi_i} \tag{3.135}$$

Using expression of activity coefficients represented in term of g ($g=(G^E/RT)$ and applying the substitution in preceding equation for a binary mixture,

$$\ln\gamma_1 = g + x_2\frac{dg}{dx_1} \tag{3.136}$$

$$\ln\gamma_2 = g - x_1\frac{dg}{dx_1} \tag{3.137}$$

Then the following expression is obtained

$$P = \frac{x_1 P_1^{sat}}{\Phi_1}\exp\{g + x_2\frac{dg}{dx_1}\} + \frac{x_2 P_2^{sat}}{\Phi_2}\exp\{g - x_1\frac{dg}{dx_1}\} \tag{3.138}$$

In this method, the experimental P-x data must be fitted to some appropriate expression and then P values are interpolated at fixed intervals in x_1. The above P equation was expressed in finite –difference form for each grid point using central differences. They applied Newton's method to the total pressure non-linear expressions and then solving the equations by block relation in case of binary systems or point relation techniques for ternary systems. Mixon et al. (1965) applied his method to multicompnent systems and obtained good results. For more details, the reader is referred to Mixon et al. (1965).

3.6.2.1 Barker's Method

Barker (1953) presented a method based on the assumption that the Gibbs excess free energy can be expressed as a polynomial function of composition. Therefore, it is a model-based method. In this method, the total pressure is presented as a function of liquid phase activity coefficients. In its turn activity coefficients are expressed in terms of parameters, which have to be determined by using a successive approximations technique. This method allows calculation of the vapour composition from the total pressure data with the help of the Gibbs-Duhem equation.

3.6.2.1.1 Formulation of Barker's method

Barker's method is formulated below:
Excess chemical potential and activity coefficients are related by the Scatchard and Raymond (1952) equation as follows:

$$\mu_1^E = RT\ln\gamma_1 \tag{3.139a}$$

$$= RT \ln (Py_1 / P_1 x_1) + (V_1 + \beta_{11})(P_1 - P) + P\delta_{12} y_1^2 \quad \textbf{(3.139b)}$$

$$\mu_2^E = RT \ln \gamma_2 \quad \textbf{(3.140a)}$$

$$= RT \ln (Py_2 / P_2 x_2) + (V_2 - \beta_{22})(P_2 - P) + P\delta_{12} y_1^2 \quad \textbf{(3.140b)}$$

Here: μ_1^E and μ_2^E are the changes in chemical potentials

P is the total pressure

P_1 and P_2 are vapour pressures of the pure components.

x and y are liquid and vapour mole fractions respectively

V_1 and V_2 are liquid molar volumes

β_{11}, β_{22} and β_{12} are second Virial coefficients in the equations of state of the pure and mixed vapours.

$$\delta_{12} = 2\beta_{12} - \beta_{11} - \beta_{22}$$

The total pressure for a binary system is written:

$$P = \gamma_1 P_1' + \gamma_2 P_2' \quad \textbf{(3.141)}$$

$$\text{w } P_2' = x_2 P_2 \exp[(V_2 - \beta_{22})(P - P_2)/RT - P\delta_{12}\, y_1^2 / RT] \quad \textbf{(3.143)}$$

here

$$P_1' = x_1 P_1 \exp[(V_1 - \beta_{11})(P - P_1)/RT - P\delta_{12}\, y_2^2 / RT] \quad \textbf{(3.142)}$$

P_1' and P_2' stand for partial pressures

Assuming that the concentration dependence of the excess free energy of mixing can be described by Scatchard (1949) equation:

$$G_x^E = x_1 \mu_1^E + x_2 \mu_2^E \quad \textbf{(3.144 a)}$$

$$= x_1 x_2 [a + b(x_1 - x_2) + c(x_1 - x_2)^2 + \ldots] \quad \textbf{(3.144b)}$$

In terms of Eq. (3.144b), the activity coefficients are given by:

$$\ln\gamma_1 = Al_1 + Bm_1 + Cn_1 + ..., \quad \textbf{(3.145)}$$

$$\ln\gamma_2 = Al_2 + Bm_2 + Cn_2 + ..., \quad \textbf{(3.146)}$$

where

$$l_1 = x_2^2, \qquad m_1 = -x_2^2(1-4x_1), \qquad n_1 = x_2^2(1-8x_1+12x_1^2), \quad \textbf{(3.147)}$$

$$l_2 = x_1^2, \qquad m_2 = +x_1^2(1-4x_2), \qquad n_1 = x_1^2(1-8x_2+12x_2^2), \quad \textbf{(3.148)}$$

and

A=a/RT, B=b/RT , C=c/RT **(3.149)**

3.6.2.1.2 Computational procedure of Barker's method

The parameters (constants) are calculated by a process of successive approximations. For the first approximation it is assumed that the solution behaves like a regular solution, so B and C are set to zero.

By neglecting the corrections for vapour phase non-ideality, A is given by

$$A = 4\ln\left(\frac{2P^*}{P_1 + P_2}\right), \quad \textbf{(3.150)}$$

P^* represents the pressure for an equimolar mixture, and it can be obtained from P-x data. The value of A is used for calculating approximate vapour compositions, which are sufficiently accurate to use in the small correction term $P\delta_{12}y^2/RT$ in Eqs. (3.142) and (3.143).

Then P_1' and P_2' can be calculated for the experimental liquid compositions. γ_1 and γ_2 are obtained by using the first approximation for A in Eqs. (3.145), total pressure P by Eq. (3.141), pressure residuals, as $R = P\exp t - Pcalc$ and the derivatives dP/dA, dP/dB, dP/dC, which are given by

$$dP/dA = l_1 \gamma_1 P_1' + l_2 \gamma_2 P_2' \,, \tag{3.151}$$

$$dP/dB = m_1 \gamma_1 P_1' + m_2 \gamma_2 P_2' \,, \tag{3.152}$$

$$dP/dC = n_1 \gamma_1 P_1' + n_2 \gamma_2 P_2' \,, \tag{3.153}$$

The changes δA, δB, δC are used to improve values in A, B ,C which will reduce the pressure residuals to zero ,by fitting by least squares to the following equation

$$(dP/dA)\delta A + (dP/dB)\delta B + (dP/dC)\delta C = R \tag{3.154}$$

Then, the following equations are solved.

$$\delta A \sum (dP/dA)^2 + \delta B \sum (dP/dA)(dP/dB) + \delta C \sum (dP/dA)(dP/dC) = \sum R(dP/dA), \tag{3.155}$$

$$\delta A \sum (dP/dA)(dP/dB) + \delta B \sum (dP/dB)^2 + \delta C \sum (dP/dB)(dP/dC) = \sum R(dP/dB) \tag{3.156}$$

$$\delta A \sum (dP/dA)(dP/dC) + \delta B \sum (dP/dB)(dP/dC) + \delta C \sum (dP/dC)^2 = \sum R(dP/dC) \tag{3.157}$$

The summations Σ are taken over all the experimental points. Adding these increments to the initial values of A, B, C, the improvement is noted and the process can be repeated until A, B, C do not change significantly. Mc Dermott and Ellis (1965) developed a procedure for generalizing Barker's method to ternary systems.

3.7 Thermodynamic consistency test for binary systems

The thermodynamic test serves to assess the validity of data and is based on the Gibbs-Duhem equation. As systematic errors can be introduced in experimental measurement and values of γ_i^* may not satisfy the Gibbs-Duhem equation, they may not be consistent. Asterisks denote experimental values. Unfortunately this test cannot be applied in the static method. The test proposed by Van Ness (1995) is formulated as follows:

For a binary system,Gibbs-Duhem equation can be written,

$$(\frac{G^E}{RT})^* = x_1 \ln \gamma_1^* + x_2 \ln \gamma_2^* \quad \textbf{(3.158)}$$

Differentiating this equation gives,

$$\frac{d(G^E/RT)^*}{dx_1} = x_1 \frac{d \ln \gamma_1^*}{dx_1} + \ln \gamma_1^* + x_2 \frac{d \ln \gamma_2^*}{dx_1} - \ln \gamma_2^* \quad \textbf{(3.159)}$$

or

$$\frac{d(G^E/RT)^*}{dx_1} = \ln \frac{\gamma_1^*}{\gamma_2^*} + x_1 \frac{d \ln \gamma_1^*}{dx_1} + x_2 \frac{d \ln \gamma_2^*}{dx_1} \quad \textbf{(3.160)}$$

Subtracting

$\frac{d(G^E/RT)}{dx_1} = \ln \frac{\gamma_1}{\gamma_2}$ from this equation yields:

$$\frac{d(G^E/RT)}{dx_1} - \frac{d(G^E/RT)^*}{dx_1} = \ln \frac{\gamma_1}{\gamma_2} - \ln \frac{\gamma_1^*}{\gamma_2^*} - (x_1 \frac{d \ln \gamma_1^*}{dx_1} + x_2 \frac{d \ln \gamma_2^*}{dx_1}) \quad \textbf{(3.161)}$$

The difference between the like terms are residuals and can be represent by a δ.

$$\frac{d\delta(G^E/RT)}{dx_1} = \delta \ln \frac{\gamma_1}{\gamma_2} - (x_1 \frac{d \ln \gamma_1^*}{dx_1} + x_2 \frac{d \ln \gamma_2^*}{dx_1}) \quad \textbf{(3.162)}$$

If a data set is reduced to make the G^E/RT residuals scatter about zero, then the derivative $d\,\delta(G^E/RT)/dx_1$, is effectively zero and

$$\delta \ln \frac{\gamma_1}{\gamma_2} = x_1 \frac{d \ln \gamma_1^*}{dx_1} + x_2 \frac{d \ln \gamma_2^*}{dx_1} \quad \textbf{(3.163)}$$

The right –hand side of this equation needs to be zero for a consistency test.

According to Van Ness and Abbott (1982), the residual on the left is a direct measure of deviations from the Gibbs-Duhem equation and failure to scatter about zero measures the departure of the data from consistency.

Chapter 4

EQUIPMENT AND EXPERIMENTAL PROCEDURE

In this chapter the apparatus used in this project is described and some of its advantages over other prior designs are discussed.

4.1 A New Static Equilibrium Cell Cluster

The original design of this assembly was done by Raal and Mühlbauer (1998) and consisted of a six-cell cluster. Both the equilibrium cell and the degassing condenser, made in stainless steel, were joined together by means of a silicone gasket. During degassing and equilibration periods the assembly was fully immersed in a constant-temperature water bath. Unfortunately, no thesis has been done on this apparatus, and only one set of isotherm data is reported in Raal and Mühlabauer (1998).

The following weaknesses of the old design were highlighted on the basis of observation:

- The equilibrium cell and degassing condenser are joined together by a silicone gasket which may cause leaks.
- It is not possible to see what happens inside the opaque stainless steel degassing condenser.
- As the majority of the static cells at low pressure published up to date employ the technique of submersion of the equilibrium cell in the water bath for getting constant temperature, this causes corrosion inside the circular base on which the apparatus stands.
- Portions of the equilibrium cell near the septum are ineffectively mixed, which could cause large errors in VLE measurement.
- The metallic stirring bar can easily corrode and it is fixed on the equilibrium cell base. This does not allow easy cleaning. This should be replaced by a removable plastic-coated magnetic stirrer bar.
- The Condenser fitting to the manifold is fixed and it does not allow easy connection/disconnection for cleaning the apparatus.

All the above weaknesses were taken in account in the new design for improving its efficiency.

The new apparatus (Figure 4-1) is consisted of 4 cells and they were constructed by the glassblower, Mr Peter Siegling. One unit of this apparatus consists of an equilibrium cell attached to a multiwalled-degassing condenser both made of glass. In this new design silicone gasket was eliminated since it should cause leaks.

The new assembly is mounted symmetrically on a circular base. Each unit cell condenser is connected to a small hexagonal manifold via stainless steel valves using 1/8" stainless steel tubing. The manifold has a small cavity of approximately 1.5 mm diameter, which is linked with six isolating valves and is connected to the vacuum pump, and pressure transducer. A small cartridge heater is inserted into the manifold for maintaining the temperature a few degrees above equilibrium cell temperature for avoiding vapour condensation.

The four equilibrium cells stand on top of a cylindrical base, in which stirring paddles with soft iron cores are attached to the bottom of the draft tube, activated by rotating magnets. The magnets are driven by o-ring pulleys from a central shaft, which is in turn driven by a small MAXON DC motor. For more details see the illustration of the equipment in Figure 4-2.

The particular interest of the condenser is the built-in draft tube, in which a gentle draft down the tube is induced by the magnetically driven impeller and produces a circulation of vapour in the condenser, returning it in the liquid surface thereby ensuring good mixing between the phases and accelerating equilibrium time. The fitting tubes connected to the condenser and to the manifold are heated electrically using nichrome resistance wire in order to maintain a temperature a few degrees higher than the cell temperature. Both manifold and stainless steel fittings are insulated in order to avoid heat loss and their temperature is maintained a little higher than the cell temperature, to prevent vapour condensation. These temperatures are monitored by a thermocouple.

The modified static cell is made from glass with both condensers 20 cm in length and the equilibrium cell whose length 6.5 cm with total volume of $38\,cm^3$. Each cell is charged with approximately 12 cm^3 of a binary mixture of known composition, prepared gravimetrically and the rest of volume is occupied by the vapour phase. All cells are equipped with sampling septa, which allow the sampling of the liquid phase with a syringe needle. This new equilibrium cell is surrounded by a water jacket in which hot water circulates in order to maintain an equilibrium cell temperature constant. The septum fixed to the top of the condenser allows the connection to the stainless steel fitting tube (see caption 7 in Figure 4-2). It also helps to connect/ disconnect the cell easily without damaging the valves nuts on manifold. This is one of the advantages of the new design over the old one. The water cell jacket is connected to the tube that draws hot water from

water bath for maintaining a constant temperature in equilibrium cell. Another advantage of the new design is that, the equilibrium cell and the degassing condenser form one unit (Figure 4-1) whereas in the old design both units are attached together by silicone gasket. Hence this could cause leaks in the latter one. Figure 4-2 shows the photograph of one unit of the modified static cell cluster used in this project.

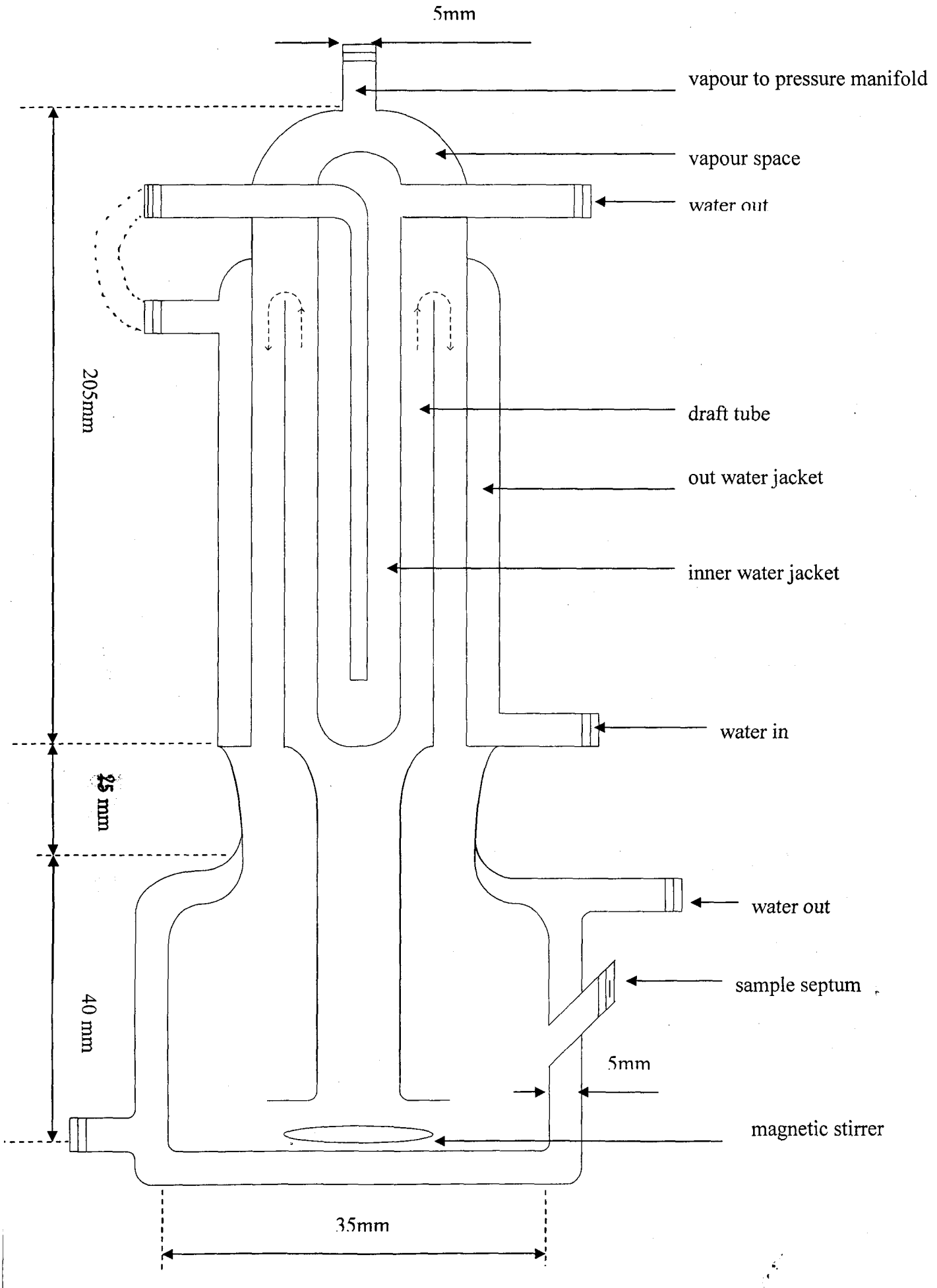

Figure 4-1: The modified static cell with degassing condenser

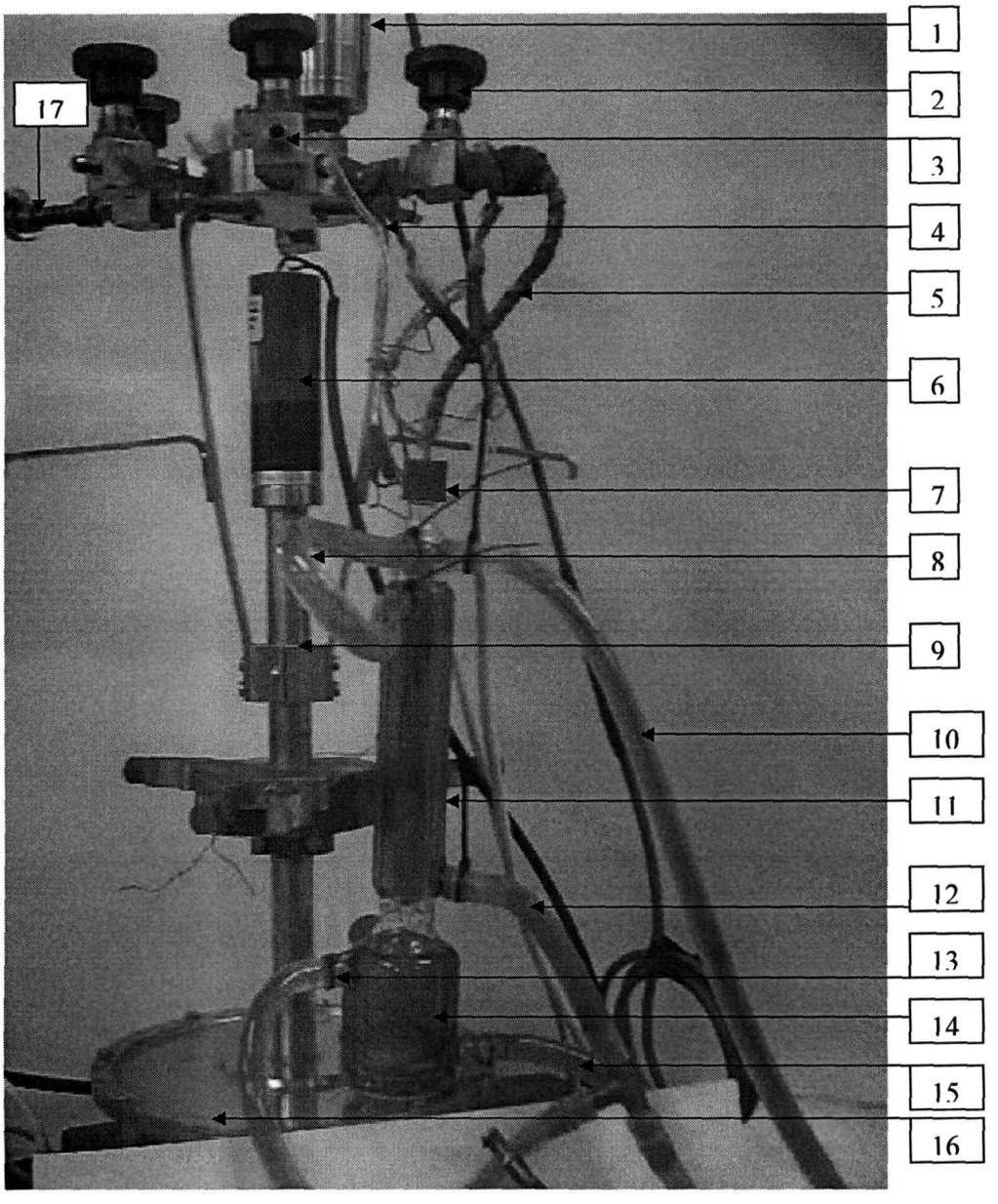

Figure 4-2: Photograph of one unit of the modified static cell cluster (used in this project).

1,pressure transducer; 2,Bellow valve; 3, connection hole to the fitting tube; 4, cartridge wire; 5, fitting tube surrounded by nichrome resistance wire (with insulator); 6, motor; 7, septum (fitted to the top of the condenser); 8, tube connecting the inner water jacket to the outer water jacket; 9, stem; 10, water out (or cooling water); 11, multiwalled-degassing condenser; 12, condenser water in (or cooling water); 13, water jacket out; 14, equilibrium cell + water jacket; 15, water jacket in; 16, cylindrical base; 17, connection to vacuum pump.

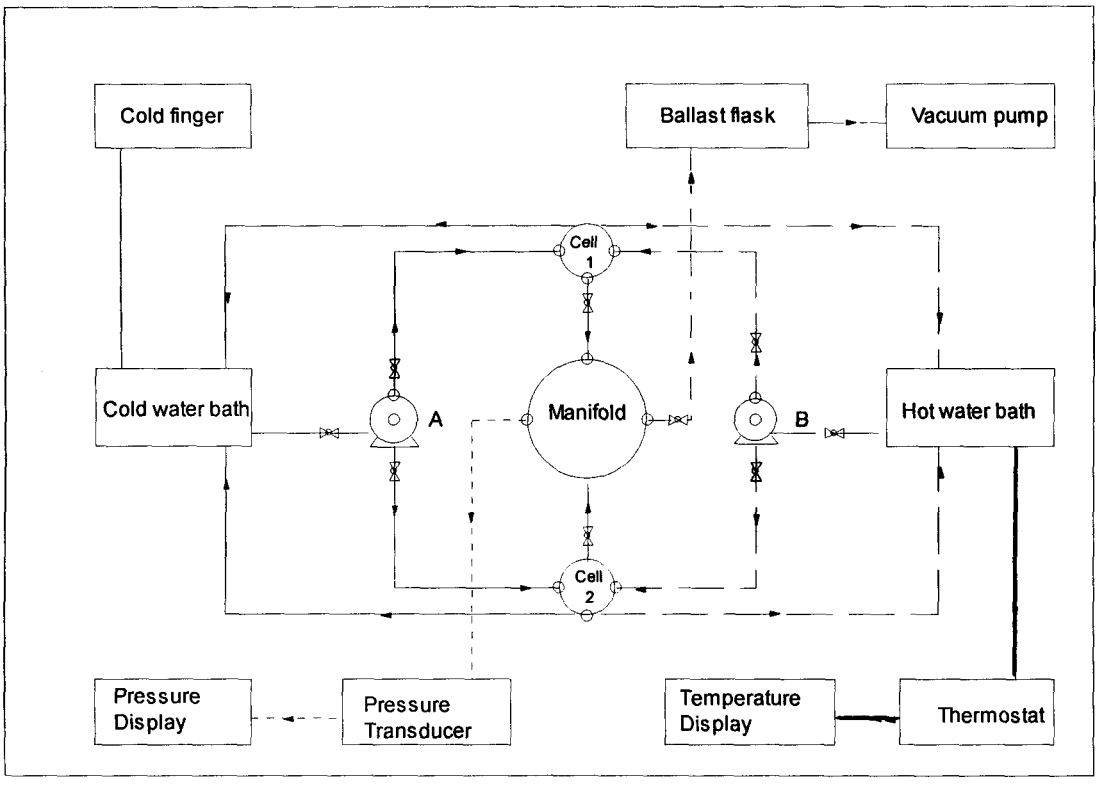

Figure 4-3: Schematic block diagram of equipment (two static cells are shown)

——— Cold water circuit

– – – – – Hot water circuit

–·–·–·– Vacuum

---------- Pressure measurement

▬▬▬ Temperature measurement

4.2 Procedures

Preparation of the equilibrium cell and associated equipment for experimentation is done as following:

The assembly is initially thoroughly degassed by opening the four isolating valves, which are already connected to the manifold and in its turn opened to the vacuum system. The degassing process is started by the circulation by means of a pump of the hot water in equilibrium cell jacket and though the condenser. During this process the fitting tubes and manifold are heated using the procedure described above.

After a degassing time of between 6 to 8 hours, which is usually sufficient (for heavy chemicals like NMP), the isolating valves are closed and the crucial operation of degassing the liquid begins. The refrigerant (ethylene glycol +water at $-14^{\circ}C$) is circulated in the condenser by means of the pump. The hot water continues circulating in the water jacket from the water bath, which is maintained to a constant temperature by the temperature controller.

The cells are loaded by injecting through the septum the required volume of known composition using a syringe. Due to the high vacuum created in the cells, a smooth ebullition of the liquid is observed. The vapour is driven up through the condenser where condensate is returned to the cell whereas non-condensable gases are expelled by opening each cell individually to the vacuum, slowly and briefly half an hour after loading the equilibrium cell. This is done in this way because it helps to eliminate the non-condensable gas only and avoid a loss of more volatile component since the degassing condenser is connected to high vacuum system.

Once the degassing is concluded, the equilibration stage of the experiment starts; the refrigerant in the condenser is replaced by hot water pumped from a water bath. The water jacket and the condenser are maintained at the same temperature by connecting both at same water bath to ensure a uniform temperature distribution which is usually sufficient to bring the mixture to boil due to the sub-atmospheric pressure in cells. The hot water is then pumped from the water bath, which is maintained at constant temperature by a thermostat. By experience, after 15 minutes of hot water circulation, the equilibrium cell reaches the water bath temperature. The isolating valve of a single cell is opened to the manifold and the pressure is checked intermittently to ensure that equilibrium is reached and if consecutive pressure readings show no discrepancy, then the equilibrium is assumed to have been reached. The pressure of each cell is read after evacuating the manifold by opening it to the vacuum system for 15 minutes. The pressures of the remaining cells are then read in turn using the same procedure.

The time taken for equilibration for each cell is 30 minutes due to the draft tube-magnetic stirring assembly. This is very important since the equilibration time for many static cells is much longer as indicated by Maher and Smith (1979).

The final stage of the experimental run is the sampling of the liquid phase using a gas-tight syringe of each cell for gas chromatograph (GC) analysis or for storing it in a sample bottle in the fridge for later analysis. The area ratio method of Raal and Mühlbauer (1997) is used in this analysis and in the GC calibration.

4.3 Calibration of different devices

The pressure and temperature calibration was carried out using ASHCROFT, Model: ST-2A apparatus. This standard apparatus is equipped with pressure and temperature sensors.

The accuracy is determined by each sensor as follows:

Pressure sensor:

Range: 0-30 inches of mercury Vacuum.

Accuracy: 0.05% FS

Temperature sensor:

Range:0-100 °C

Accuracy: 0.05%

4.3.1 Pressure calibration

The pressure display used in this project was calibrated using a pressure standard. The standard pressure and transducer-display were connected to the manifold. High vacuum was created in the manifold and slowly the isolating valve was opened to allow air in. Pressure readings on both sides are registered and various set points are obtained. The relationship between both readings is linear and is represented in Figure 4-4. Pressure display accuracy as it is shown by the manufacturer is 0.15 %

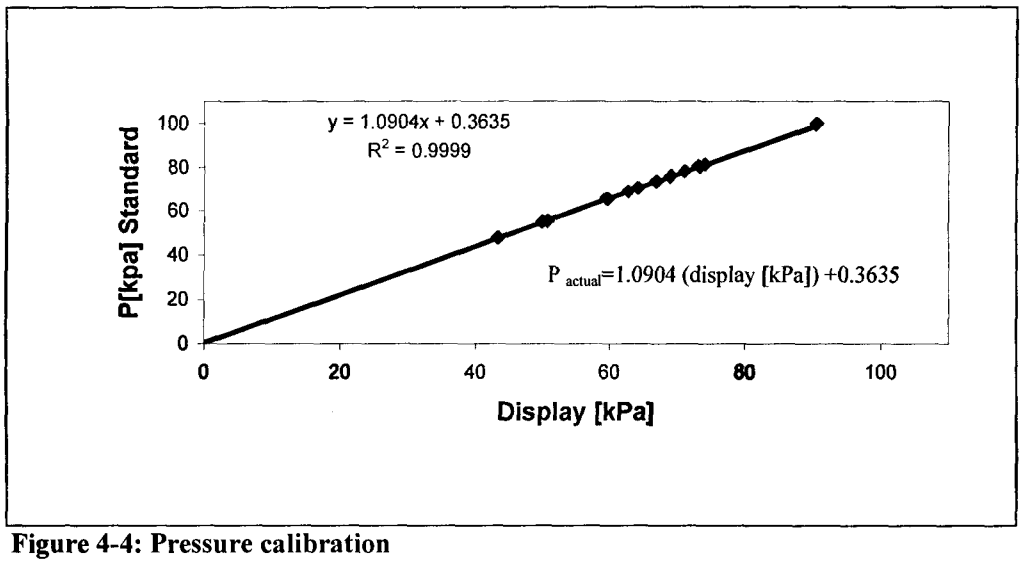

Figure 4-4: Pressure calibration

4.3.2 Temperature calibration

The temperature in this project was measured by means of Pt-100 sensor, which is a preferred device for the temperature range between 0 and 100°C.

Both standard and Eurothem display probes were totally immersed in a water bath, where the temperature is raised for getting various set points. A plot of the two readings shows the linear relationship as in Figure 4-5. Actual temperature is obtained using the linear equation. The accuracy of the temperature measurement is estimated to be 0.13%.

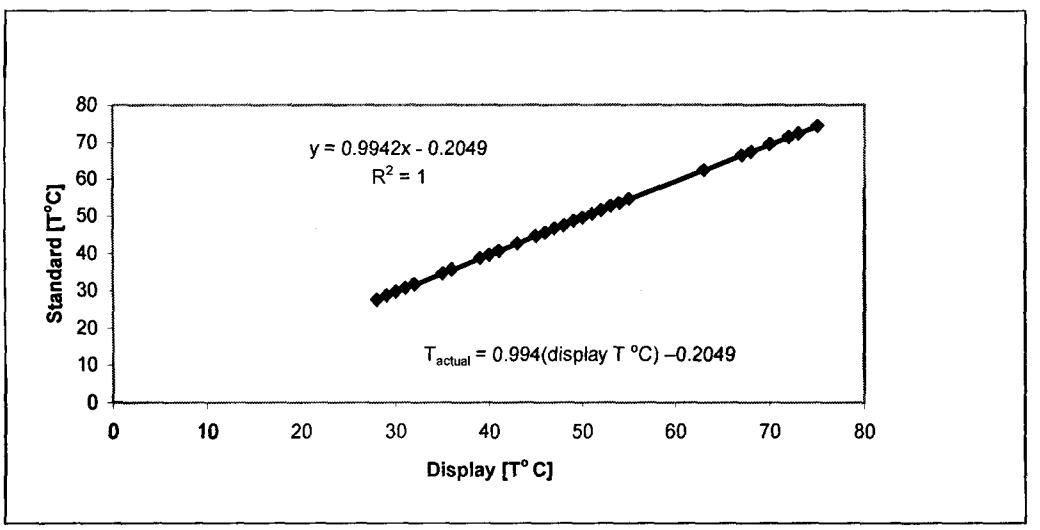

Figure 4-5: Temperature calibration

4.3.3 Gas chromatograph detector calibration

Gas chromatography or GC is a method used for the separation of mixtures of substances into their individual components. The accuracy of gas chromatography is limited by the accuracy of peak area determination and the accuracy of calibration. Detector calibration was conducted for all binary systems used in this project. In general, the number of the moles (n) passing the detector is proportional to the peak area (A), obtained from the electronic integrator. The proportionality constant between the number of the moles and the peak area is defined as the response factor (F):

$$n_1 = A_1 F_1 \tag{4.1}$$

$$\frac{n_1}{n_2} = \left(\frac{A_1}{A_2}\right)\left(\frac{F_1}{F_2}\right) = \frac{x_1}{x_2} \tag{4.2}$$

where x_i is the mole fraction of component i.

In all cases plots of area ratio (A_2/A_1) versus composition ratio (x_2/x_1) were straight lines passing through the origin. The reverse plot of (A_1/A_2) versus (x_1/x_2) is similarly used for the mole fraction ratio (x_1/x_2) in the range from 0 to 1.3. The reason for doing this is for checking the linearity of the thermal conductivity detector (TCD) response factor where the area recorded by the integrator is proportional to the number of moles.

As suggested by Raal and Mühlbauer (1998) in their calibration procedure, the slope of the above plots should be $slope(1) = \frac{1}{slope(2)}$ or ($F_1/F_2 \equiv F_2/F_1$) (as seen in Figures 4-6 and 4-7). This implies that the response factor ratios are exactly constant over the full composition range. Thus, the equation (4.2) can be written as follows:

$$\frac{A_1}{A_2} = \frac{x_1}{x_2} \tag{4.3}$$

This equation (4.3) is used to calculate the equilibrium compositions of the compounds. The detector response factor ratios for each binary system are shown in the chapter of experimental results. In this project, a Chrompak 9000 GC equipped with capillary column (J & W. scientific GS-Q) and a TCD detector was used. The calibration graphs for the other systems are shown in Appendix B.

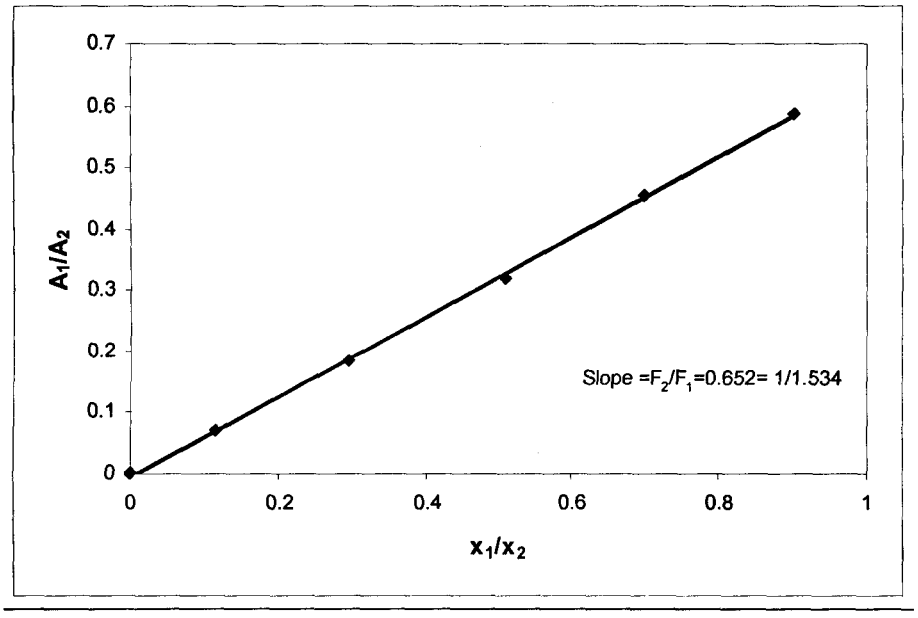

Figure 4-6: Gas chromatograph calibration for cyclohexane (1)/ethanol (2)

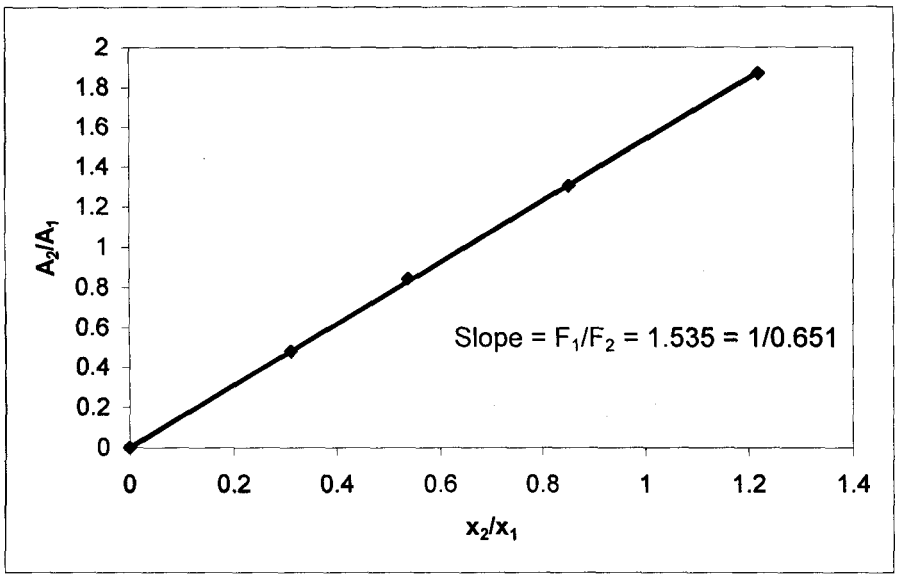

Figure 4-7: Gas chromatograph calibration for cyclohexane (1)/ethanol (2)

Table 4-1: Operation conditions of gas chromatograph

Operating Conditions	Cyclohexane/ Ethanol	Water/ NMP	1-hexene/ NMP
Capillary column	150 °C	230 °C	230 °C
Detector (TCD)	240 °C	240 °C	240 °C
Injector	220 °C	230 °C	230 °C
Gas flow rate	30 ml/min	30 ml/min	30 ml/min

The GC-column temperature was kept constant during analysis of each binary system.

4.4 Characteristics of reagents

The characteristics of the reagents used in this project are summarized in Table 4-2

Table 4 -2: Pure component specification

Chemical	Supplier	Purities	Refractive Index at 298.15 K	
		(mass %)	Experimental	Literature®
Cyclohexane	AnalaR	99.70%	1.4264	1.4266
Ethanol	AnalaR	99.70%	1.3610	1.3612
Water	Distilled	-	1.3328	1.3327
1-Hexene	ACROS	97%	1.3837	1.3836
NMP	MERCK	99.50%	1.4684	1.4683

®Weast&Grasselli(1989)

4.5 Detection of leaks in the manifold and in all assembly connections

A small leak can disturb measurements of vapour pressure, which is a key measurement in this project. All systems were held under high vacuum, which should be maintained for approximately 2 hours after switching off the vacuum pump.

Once a variation of the vacuum was observed, a thorough inspection was made around all valves and connections. For detecting which part of the system caused the leaks, the manifold is isolated first by closing all valves; if the vacuum remains constant it means that the leaks are from the connections of the tubes fitted to the condensers. In this case, the o-rings are replaced to ensure 100% seals. It is very important to ensure that the nuts are not over- tightened because they can be damaged.

CHAPTER 5

EXPERIMENTAL RESULTS

This chapter compiles the experimental results obtained in this work at low pressures using the modified static cell cluster of Raal and Mühlbauer (1998). All data except that of cyclohexane/ ethanol at 323.15 K are new because they were not found in the literature (at 313.15 K, 323.15 K, and 333.15 K). Vapour-liquid equilibrium data were measured for binary mixtures of the following three systems:

- Cyclohexane + ethanol at 35°C, 50°C
- 1-Hexene + N-methyl-2-pyrrolidone at 40°C, 50°C, 60°C
- water + N-methyl-2-pyrrolidone at 40°C, 50°C, 60°C

The accuracy of the data depends on various factors such as the precision in measurements of the temperature, pressure and liquid composition and the purity of the reagents. More explanations about how the measurements were carried out are found in chapter 4.

In this work thorough degassing is essential, and if it is not attained, large errors can result; of course incomplete degassing is one of the possible sources of error. According to Gibbs and Van Ness (1972) no general test for completeness of degassing is available, and one must rely on experience, on repeatability tests, and on comparison of pure component vapour pressures with literature values when they are available.

As vapour pressures are highly temperature dependent, fluctuations in water bath temperature can affect the results. In this project the temperature controller was maintained to within a limit of 0.01 to 0.08°C.

This new design has significantly reduced the experimental time taken for degassing the solutions to half an hour. The normal degassing method (which is applied to various static cells) was lengthy freezing-evacuation-thawing cycles. Seven to nine cycles were required, with about 1 hour per cycle [Maher and Smith (1979)]. And this work the time taken to reach equilibrium in each cell was 30 minutes due to the draft tube- magnetic

stirring assembly. This is very important since the equilibration time for many static cells is much longer as indicated by Maher and Smith (1979).

5.1 Antoine constants Characteristics of reagents

The Antoine constants characteristics of the reagents used in this project are summarized inTable5-1

Table 5-1: Antoine constants at low pressure of the chemicals

System	A*	B*	C*	T_{min}/ °C	T_{max}/ °C
Cyclohexane	6.8515	1206.47	223.136	7	81
Ethanol	8.2042	1642.89	230.341	-57	80
1-hexene	6.8658	1152.97	225.849	-30	87
Water	8.0711	1730.63	233.426	1	100
NMP	7.5483	1979.68	222.162	6	**206**

*Dortmund Data Bank Software [DDB (1998)]

5.2 Vapour pressure measurements of pure compounds

The vapour pressures of cyclohexane and of ethanol were measured so as to test the new apparatus and were compared to those obtained by the Antoine equation. Different sets of points are shown in Figures 5-1 and 5-2 and ΔP errors (Pmeasured-Pcalculated) for both compounds are shown in the tables 5-2 and 5-3. In the Antoine equation the pressure is expressed in mmHg; its constants are listed in Table 5-2 and are from DECHEMA (1999).

$$\text{Ln[P/mmHg]} = A - \frac{B}{T/^{\circ}C + C}$$

5.2.1 Vapour pressure measurement for Cyclohexane

Table 5-2: Measured Vapour pressures for Cyclohexane

T[°C]	$P_{measured}$ [kPa]	$P_{calculated}$ [kPa]	ΔP[kPa]
29.320	15.752	16.108	-0.356
35.380	20.388	20.415	-0.027
41.830	26.485	26.415	0.166
45.500	30.562	30.076	0.485
53.480	41.186	40.707	0.479
58.670	49.559	49.631	-0.071
62.600	56.755	56.731	0.024
65.410	62.385	62.189	0.196

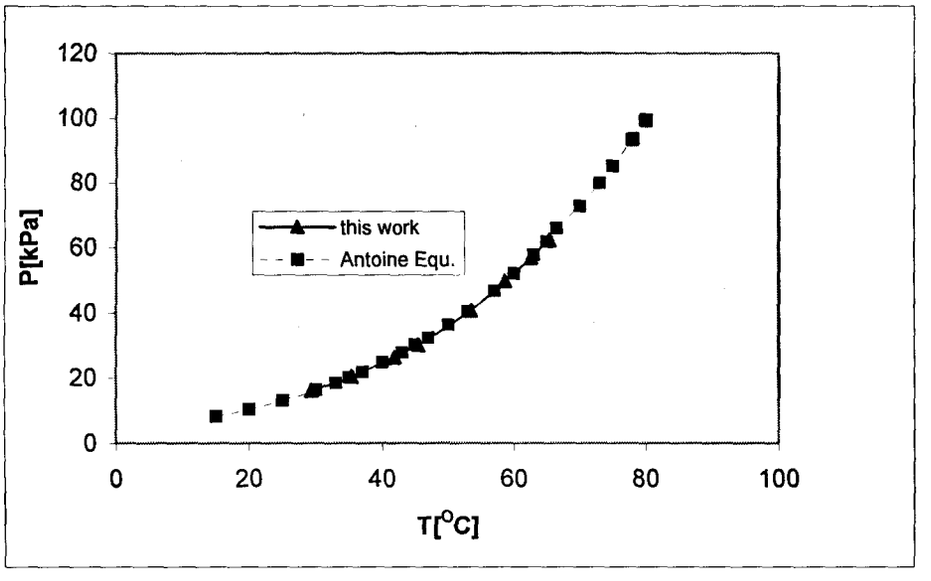

Figure 5-1: Vapour pressure measurement for Cyclohexane

5.2.2 Vapour pressure measurement for Ethanol

Table 5-3: Measured Vapour pressures for Ethanol

T[°C]	$P_{measured}$ [kPa]	$P_{calculated}$ [kPa]	ΔP[kPa]
32.400	12.216	11.914	0.303
36.480	14.820	14.848	-0.028
44.730	22.550	22.716	-0.166
52.263	32.413	32.774	-0.361
55.760	38.155	38.600	-0.445
59.128	44.451	45.019	-0.568
61.347	49.413	49.725	-0.312

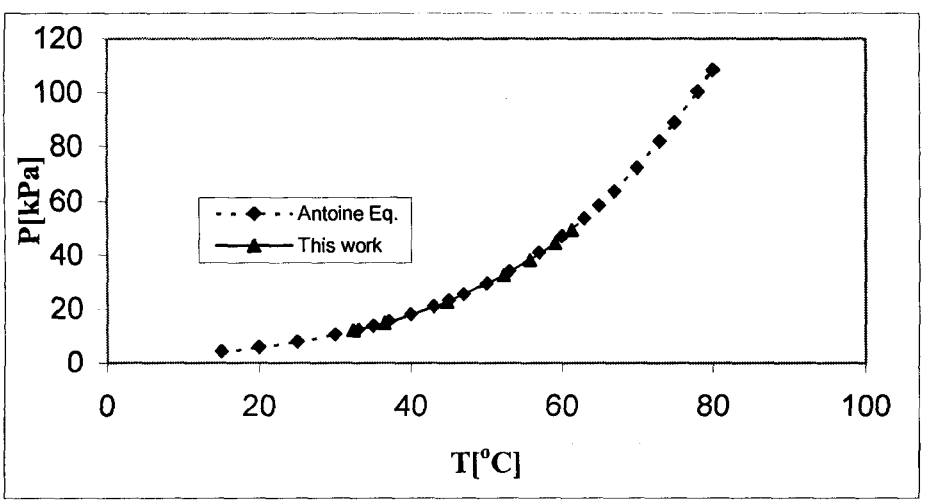

Figure 5-2: Vapour pressure measurement for Ethanol

5.3 VLE measurements for Cyclohexane + Ethanol system

The cyclohexane(1) + ethanol(2) system has been chosen for testing the static cell cluster . This binary mixture has been selected for its following characteristics:

- This system was studied by different authors such us Nagai and Isii (1935), Washburn and Handorf (1935), Joseph et al. (2001) and is available in the literature.
- This mixture is non-ideal and exhibits a wide deviation from Raoult law. Scatchard and Satkiewicz (1964) attributed this deviation to the great difference in polarity and internal pressure of the two compounds.
- Cyclohexane and ethanol are not expensive and are available at high purity (>99%).

Table 5-4:VLE data for Cyclohexane (1) + Ethanol (2) system at 308.15 K

x_1	P[kPa]	x_1	P[kPa]
0.000	14.026	0.469	30.436
0.055	21.517	0.478	30.763
0.123	25.355	0.785	30.294
0.134	26.325	0.825	29.924
0.184	27.612	0.863	29.618
0.206	28.561	0.922	29.520
0.265	29.259	0.974	27.745
0.387	30.330	1.000	20.895

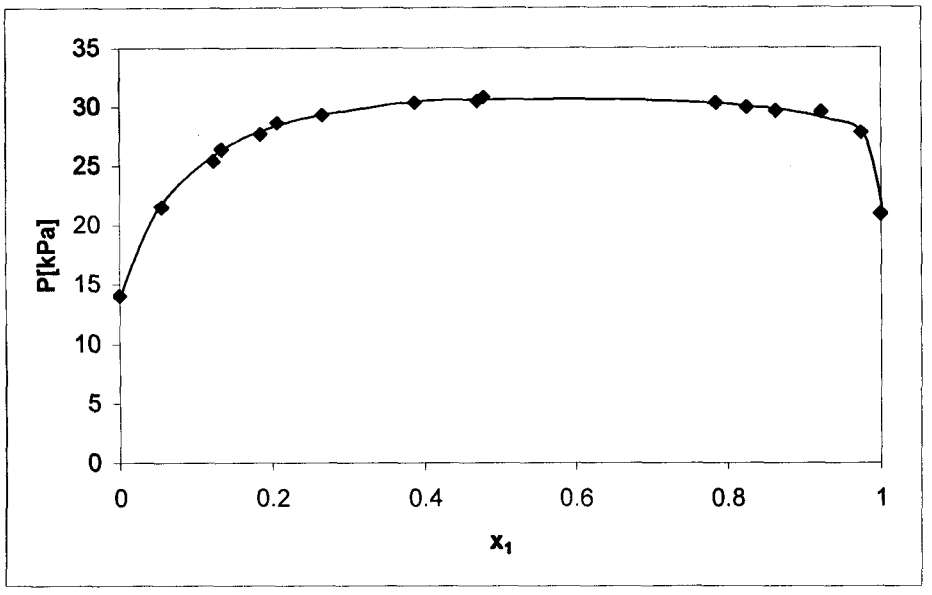

Figure 5-3: Experimental P-x_1 data for Cyclohexane (1) + Ethanol (2) system at 308.15K

Table 5-5: VLE Data for Cyclohexane (1) + Ethanol (2) system at 323.15 K

x_1	P[kPa]	x_1	P[kPa]
0.000	29.520	0.679	57.260
0.047	40.163	0.701	57.294
0.096	45.724	0.813	56.693
0.150	51.034	0.890	54.775
0.199	52.575	0.907	54.120
0.262	54.556	0.927	53.030
0.376	56.410	0.975	48.559
0.501	57.361	1.000	36.310

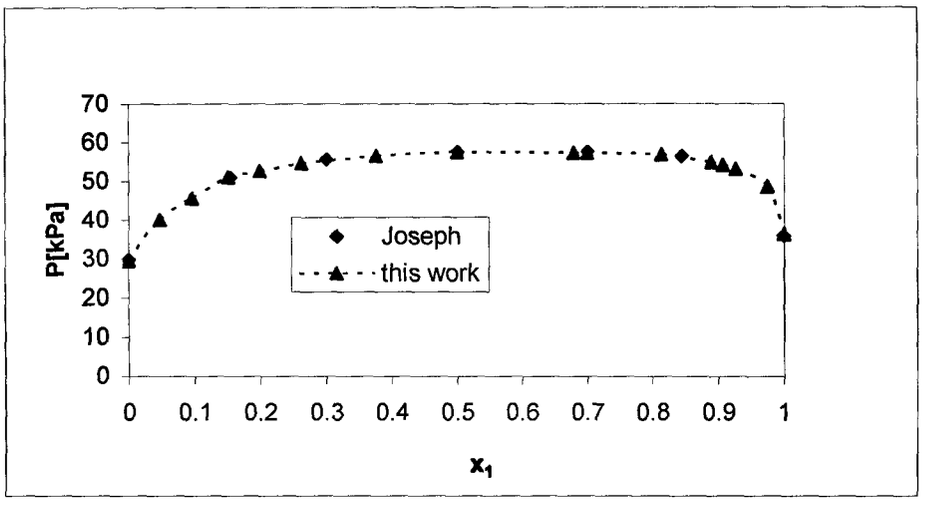

Figure 5-4: Experimental P-x_1 data for Cyclohexane (1) + Ethanol (2) system at 323.15 K

5.4 VLE measurements for 1-Hexene/NMP system

Phase equilibrium data for 1-hexene/NMP have been measured at 313.15 K, 323.15 K and 333.15 K and their data are gathered in Table 5-6 to 5-8, and are illustrated in Figures 5-5 to 5-7 These data are new VLE data.

Table 5-6: VLE Data for 1-Hexene (1) + NMP (2) system at 313.15 K

x_1	P[kPa]	x_1	P[kPa]
0.000	0.132	0.380	38.745
0.039	9.141	0.455	39.149
0.078	17.330	0.518	40.501
0.107	21.211	0.649	41.635
0.142	24.880	0.781	43.371
0.182	28.101	0.860	44.462
0.252	34.307	0.901	44.491
0.310	36.150	0.913	44.686
0.345	38.254	0.945	44.723
		1.000	44.961

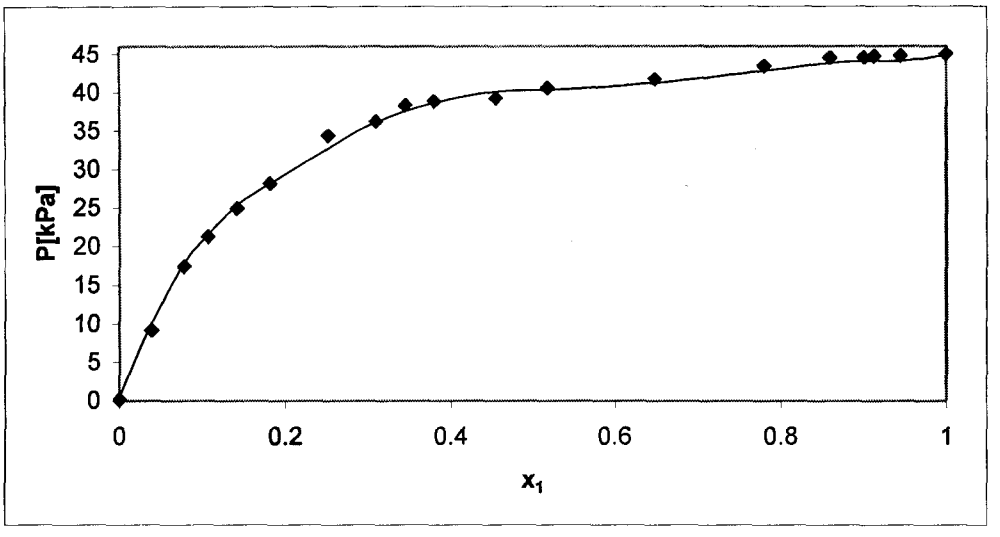

Figure 5-5: Experimental P-x_1 data for 1-Hexene (1) + NMP (2) system at 313.15K

Table 5-7: VLE Data for 1-Hexene (1) + NMP (2) system at 323.15 K

x_1	P[kPa]	x_1	P[kPa]
0.000	0.250	0.379	50.565
0.040	12.445	0.477	53.705
0.080	22.531	0.535	54.501
0.102	27.907	0.692	56.737
0.175	36.859	0.822	60.571
0.209	40.686	0.859	61.529
0.247	45.401	0.890	62.133
0.308	49.049	0.908	62.509
0.350	50.303	0.951	63.068
		1.000	64.574

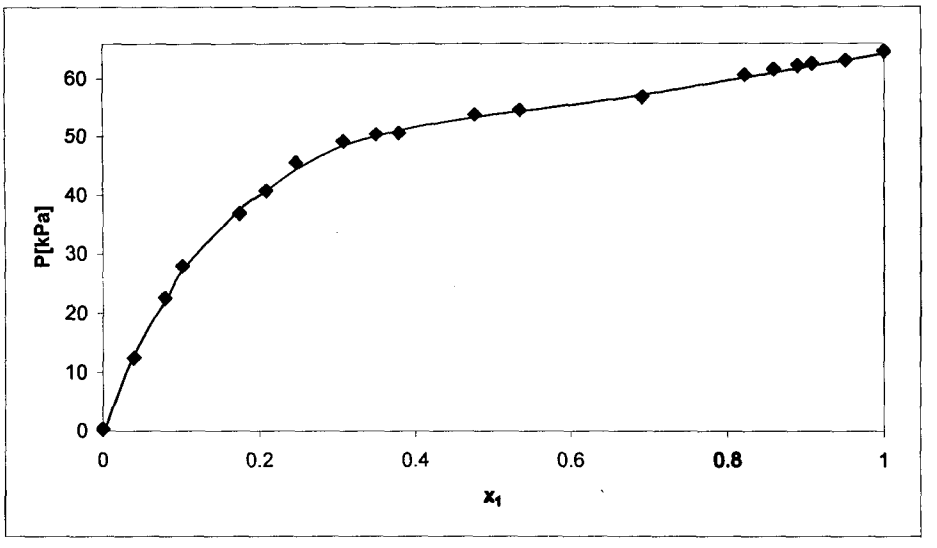

Figure 5-6: Experimental P-x_1 data for 1-Hexene (1) + NMP (2) system at 323.15K

Table 5-8: VLE Data for 1-Hexene (1) + NMP (2) system at 333.15 K

x_1	P[kPa]	x_1	P[kPa]
0.000	0.453	0.374	66.970
0.050	15.629	0.434	69.310
0.069	29.041	0.480	71.893
0.105	36.074	0.572	73.454
0.148	46.359	0.738	78.018
0.210	52.030	0.851	82.972
0.249	59.081	0.895	85.302
0.290	62.900	0.910	85.352
0.353	66.518	0.949	87.857
		1.000	90.473

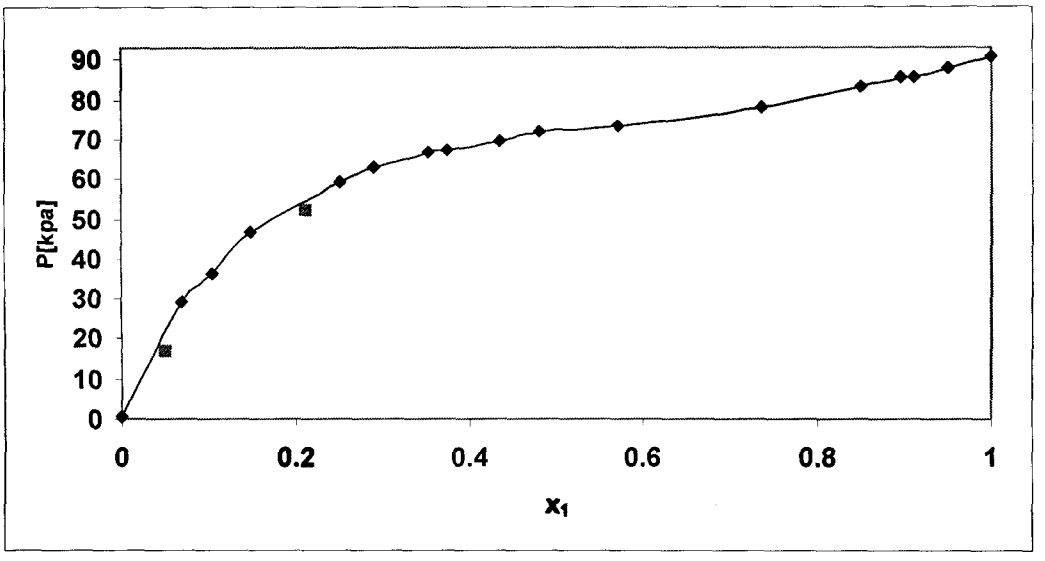

Figure 5-7: Experimental P-x_1 data for 1-Hexene (1) + NMP (2) system at 333.15K

5.5 VLE measurements for Water/NMP system

Water/NMP system was measured at 313.15 K, 323.13 K and 333.15 K. The VLE data are shown in Table 5-9 to 5-11 and are illustrated in Figure 5-8 to 5-10.

Table 5-9: VLE Data for Water (1) + NMP (2) system at 313.15 K

x_1	P[kPa]	x_1	P[kPa]
0.000	0.253	0.493	3.567
0.032	0.312	0.500	3.617
0.061	0.591	0.606	4.355
0.095	0.787	0.650	4.700
0.102	0.838	0.771	5.578
0.118	0.953	0.862	6.237
0.135	1.023	0.906	6.673
0.165	1.194	0.961	7.086
0.180	1.302	0.981	7.298
0.231	1.673	0.991	7.381
		1.000	7.512

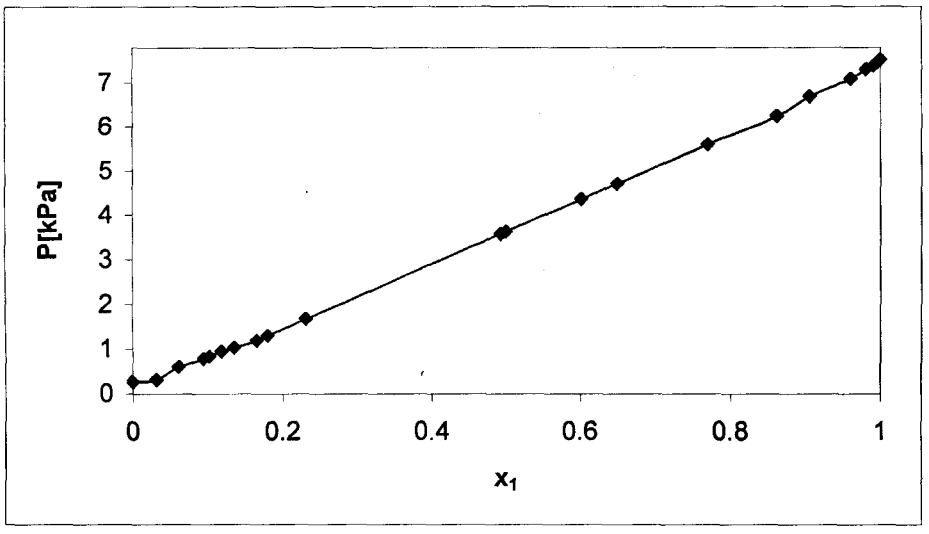

Figure 5-8: Experimental P-x_1 data for Water (1) + NMP (2) system at 313.15K

Table 5-10: VLE Data for Water (1) + NMP (2) system at 323.15 K

x_1	P[kPa]	x_1	P[kPa]
0.000	0.300	0.603	7.231
0.032	0.530	0.715	8.692
0.070	0.950	0.831	10.103
0.087	1.257	0.867	10.540
0.105	1.386	0.920	11.453
0.235	2.857	0.946	11.701
0.301	3.657	0.978	12.112
0.420	5.206	0.987	12.224
0.562	7.023	1.000	12.568

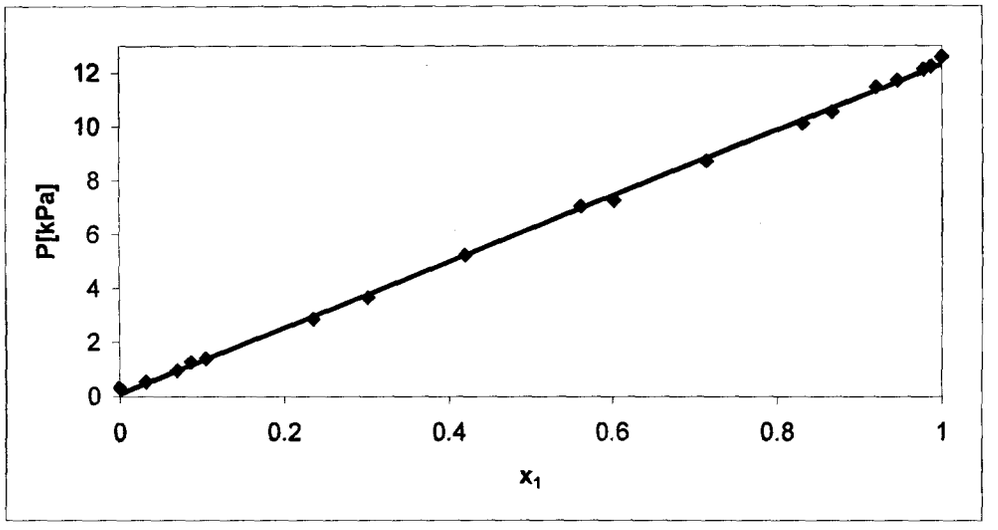

Figure 5-9: Experimental P-x_1 data for Water (1) + NMP (2) system at 323.15K

Table 5-11: VLE Data for Water (1) + NMP (2) system at 333.15 K

x_1	P[kPa]	x_1	P[kPa]
0.000	0.613	0.345	7.331
0.013	0.770	0.464	9.707
0.017	0.836	0.512	10.643
0.200	0.805	0.653	13.105
0.023	0.881	0.762	15.305
0.025	0.954	0.816	16.701
0.041	1.482	0.827	17.102
0.071	2.141	0.858	17.521
0.104	2.812	0.891	18.011
0.124	3.102	0.921	18.509
0.175	4.031	0.932	18.791
0.231	5.201	0.974	19.742
0.278	5.728	1.000	20.551

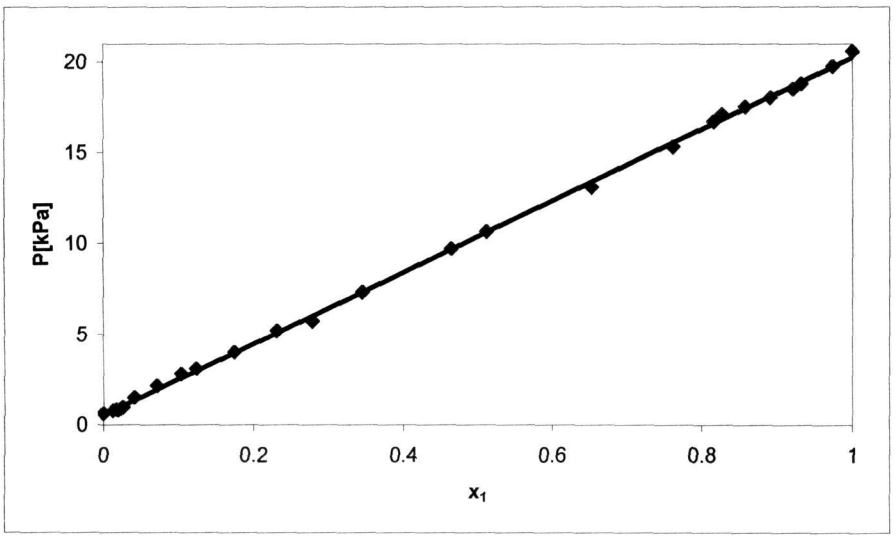

Figure 5-10: Experimental P-x_1 data for Water (1) + NMP (2) system at 333.15K

CHAPTER 6

VLE DATA ANALYSIS

This chapter illustrates the results of different techniques used in modelling the data obtained in this work. The measured data are presented in Chapter 5. This new design has advantages over prior designs:

As described earlier in chapter four, the new design of the static cell with a water jacket around the equilibrium cell for circulation of hot water has significantly reduced the experimental time taken for the degassing to half an hour for each cell. The previous normal degassing method (which was applied to various static cells) was lengthy freezing-evacuation-thawing cycles. Seven to nine cycles were required, with about 1 hour per cycle [Maher and Smith (1979)].

6.1 Sources and purities of chemicals

The reagents used in this project were purchased from the various companies as summarised in Table 4-2. They were used without further purification since a gas chromatographic analysis did not show any significant impurities. In addition a comparison of the measured refractive indexes with the literature values shows only a small discrepancy. These are listed in Table 4-2. The GC calibration plots for cyclohexane and ethanol are presented in Figure 4-6 and Figure 4-7. Other calibration graphs for the rest of the systems are found in Appendix B. The procedure used in this work is that of Raal and Mühlbauer (1998) as summarised in Section 4.3.3 of this thesis. The measurement accuracy was 0.0001.

6.2 Experimental vapour pressures data

Vapour pressure is very useful for separation system design. An important but neglected part of data reduction is the pure component vapour pressures as pointed out by Van Ness et al.(1973). According to Maher & Smith (1979), the vapour pressures of pure components provide information on the purities and the stabilities of chemicals used on the accuracies of the temperatures and pressure measurements. Vapour pressures are very sensitive to the conditions under which they are measured and Van Ness et al.(1973) stressed the importance of including them in the set of measured P-x data. In this work, the Vapour pressures of pure components, cyclohexane and ethanol were measured for testing the assembly. The values obtained were compared to those predicted using the three-constant Antoine equation. The ΔP are shown in Tables 5-2 and 5-3. The average deviation was calculated using the following formula

$$\Delta P_{avg} = \frac{\left|P_{\exp} - P_{lit}\right|}{n_{\exp}} \qquad \textbf{(6.1)}$$

and is 0.225 kPa for cyclohexane and 0.291 kPa for ethanol.

6.3 Data reduction

Data reduction is a process of computing liquid phase activity coefficients from experimental VLE data. An important aspect of data reduction is the fitting of the experimental data to a suitable analytical expression. According to Van Ness et al.(1978), different objective functions give different parameters for a given model unless the VLE data are perfect , hence the problem of choosing which objective function produces the best results exists. The following year they compared all these objective functions and according to the results obtained, the objective function $\sum_i (P_{\exp} - P_{calc})_i^2$ used by Barker (1953) performed the best. The results of data regression are significantly affected by the correlating expression to the extent that certain expressions do not produce thermodynamically consistent results, or sometimes, no solution at all (Van Ness [1970]. Low pressure VLE data are analysed at either constant pressure or constant temperature where a (P_i,x_i,y_i) or (T_i,x_i,y_i) set forms a complete data set. The approach recommended when using P-T-x data is to use the difference in calculated and experimental total pressure (squared). This approach is also favoured when otherwise accurate data are believed to have a high margin of error in the vapour composition. The quality of

pressure fit greatly influences the results of any data reduction procedure. The following expression is therefore utilised for calculating the average error which are listed in Tables 6-14 to 6-16:

$$\Delta P_{avg} = \frac{\left|P_{\exp} - P_{calc}\right|}{n_{\exp}} \qquad (6.2)$$

The minimisation of the pressure residual is the simplest and most direct method (Van Ness [1995]). For carrying out this computing work, the Matlab function called *fminsearch* was employed.

In this work data reduction was studied at constant temperature where the variables in an isothermal set (P_i, x_i) are not independent of each other but related through the Gibbs-Duhem equation. This equation is normally used to test the thermodynamic consistency of the measured data. However, in this project this test was not necessary as the Gibbs-Duhem equation was utilised in Barker's Method for calculation of vapour composition from the total pressure data.

6.3.1 The Barker's Method (1953)

Barker (1953) presented a method based on the assumption that the Gibbs excess free energy can be expressed as a polynomial function of composition. In this method, the total pressure is presented as a function of liquid phase activity coefficients. In turn, activity coefficients are expressed in terms of parameters, which have to be determined by using a technique of successive approximations. For the first approximation it is assumed that the solution behaves like a regular solution. The errors, or residuals, ($\delta P = P_{exp} - P_{calc}$) between the experimentally measured pressures and those calculated are minimised by fitting the data using the method of least squares. Excess chemical potential and activity coefficients are related by the method of Scatchard and Raymond (1952). More details about formulation and computational procedure of Barker's method are presented in Chapter 3.

In addition to Barker's method, the NRTL and Wilson equations were used for fitting the data. In these models, the objective function is based on pressure, and its residuals $(\delta P)^2$ are minimised to obtain the best fit. These equations were chosen because, as discussed in the review chapter, they generally are a superior representation of activity-coefficient behaviour [Walas (1985)]. The vapour phase deviations from ideality were taken in account by using second Virial coefficients from the Hayden and O'Connell correlation.

6.3.2 The Hayden and O'Connell (1975) correlation

This method was used for predicting pure component and cross second Virial coefficients. The literature survey shows that this correlation was chosen by several authors for computation of vapour non-ideality. The critical properties of chemicals used in this project were found in the Dortmund Data Bank (DBR). The methods of Reid et al. (1998) were used for predicting those properties that are not available in the literature. The values used for the pure components and mixtures are summarised in Appendix C. The required input parameters for each compound are: critical temperature, T_c; critical pressure, P_c; dipole moment, μ; acentric factor, ω; association and solvation parameters, η; and mean radius of gyration, R_D.

Acentric factor which is a macroscopic measure of how much the force field around the molecule deviates from spherical symmetry is estimated by using the Pitzer equation:

$$\omega = -\log\left(\frac{P^{sat}}{P_c}\right)_{T/T_c=0.7} - 1.000 \qquad \textbf{(6.3)}$$

The liquid molar volume was estimated from the Rackett (1970) equation

$$V = V_c Z_c^{(1-T_r)0.2857} \qquad \textbf{(6.4)}$$

where Z_c is critical compressibility factor, V_c is critical molar volume, T_r is reduced temperature and is calculated from T/T_c.

The mean radius of gyration can be estimated from Harlacher and Braun (1970) correlation which relate R_D with the parachor, P'

$$P' = 50 + 7.6R_D + 13.75R_D^2 \qquad \textbf{(6.5)}$$

Prausnitz et al. (1980) suggested that the association and solvation parameters should be chosen for a chemically similar system. More details about this correlation are found in Chapter 3. Some of these parameters are listed in Appendix C. The best fit model correlation over all the data is illustrated in this chapter, and the values of the activity model parameters regressed for the systems used in this work are shown in Tables 6-14 to 6-16. Based on the deviation between the measured and calculated pressures, the best model for each isotherm of the three systems was the NRTL model, which fitted the best because it minimised the pressure residuals better. Normally the difference between the NRTL and the Wilson models is small. If the comparison is based on number of adjustable parameters, the Wilson fits better because it uses 2 whereas the NRTL method has 3 adjustable parameters.

6.3.3 Reliability of computational procedure of Barker's Method

The data of Brown (1952), on a system of benzene + n-heptane at 80°C, were used for testing the reliability of the Barker's method program developed in this project. These data were chosen because Barker utilised the same data for describing his method. More explanations about formulation and computational procedure of Barker's method can be found in Chapter 3. The results obtained are compared to those of Barker (1953) and the difference is very small. This shows that the programme written in Matlab language for calculating vapour composition is reliable. The sets of these data are reproduced in Table 6-1 and 6-2.

Table 6-1 Result obtained by Barker (1953) using Brown (1952) data on Benzene + n-Heptane system at 80°C.

x_1	Pexp[kPa]	Pcalc[kPa]	ΔP[kPa]	$y_1$exp	$y_1$calc	Δy_1
0.046	454.620	454.730	-0.110	0.098	0.099	–0.000
0.086	476.250	476.400	-0.150	0.173	0.173	0.000
0.200	534.380	534.070	0.310	0.347	0.346	0.001
0.279	569.490	569.910	-0.420	0.441	0.440	0.000
0.384	613.530	613.090	0.440	0.546	0.545	0.000
0.486	650.160	649.770	0.390	0.630	0.630	0.000
0.582	679.740	680.610	-0.870	0.701	0.701	0.000
0.690	708.780	708.920	-0.140	0.775	0.775	0.001
0.784	729.770	729.560	0.210	0.838	0.836	0.002
0.897	748.460	748.510	-0.050	0.914	0.915	0.000

Table 6-2 Result obtained in this work using Brown (1952) data on benzene (1) + n-heptane system at 80°C

x_1	Pexp[kPa]	Pcalc[kPa]	ΔP[kPa]	$y_1$exp	$y_1$calc	Δy_1
0.046	455.180	454.620	0.563	0.099	0.099	0.000
0.086	475.910	476.250	-0.340	0.173	0.174	-0.001
0.200	533.320	534.380	-1.056	0.347	0.354	-0.007
0.279	569.910	569.490	0.418	0.441	0.452	-0.011
0.384	613.810	613.530	0.276	0.546	0.558	-0.012
0.486	650.590	650.160	0.426	0.630	0.642	-0.011
0.582	680.560	679.740	0.822	0.701	0.711	-0.010
0.690	708.650	708.780	-0.134	0.776	0.780	-0.005
0.784	728.770	729.770	-1.003	0.838	0.840	-0.001
0.897	747.640	748.460	-0.822	0.915	0.917	-0.002

6.3.4 The Cyclohexane/ethanol system

The vapour pressures of two pure single components (cyclohexane and ethanol) were measured and compared to those of the Antoine equation (see section 6.2). A literature survey showed that the binary system of both components has been studied by different authors at different temperatures such as Nagai and Isii (1935), Joseph et al. (2001). This binary mixture exhibits a wide deviation from Raoult's law. Scatchard and Satkiewicz (1964) attributed this deviation to the great difference in polarity and internal pressure of the two components. The vapour pressure data at various temperatures and deviations of the measured pressures from those predicted for this system are included in Tables 6-3 and 6-4. The activity coefficients model parameters for this mixture are summarised in Table 6-14. The comparison of the measured data with the literature shows good agreement (Figure 5-4). This result indicates that the computational procedure of the Barker's method is reliable.

This binary system has been selected as a test system to ensure that the static-cell cluster was operating correctly and the experimental procedure was accurate. The following characteristics are the basis of its choice:

- As mentioned above the cyclohexane/ethanol system was studied by different authors and is available in the literature.
- It is a non-ideal mixture and these two components are not expensive and are available at high purity (>99%).

Table 6-3 Measured P-x_1 and y_1 calculated data for cyclohexane (1) +ethanol (2) system at 308.15 K

x_1	Pcalc[kPa]	Pexp[kPa]	ΔP[kPa]	$y_1$calc
0.000	15.075	14.026	-1.049	0.000
0.055	20.425	21.517	1.092	0.310
0.123	25.096	25.355	0.259	0.478
0.134	25.679	26.325	0.646	0.495
0.184	27.827	27.612	-0.215	0.554
0.206	28.541	28.561	0.020	0.573
0.265	29.894	29.259	-0.635	0.608
0.387	30.938	30.330	-0.608	0.637
0.469	30.967	30.436	-0.531	0.639
0.478	30.957	30.763	-0.194	0.639
0.785	30.891	30.294	-0.597	0.612
0.825	30.696	29.924	-0.772	0.620
0.863	30.208	29.618	-0.590	0.636
0.922	28.289	29.520	1.231	0.698
0.974	24.300	27.745	3.445	0.841
1.000	20.895	20.895	0.000	1.000

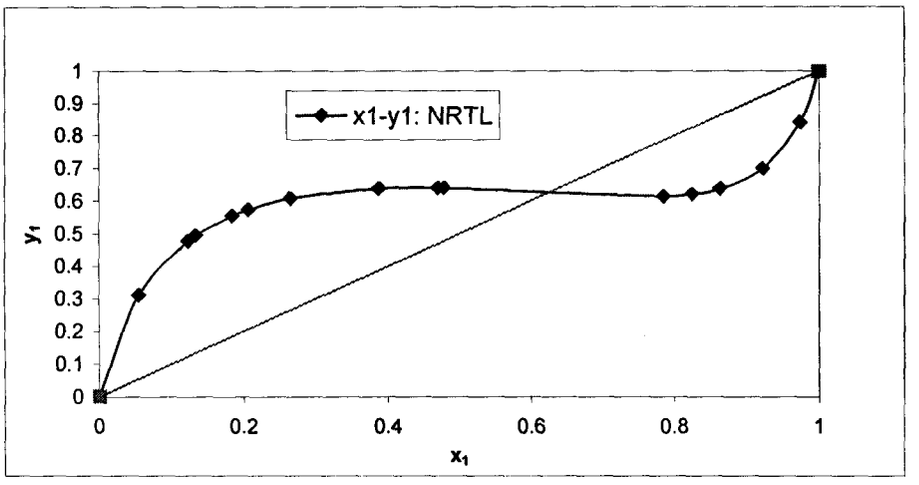

Figure 6-1 Measured x_1 and calculated y_1 diagram for cyclohexane (1)/ ethanol (2) system at 308.15 K (new data at this isotherm) fitted with NRTL

Table 6-4 Measured P-x_1 and calculated y_1 data for the system cyclohexane (1) + ethanol (2) at 323.15 K.

x_1	Pcalc[kPa]	Pexp[kPa]	ΔP[kPa]	$y_1$calc
0.000	31.445	29.520	-1.924	0.000
0.047	38.668	40.163	1.495	0.230
0.096	44.723	45.724	1.001	0.369
0.150	49.714	51.034	1.320	0.462
0.199	52.894	52.575	-0.318	0.514
0.262	55.634	54.556	-1.077	0.559
0.376	57.646	56.410	-1.236	0.594
0.500	57.816	57.361	-0.454	0.599
0.679	57.907	57.260	-0.646	0.577
0.700	57.982	57.294	-0.687	0.574
0.813	57.882	56.693	-1.189	0.574
0.890	55.339	54.775	-0.564	0.613
0.907	54.011	54.120	0.109	0.633
0.927	52.020	53.030	1.010	0.664
0.975	46.607	48.559	1.952	0.817
1.000	36.310	36.310	0.000	1.000

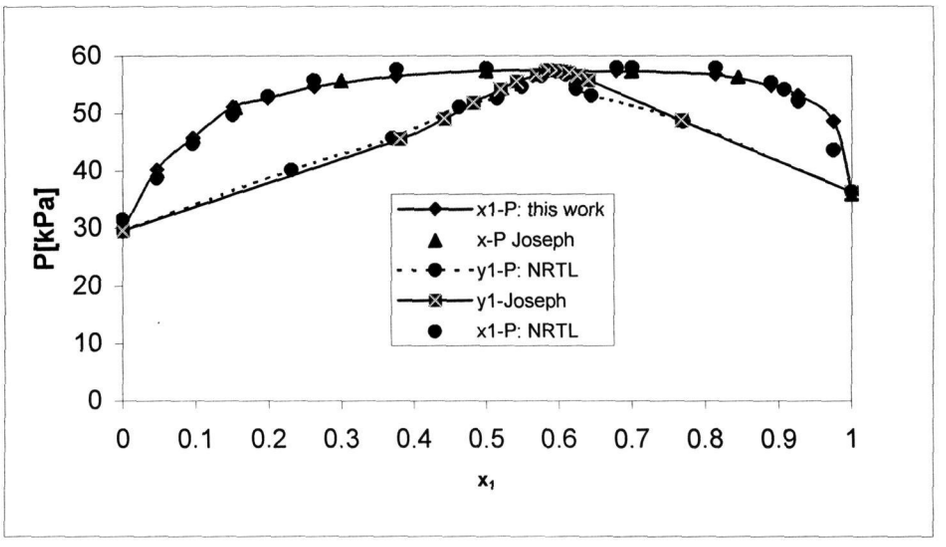

Figure 6-2 Measured P-x_1 and y_1 calculated data compared to literature [Joseph et al. (2001)] for the system cyclohexane (1) +ethanol (2) at T=323.15K.

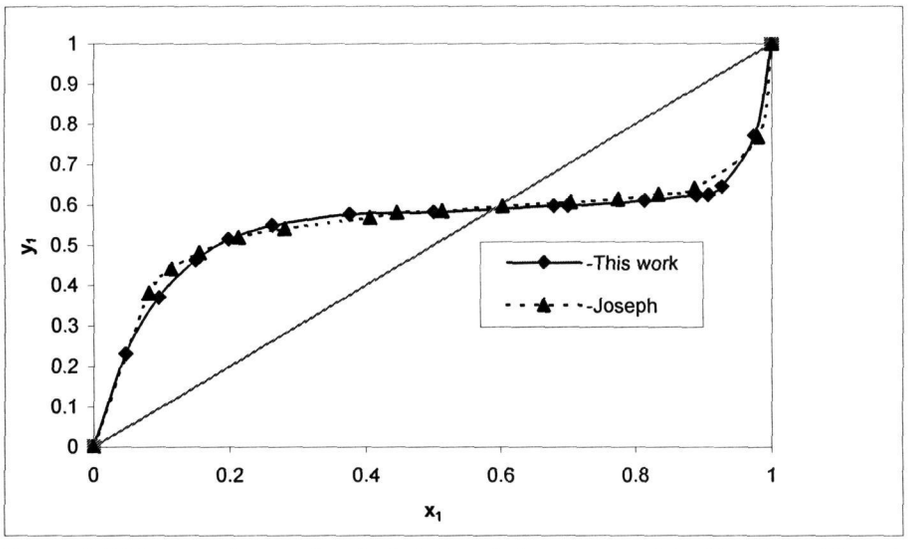

Figure 6-3 Measured x_1 and calculated y_1 data compared to literature (Joseph et al. (2001)) for the system cyclohexane (1) + ethanol (2) at T=323.15K.

Table 6-5 Calculated activity coefficients for cyclohexane (1)/ ethanol (2) system at 308.15 K, 323.15K using NRTL model.

T=308.15 K			T=323.15 K		
x_1	γ_1	γ_2	x_1	γ_1	γ_2
0.000			0.000		
0.310	5.513	1.058	0.047	5.221	1.051
0.477	4.654	1.056	0.096	4.697	1.047
0.495	4.527	1.058	0.151	4.165	1.053
0.554	3.993	1.073	0.199	3.733	1.070
0.572	3.778	1.083	0.262	3.222	1.110
0.607	3.260	1.125	0.376	2.481	1.247
0.637	2.422	1.288	0.500	1.885	1.543
0.639	2.006	1.481	0.679	1.339	2.539
0.638	1.967	1.508	0.700	1.294	2.737
0.612	1.145	3.924	0.813	1.112	4.402
0.619	1.096	4.700	0.890	1.039	6.483
0.636	1.059	5.654	0.907	1.028	7.149
0.697	1.019	7.739	0.927	1.017	7.994
0.841	1.002	10.501	0.975	1.002	10.724
1.000				1.000	

6.3.5 The 1-hexene/NMP system

The 1-hexene + NMP system has been measured at three temperatures (313.15 K, 323.15 K and 333.15 K) and experimental results are summarised in Tables 6-6 to 6-8 together with pressure deviations. Activity coefficients are illustrated in Table 6-9. This system is new, since no reliable values were found at the temperatures mentioned above. The literature survey shows that this mixture was previously studied at 90°C and 140°C by Fischer and Gmehling (1996). The experimental P, x values are compared with those obtained from the NRTL correlation in Figures 6-4 to 6-9 and the deviations are small. The experimental results of this mixture show a strong positive deviation from Raoult's law. No azeotrope was observed since the vapour pressure ratio is quite large. In all three systems studied, the non-ideal behaviour of vapour phase was taken into account and was described using the Hayden and O'Connell (1975) correlation (see section 6.2.2). Some of the parameters used in this method are shown in Appendix C.1 and C.3. The (x_1, y_1) diagrams in Figures 6-4, 6-6 and 6-8 illustrate that 1-hexene is more volatile than NMP because their representative curves are located far from 45^0 diagonal and can be easily separated by distillation. The reduction of experimental data was carried out utilising Barker's Method, NRTL and Wilson. The activity coefficients model parameters for 1-hexene + NMP are presented in Table 6-15. Infinite dilution activity coefficients for this

system are calculated using Ellis and Johan (1962) as modified by Maher and Smith (1979). This method is described in section 6.3 and the obtained γ_i^{∞} values are listed in Table 6-18 and are plotted with other γ_i in Figures 6-23 to 6-25. Based on the mean deviations between the experimental and calculated pressures in the determination of the system optimum parameters using above models, the NRTL model comes as the best fit for each of the 1-hexene/NMP system isotherms.

Table 6-6 Measured P-x_1 and calculated y_1 data for the system 1-hexene (1) + NMP (2) at 313.15 K.

x_1	Pcalc[kPa]	Pexp[kPa]	ΔP[kPa]	$y_1$calc
0.000	0.697	0.132	-0.565	0.000
0.039	10.262	9.141	-1.121	0.951
0.078	17.160	17.330	0.170	0.978
0.107	21.118	21.211	0.092	0.985
0.142	24.965	24.880	-0.085	0.990
0.182	28.470	28.101	-0.368	0.993
0.252	33.087	34.307	1.220	0.995
0.310	35.931	36.150	0.218	0.996
0.345	37.326	38.254	0.928	0.997
0.380	38.512	38.745	0.233	0.997
0.455	40.417	39.149	-1.267	0.997
0.518	41.408	40.501	-0.906	0.997
0.649	42.032	41.635	-0.397	0.997
0.781	41.716	43.371	1.654	0.997
0.860	41.855	44.702	2.847	0.998
0.901	42.256	44.491	2.234	0.998
0.913	42.436	44.686	2.249	0.998
0.945	43.089	44.723	1.634	0.999
1.000	44.961	44.961	0.000	1.000

Table 6-7 Measured P-x_1 and y_1 calculated data for the system 1-hexene (1) + NMP (2) at 323.15 K.

x_1	Pcalc[kPa]	Pexp[kPa]	ΔP[kPa]	y1calc
0.000	0.783	0.250	-0.533	0.000
0.040	13.621	12.445	-1.175	0.956
0.080	23.036	22.531	-0.505	0.979
0.102	27.173	27.907	0.734	0.984
0.175	37.352	36.859	-0.492	0.991
0.209	40.798	40.686	-0.111	0.993
0.247	43.985	45.404	1.418	0.994
0.308	48.007	49.049	1.041	0.995
0.350	50.176	50.303	0.126	0.996
0.379	51.442	50.565	-0.877	0.996
0.477	54.590	53.705	-0.885	0.997
0.535	55.787	54.501	-1.286	0.997
0.692	57.480	56.737	-0.742	0.997
0.822	58.661	61.295	2.633	0.997
0.859	59.274	61.829	2.555	0.997
0.890	59.969	62.133	2.163	0.998
0.908	60.469	62.509	2.040	0.998
0.951	62.018	63.068	1.050	0.999
1.000	64.574	64.674	0.100	1.000

Table 6-8 Measured P-x_1 and y_1 calculated data for 1-hexene (1) + NMP (2) system at 333.15K.

x_1	Pcalc[kPa]	Pexp[kPa]	ΔP[kPa]	y1calc
0.000	0.850	0.453	-0.397	0.000
0.050	20.690	17.629	-3.061	0.965
0.069	26.550	28.041	1.491	0.974
0.105	35.949	36.076	0.126	0.982
0.148	44.709	46.359	1.650	0.987
0.210	53.953	52.030	-1.923	0.991
0.249	58.298	59.081	0.782	0.992
0.290	61.972	62.900	0.928	0.993
0.353	66.281	66.518	0.236	0.994
0.374	67.438	66.970	-0.467	0.994
0.434	70.157	69.310	-0.847	0.994
0.480	71.782	71.893	0.110	0.994
0.572	74.246	73.454	-0.791	0.995
0.738	77.817	78.018	0.201	0.995
0.851	81.283	82.972	1.688	0.996
0.895	83.260	85.302	2.042	0.997
0.910	84.050	85.352	1.302	0.997
0.949	86.441	87.857	1.416	0.998
1.000	90.473	90.473	0.000	1.000

Table 6-9 Calculated activity coefficients for 1-hexene (1)/ NMP (2) system at 313.15 K, 323.15 K, 333.15 K using NRTL model.

T=313.15 K			T=323.15 K			T=333.15 K		
x_1	γ_1	γ_2	x_1	γ_1	γ_2	x_1	γ_1	γ_2
0.000				0.000			0.000	0.000
0.039	5.690	3.861	0.040	4.697	1.002	0.050	4.553	1.621
0.078	4.871	2.965	0.080	4.140	1.010	0.069	4.278	1.548
0.107	4.391	2.507	0.102	3.871	1.017	0.105	3.822	1.436
0.142	3.920	2.110	0.175	3.134	1.052	0.148	3.373	1.341
0.182	3.490	1.800	0.209	2.857	1.076	0.210	2.865	1.260
0.252	2.928	1.486	0.247	2.589	1.107	0.249	2.608	1.236
0.310	2.583	1.364	0.308	2.233	1.172	0.290	2.378	1.230
0.345	2.409	1.332	0.350	2.031	1.228	0.353	2.087	1.256
0.380	2.256	1.327	0.379	1.910	1.272	0.374	2.004	1.273
0.455	1.976	1.394	0.477	1.582	1.465	0.434	1.794	1.349
0.518	1.777	1.533	0.535	1.437	1.616	0.480	1.659	1.435
0.649	1.439	2.134	0.692	1.172	2.233	0.572	1.439	1.687
0.781	1.187	3.489	0.822	1.054	3.107	0.738	1.167	2.551
0.860	1.082	5.039	0.859	1.033	3.449	0.851	1.056	3.678
0.901	1.042	6.241	0.890	1.020	3.777	0.895	1.029	4.322
0.913	1.033	6.665	0.908	1.014	3.988	0.910	1.022	4.579
0.945	1.013	8.001	0.951	1.004	4.560	0.949	1.007	5.352
1.000				1.000			1.000	0.000

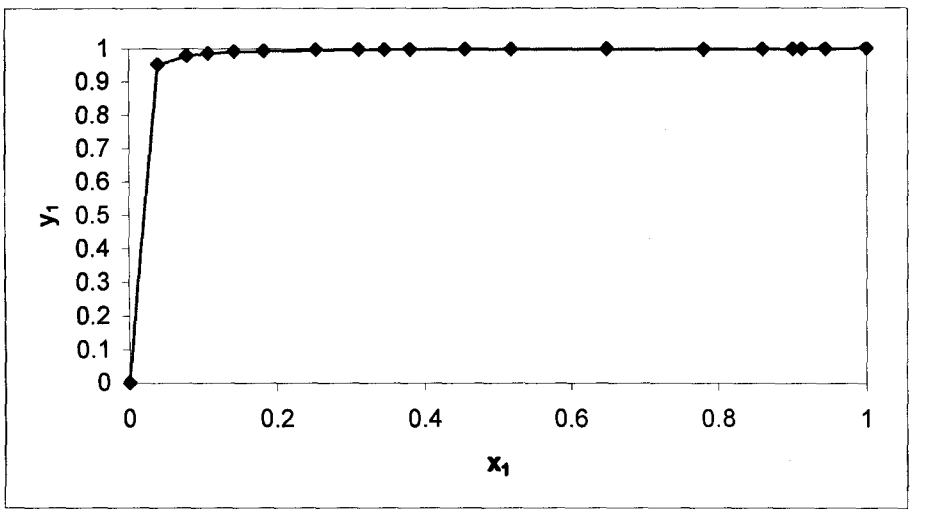

Figure 6-4 Measured x_1 and calculated y_1 diagram for 1-hexene (1)/ NMP (2) system at 313.15 K.

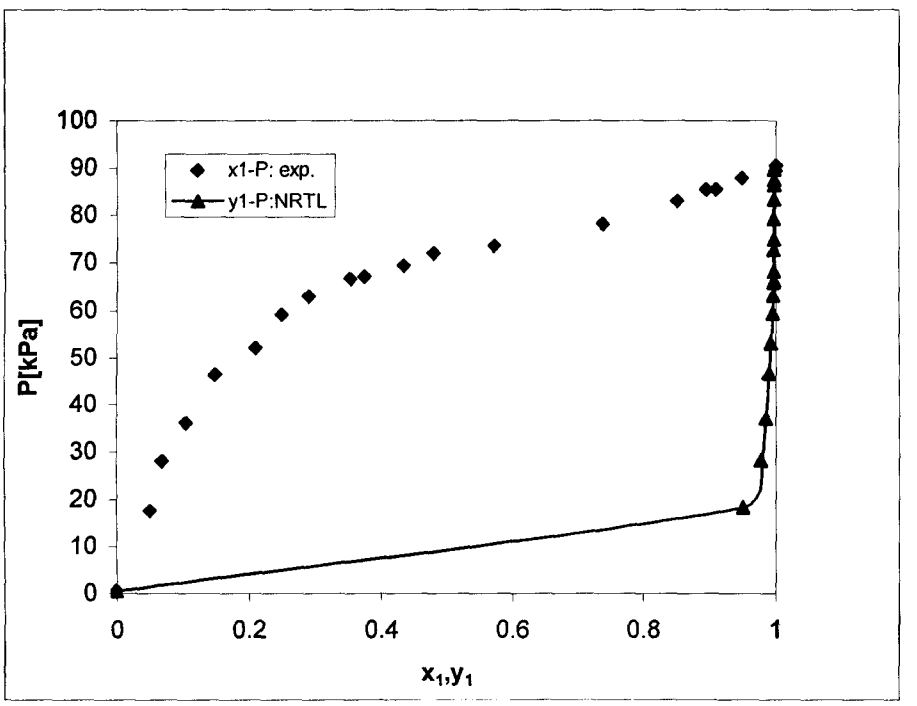

Figure 6-5 Measured P-x_1 and calculated y_1 diagram for 1-hexene (1)/ NMP (2) system at 313.15 K.

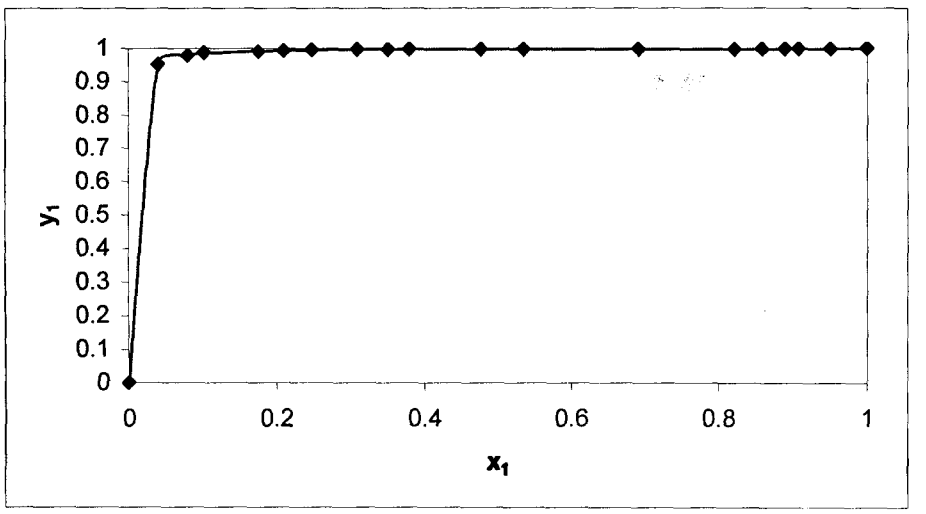

Figure 6-6 Measured x_1 and calculated y_1 diagram for 1-hexene (1)/ NMP (2) system at 323.15 K.

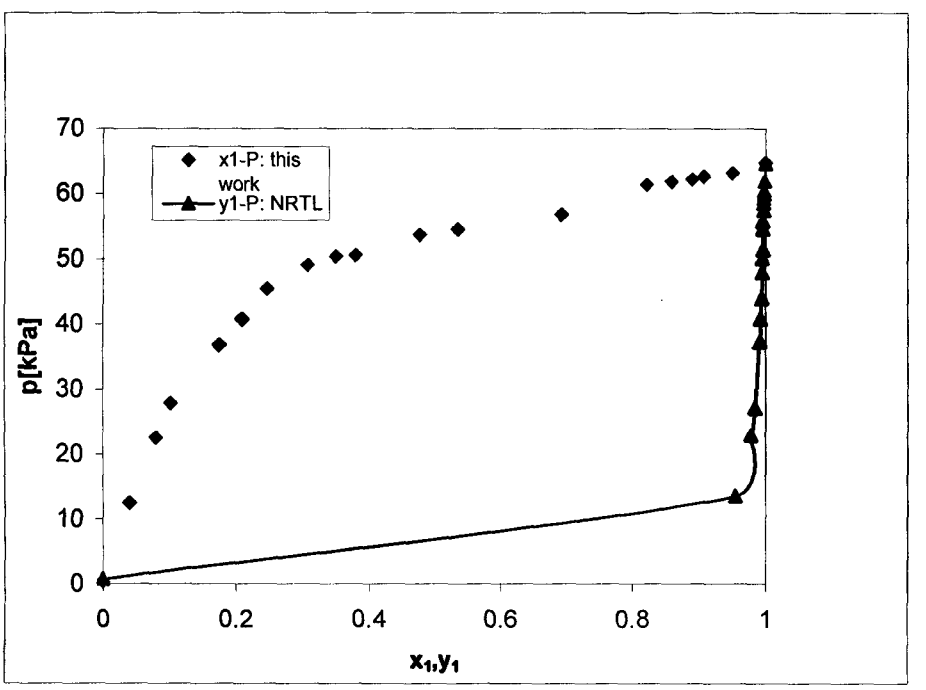

Figure 6-7 Measured P-x_1 and calculated y_1 diagram for 1-hexene (1)/ NMP (2) system at 323.15 K.

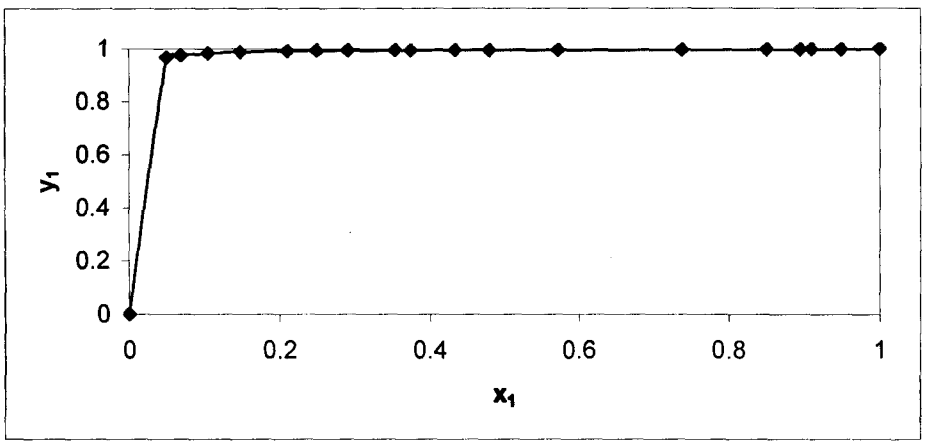

Figure 6-8 Measured x_1 and calculated y_1 diagram for 1-hexene (1)/ NMP (2) system at 333.15 K.

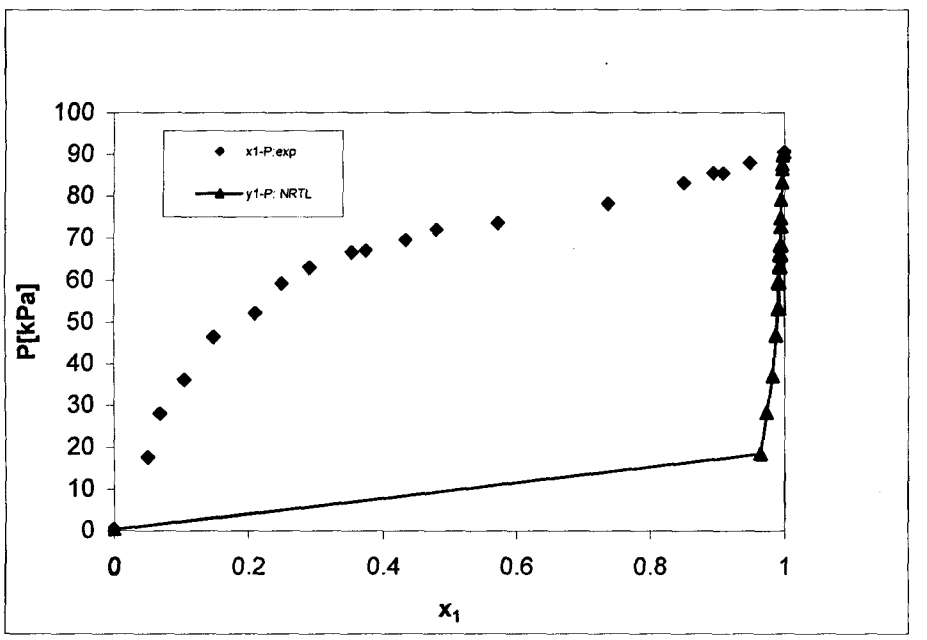

Figure 6-9 Measured P-x_1 and calculated y_1 diagram for 1-hexene (1)/ NMP (2) system at 333.15 K.

6.3.6 The Water/NMP system

In this project, the binary mixture of water and NMP has been studied experimentally by measuring isothermal P-x at 313.15 K, 323.15 K and 333.15 K. This system has been described by other authors such Fisher and Gmehling (1996) but no reliable data was found on the above mentioned isotherms. The water used in this experiment was distilled and its refractive index was measured to ensure that it does not contain impurities (Table 4-2). As was seen before, the principle of the VLE measurement by the static method is to determine the system pressure as a function of liquid composition. The composition of liquid phase at equilibrium was sampled through septa and analysed in a GC. In addition to Barker's method being utilised to calculate vapour phase composition, the NRTL and Wilson models were investigated. The non-ideality of system was analysed by using the Hayden and O'Connell correlation where the cross-coefficient B_{12} for this binary system and the second virial coefficient for each of the pure components were obtained. These values are tabled in Appendix C.4. Then the objective function based on pressure [F=$\sum(\delta P)^2$] was optimised. In Tables 6-10 to 6-12 the experimental pressures P as a function of liquid composition x are listed and are presented in graphical form with the regressed values from the NRTL in Figures 6-10 to 6-15. It can be seen from P-x, y data that this system shows a deviation from Raoult's law and no azeotrope was observed since the vapour pressure ratio is quite large. The (x_1, y_1) plots in Figures 6-10, 6-12 and 6-14 show that these diagrams are located far from the 45^0 diagonal which confirm that one component (water) has a much greater tendency to vaporise than the other (NMP). The activity coefficients model parameters for the water +NMP system are reported in Table 6-16. Activity coefficients are shown in Table 6-13 and are plotted in Figures 6-26 to 6-28. The calculated infinite dilution activity coefficients are not represented on same graph with the former because they are very high and the graph becomes ugly. As shown in Figures 6-11, 6-13 and 6-15, the deviations between experimental and calculated data are large, but the NRTL method minimized the pressure residuals better than Wilson; hence it comes as the best fit for this system. Renon et al. (1971), provided a method which helps to look at the consistency of the NRTL parameters generated at different temperatures; these parameters are linear function of the temperature (Figures 6-16 to 6-18).

Table 6-10 Measured P-x_1 and y_1 calculated data for the system water (1)/NMP (2) at 313.15 K.

x_1	Pcalc[kPa]	Pexp[kPa]	ΔP[kPa]	$y_1$calc
0.000	0.253	0.147	0.105	0.000
0.032	0.312	0.347	-0.035	0.552
0.061	0.591	0.536	0.054	0.699
0.095	0.787	0.763	0.023	0.781
0.102	0.838	0.810	0.027	0.793
0.118	0.953	0.919	0.033	0.816
0.135	1.023	1.036	-0.013	0.835
0.165	1.193	1.244	-0.051	0.861
0.180	1.302	1.348	-0.046	0.872
0.231	1.673	1.703	-0.030	0.899
0.493	3.567	3.526	0.040	0.965
0.500	3.617	3.575	0.041	0.966
0.602	4.355	4.317	0.037	0.978
0.650	4.700	4.681	0.018	0.983
0.771	5.578	5.646	-0.068	0.991
0.862	6.237	6.404	-0.167	0.996
0.906	6.673	6.770	-0.097	0.997
0.961	7.086	7.215	-0.128	0.999
0.981	7.298	7.369	-0.071	1.000
0.991	7.381	7.445	-0.064	1.000
1.000	7.512	7.512	0.000	1.000

Table 6-11 Measured P-x_1 and y_1 calculated data for the system water (1)/NMP (2) at 323.15 K

x_1	Pcalc[kPa]	Pexp[kPa]	ΔP[kPa]	$y_1$calc
0.000	0.303	0.155	0.147	0.000
0.032	0.531	0.509	0.021	0.673
0.070	0.952	0.951	0.001	0.812
0.087	1.257	1.155	0.102	0.841
0.105	1.386	1.372	0.013	0.863
0.235	2.857	2.961	-0.104	0.932
0.301	3.657	3.753	-0.096	0.948
0.420	5.206	5.139	0.067	0.966
0.562	7.023	6.789	0.233	0.981
0.603	7.231	7.282	-0.051	0.984
0.715	8.692	8.696	-0.004	0.991
0.831	10.103	10.273	-0.169	0.996
0.867	10.540	10.776	-0.235	0.997
0.920	11.453	11.513	-0.060	0.998
0.946	11.701	11.867	-0.166	0.999
0.978	12.112	12.290	-0.177	1.000
0.987	12.224	12.405	-0.180	1.000
1.000	12.568	12.568	0.000	1.000

Table 6 12 Measured P-x_1 and y_1 calculated data for the system water (1) + NMP (2) at 333.15 K.

x_1	Pcalc[kPa]	Pexp[kPa]	ΔP[kPa]	$y_1$calc
0.000	0.470	0.463	-0.007	0.000
0.013	0.753	0.770	0.016	0.372
0.017	0.839	0.836	-0.003	0.436
0.020	0.904	0.805	-0.099	0.476
0.022	0.947	0.881	-0.066	0.500
0.025	1.012	0.954	-0.058	0.531
0.041	1.355	1.482	0.126	0.649
0.071	1.989	2.141	0.151	0.760
0.104	2.673	2.812	0.138	0.822
0.124	3.082	3.102	0.019	0.846
0.175	4.101	4.031	-0.070	0.887
0.231	5.187	5.201	0.013	0.913
0.278	6.078	5.728	-0.350	0.929
0.345	7.327	7.331	0.003	0.945
0.464	9.532	9.707	0.174	0.965
0.512	10.435	10.643	0.207	0.971
0.653	13.195	13.105	-0.090	0.984
0.762	15.466	15.305	-0.161	0.991
0.816	16.628	16.701	0.072	0.993
0.827	16.867	17.102	0.234	0.994
0.858	17.541	17.521	-0.019	0.995
0.891	18.258	18.010	-0.247	0.997
0.921	18.904	18.509	-0.395	0.998
0.932	19.140	18.791	-0.348	0.998
0.974	20.022	19.742	-0.279	0.999
1.000	20.551	20.551	0.000	1.000

Table 6-13 Calculated activity coefficients for water (1)/ NMP (2) system at 313.15 K, 323.15 K, 333.15 K using NRTL model.

T=313.15 K			T=323.15 K			T=333.15 K		
x_1	γ_1	γ_2	x_1	γ_1	γ_2	x_1	γ_1	γ_2
0.000			0.000			0.000		
0.032	1.069	1.000	0.032	1.069	1.000	0.013	1.070	1.000
0.061	1.068	1.000	0.070	1.068	1.000	0.017	1.070	1.000
0.095	1.067	1.000	0.087	1.067	1.000	0.020	1.070	1.000
0.102	1.066	1.000	0.105	1.066	1.000	0.022	1.070	1.000
0.118	1.065	1.000	0.235	1.058	1.002	0.025	1.070	1.000
0.135	1.065	1.001	0.301	1.054	1.004	0.041	1.069	1.000
0.165	1.063	1.001	0.420	1.044	1.009	0.071	1.068	1.000
0.180	1.062	1.001	0.562	1.030	1.022	0.104	1.066	1.000
0.231	1.059	1.002	0.603	1.026	1.027	0.124	1.065	1.000
0.493	1.037	1.014	0.715	1.016	1.048	0.175	1.062	1.001
0.500	1.036	1.015	0.831	1.007	1.082	0.231	1.059	1.002
0.602	1.027	1.027	0.867	1.004	1.096	0.278	1.055	1.003
0.650	1.022	1.035	0.920	1.002	1.121	0.345	1.050	1.005
0.771	1.011	1.062	0.946	1.001	1.135	0.464	1.040	1.012
0.862	1.005	1.094	0.978	1.000	1.154	0.512	1.035	1.016
0.906	1.002	1.114	0.987	1.000	1.160	0.653	1.022	1.035
0.961	1.000	1.143	1.000			0.762	1.012	0.060
0.981	1.000	1.156				0.816	1.008	1.077
0.991	1.000	1.162				0.827	1.007	1.081
1.000						0.858	1.005	1.092
						0.891	1.003	1.107
						0.921	1.002	1.121
						0.932	1.001	1.127
						0.974	1.000	1.151
						1.000		

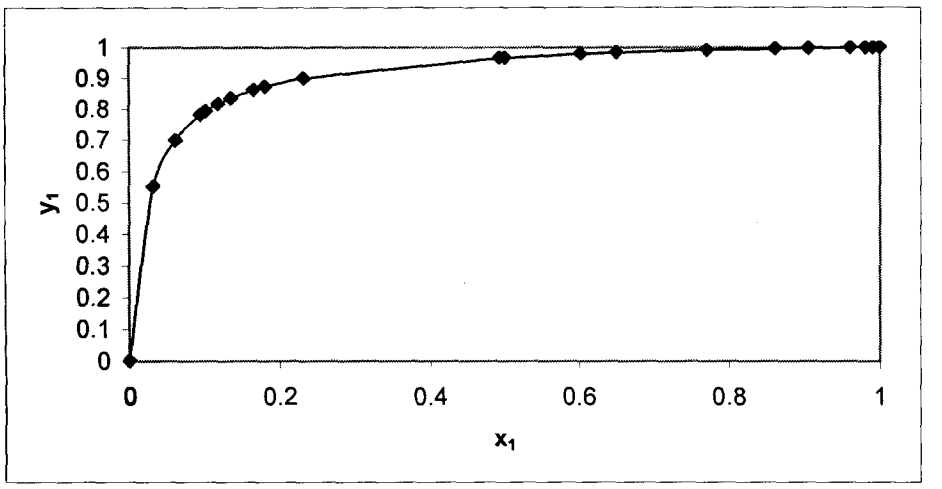

Figure 6-10 Measured x_1 and calculated y_1 diagram for water (1)/ NMP (2) system at 313.15 K.

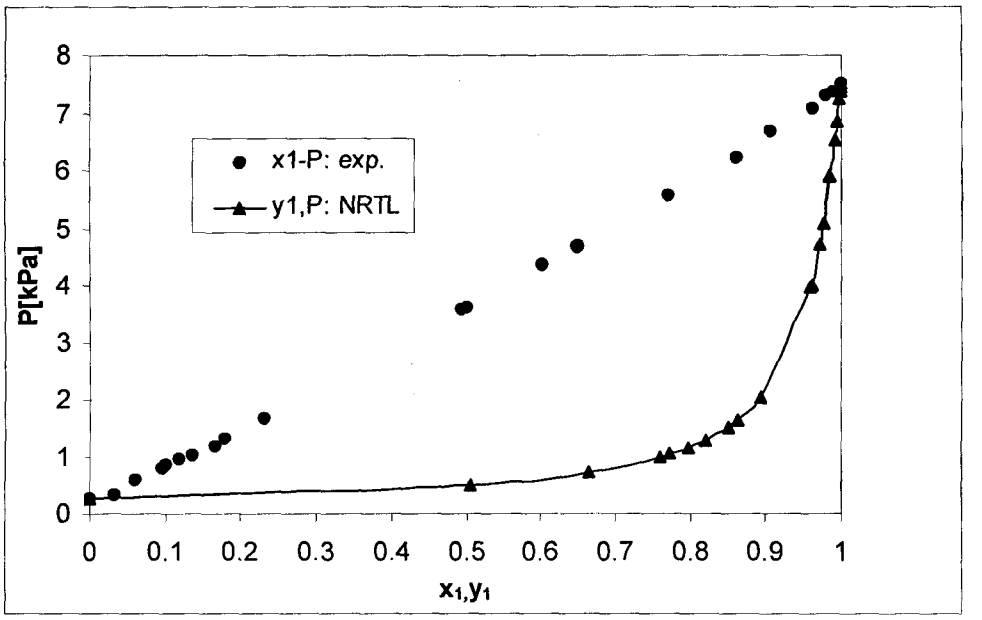

Figure 6-11 Measured P-x_1 and calculated y_1 diagram for water (1)/ NMP (2) system at 313.15 K.

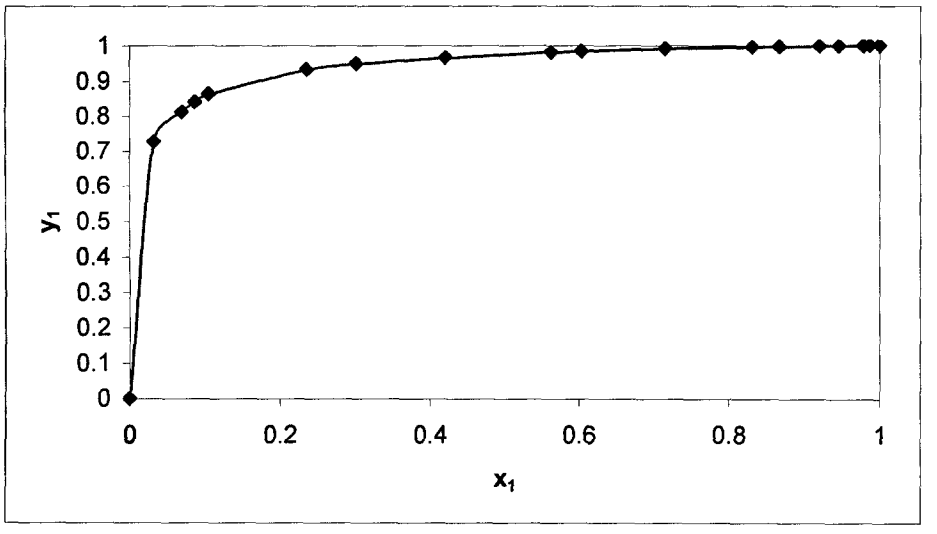

Figure 6-12 Measured x_1 and calculated y_1 diagram for water (1)/ NMP (2) system at 323.15 K.

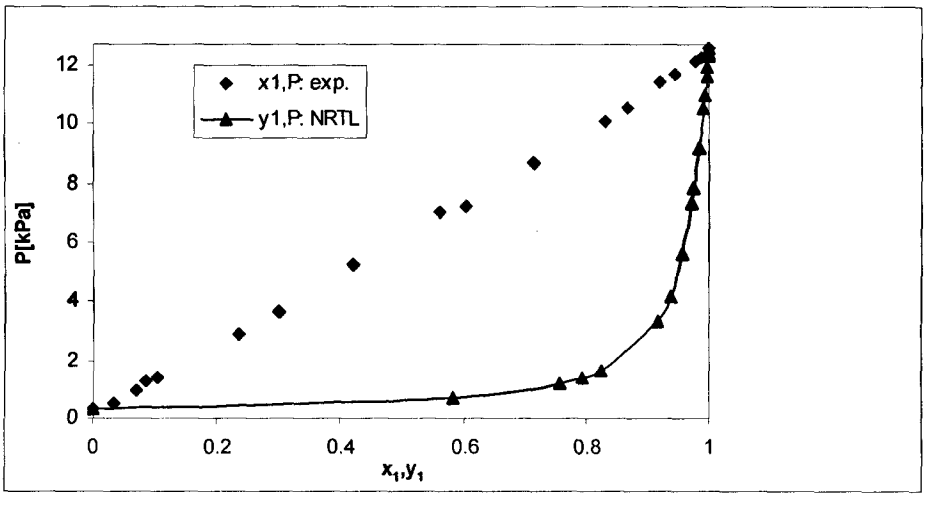

Figure 6-13 Measured P-x_1 and calculated y_1 diagram for water (1)/ NMP (2) system at 323.15 K.

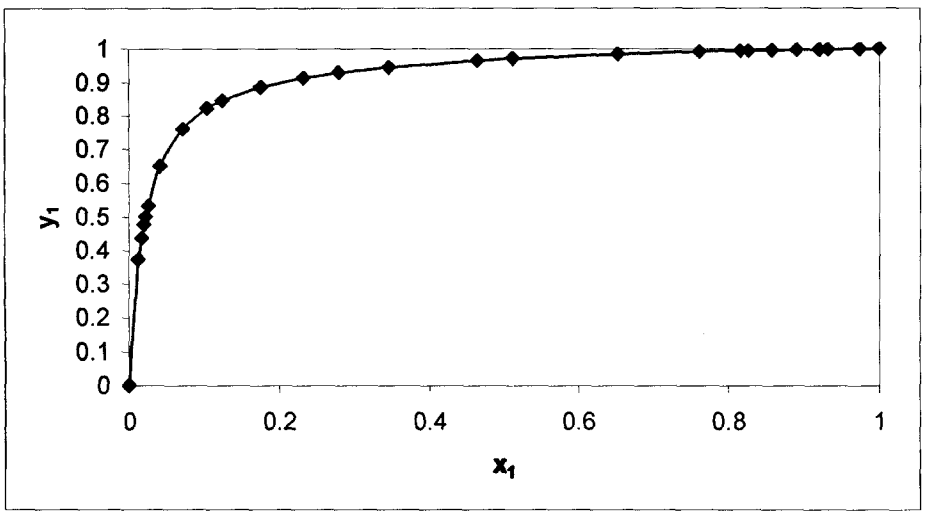

Figure 6-14 Measured x_1 and calculated y_1 diagram for water (1)/ NMP (2) system at 333.15 K.

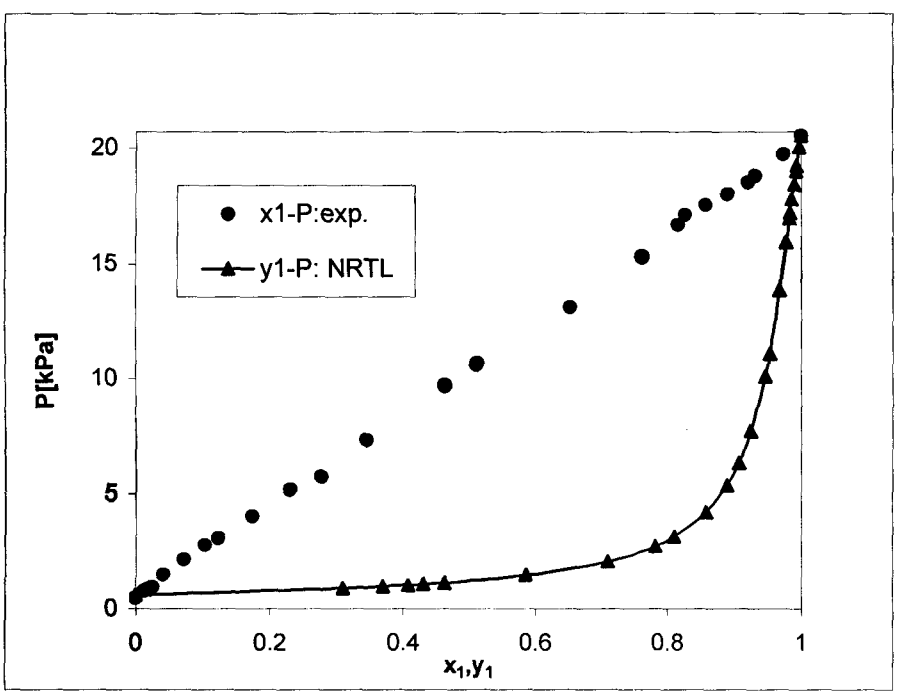

Figure 6-15 Measured P-x_1 and calculated y_1 diagram for water (1)/ NMP (2) system at 333.15 K.

6.4 Activity coefficient model parameters regressed for experimental VLE

Table 6-14 Activity coefficient model parameters for the Cyclohexane (1)/ Ethanol (2) system.

Equation	308.15 K	333.15 K
NRTL		
g_{12}- g_{11} in J/mol	1667.023	1688.21
g_{12}- g_{22} in J/mol	2219.463	2220.65
Average α	0.941	-1.2737
$\Delta P_{average}$ (kPa)	0.9581	0.5375
Wilson		
λ_{12}- λ_{11} in J/mol	-354.159	-230.041
λ_{12}- λ_{22} in J/mol	1247.3	1354.53
$\Delta P_{average}$ (kPa)	1.519	1.369

Table 6-15 Activity coefficient model parameters for the 1-hexene (1)/NMP (2) system.

Equation	313.15 K	323.15 K	333.15 K
NRTL			
g_{12}- g_{11} in J/mol	1549.69	2283.78	2769.94
g_{12}-g_{22} in J/mol	2335.84	2194.22	2654.53
Average α	-1.109	-0.016	-0.133
$\Delta P_{average}$ (kPa)	1.407	1.039	1.007
Wilson			
λ_{12}- λ_{11} in J/mol	1163.54	1263.69	1204.69
λ_{12}- λ_{22} in J/mol	2445.89	2524.10	2371.80
$\Delta P_{average}$ (kPa)	1.294	1.307	1.0405

Table 6-16 Activity coefficient model parameters for the water (1)/NMP (2) system

NRTL	313.15 K	323.15 K	333.15 K
g_{12}- g_{11} in J/mol	1041.46	1074.72	1107.98
g_{12}- g_{22} in J/mol	-520.730	-537.359	-553.988
Average α	0.957	1	0.839
Δ $P_{average}$ (kPa)	0.228	0.28773	0.274
WILSON			
λ12- λ11 in J/mol	6104.349	6299.282	6494.22
λ12- λ22 in J/mol	-2494.92	-2574.59	-2654.26
Δ $P_{average}$ (kPa)	1.436	2.041	2.016

In this work, the regressed NRTL parameters Δg_{12} and Δg_{21} are found to be linear functions of temperature. The activity coefficient model parameters in Tables 6-14 to 6-16 increase slightly as the temperature increase although there are some irregularities. The regressed parameters against temperature are plotted in the following figures (Figures 6-16 to 6-18):

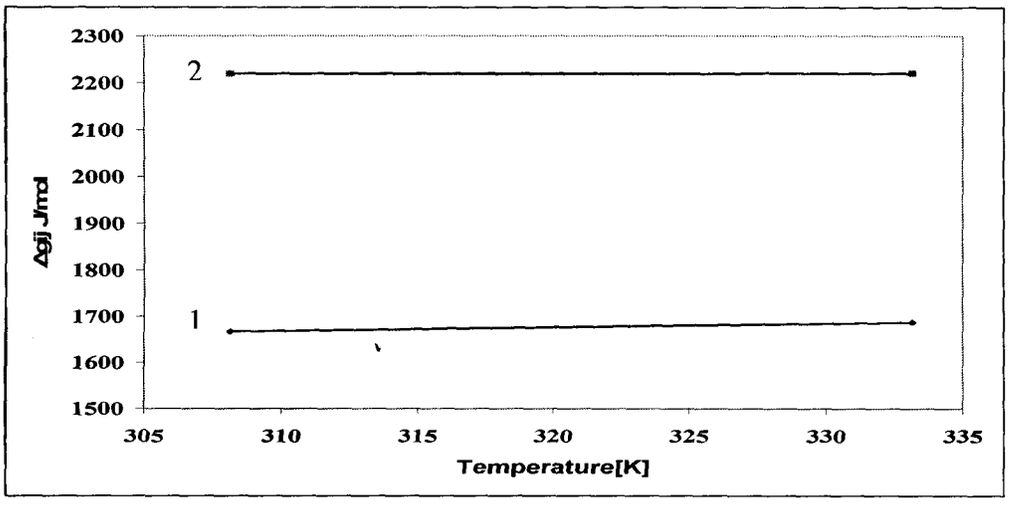

Figure 6-16: Regressed parameters for Cyclohexane (1) + Ethanol (2):
1, g_{12}-g_{11} J/mol; 2, g_{12}-g_{22} J/mol

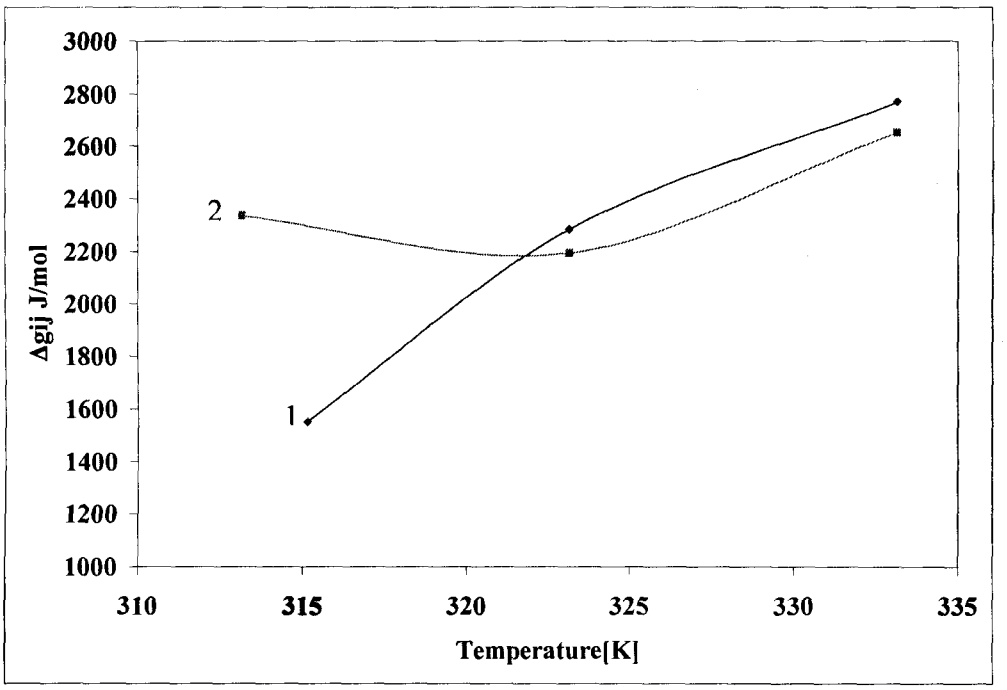

Figure 6-17: NRTL regressed parameters for 1-hexene (1) + NMP (2):
1, g_{12}-g_{11} J/mol; 2, g_{12}-g_{22} J/mol

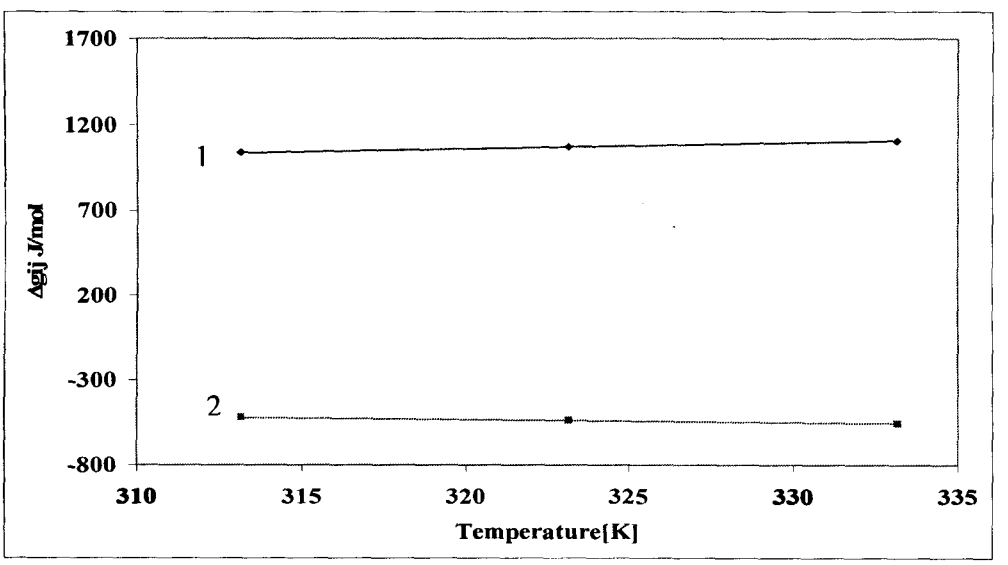

Figure 6-18: NRTL regressed parameters for Water (1) + NMP (2):
1, g_{12}-g_{11} J/mol; 2, g_{12}-g_{22} J/mol

6.5 Infinite dilution activity coefficients

Determination of activity coefficients in dilute region as explained in paragraph 3.5.5.1, were obtained using the endpoint slopes as has been described by Ellis and Jonah (1962) and modified by Maher and Smith (1979).

In this method the P_D vs x_1 data are converted to P_D vs x_1 values using

$$P_D = P - P_2^{sat} - \left(P_1^{sat} - P_2^{sat}\right)x_1 \text{ where}$$

$$\left(\frac{\partial P}{\partial x_1}\right)_{x_1=0} = \left(\frac{P_D}{x_1 x_2}\right)_{x_1=0} + P_1^{sat} - P_2^{sat},$$

$$\left(\frac{\partial P}{\partial x_1}\right)_{x_1=1} = -\left(\frac{P_D}{x_1 x_2}\right)_{x_1=1} + P_1^{sat} - P_2^{sat}$$

P_D represents the experimental deviation from Raoult's law and is independent of the equation of state used to calculate the activity coefficients [Maher and Smith, 1979)].

Both $\left(P_D/x_1x_2\right)$ and $\left(x_1x_2/P_D\right)$ are plotted vs x_1. According to Maher and Smith (1979), for some systems, the shape of the curve will allow reliable extrapolations at both ends (if the curve is linear). Often, both plots must be used with one providing a reliable extrapolation at one end while the other works better at the other end.

The values for the terminal slopes on a P_D vs x_1, plot may be obtained directly from the intercepts on a $\left(P_D/x_1x_2\right)$ or $\left(x_1x_2/P_D\right)$ vs x_1 plot.

In Figures 6-16 and 6-17 these plots are shown for cyclohexane + ethanol system at 323.15 K. The values of γ_1^∞ and γ_2^∞ obtained are compared to the literature [Joseph (2001)] in Table 6-17 except those of 1-hexene- NMP and water- NMP (listed in Tables 6-18 and 6-19) because they are new data. The differences are noted but are not very significant. The infinite dilution values calculated in this project are higher than Joseph's values. Based on the linearity shown on the plot, these values can be dependent upon the equation of state used [Maher and Smith (1979)] because they were obtained from the linear plot which gives satisfactory extrapolation and hence the calculation of γ_i^∞. The plots for the rest of binary systems at different temperatures are shown in Appendix A. Unfortunately the plots are not linear. This is a consequence of high sensitivity in dilute

region and therefore inaccuracy in measurements is very high which results in non linear plots.

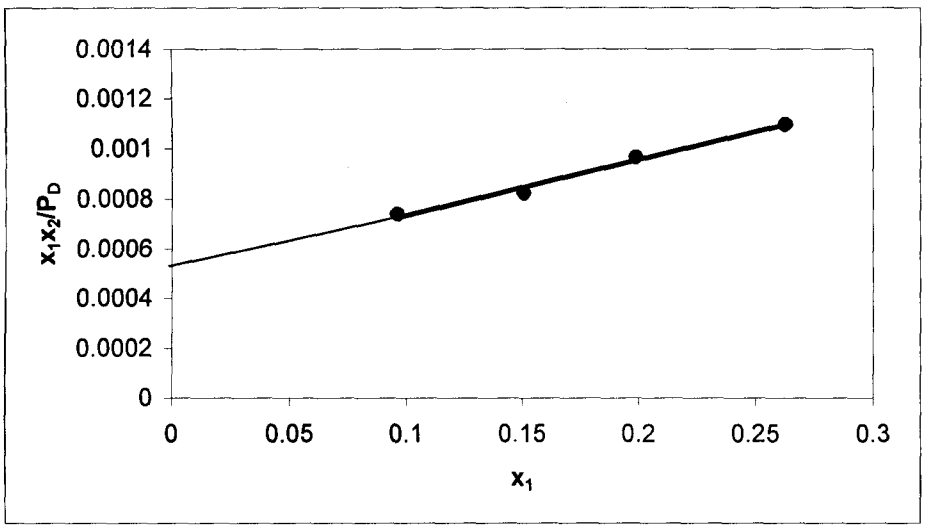

Figure 6-19: $\frac{x_1 x_2}{P_D}$ **vs.** x_1 **as** $x_1 \rightarrow 0$ **for Cyclohexane (1) + Ethanol (2) at 323.15 K**

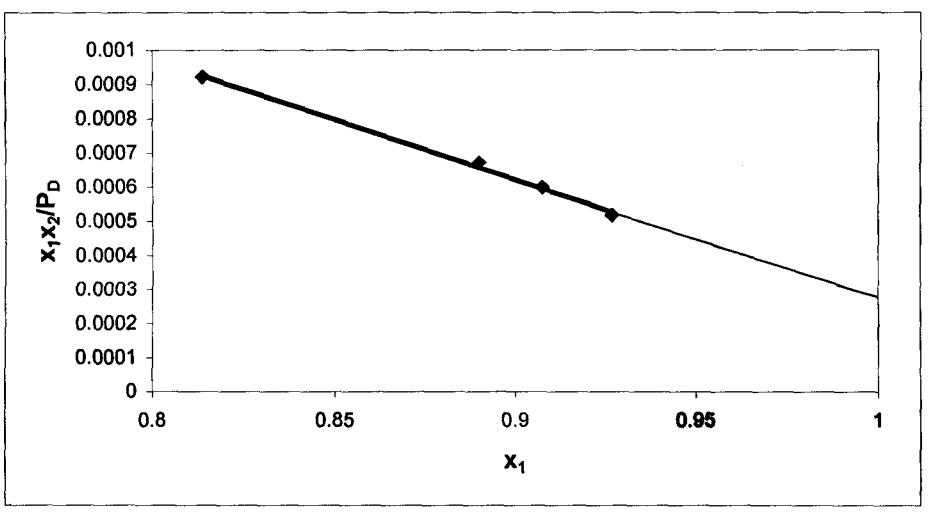

Figure 6-20: $\frac{x_1 x_2}{P_D}$ **vs.** x_1 **as** $x_1 \rightarrow 1$ **for Cyclohexane (1) + Ethanol (2) at 323.15 K**

Table 6-17 Infinite dilution activity coefficients for the cyclohexane (1) / ethanol (2) system

Temperature	308.15 K	323.15 K	
		This work	Joseph (2001)
γ_1^∞	7.58	14.174	9.2
γ_2^∞	12.502	21.167	29.5

Table 6-18 Infinite dilution activity coefficients for the 1-hexene (1) / NMP (2) system

Temperature	313.15 K	323.15 K	333.15 K
γ_1^∞	6.342	5.359	8.076
γ_2^∞	10.732	6.354	5.193

Table 6-19 Infinite dilution activity coefficients for the water (1) / NMP (2) system

Temperature	313.15 K	323.15 K	333.15 K
γ_1^∞	6.371	4.15	9.471
γ_2^∞	3.581	7.362	5.736

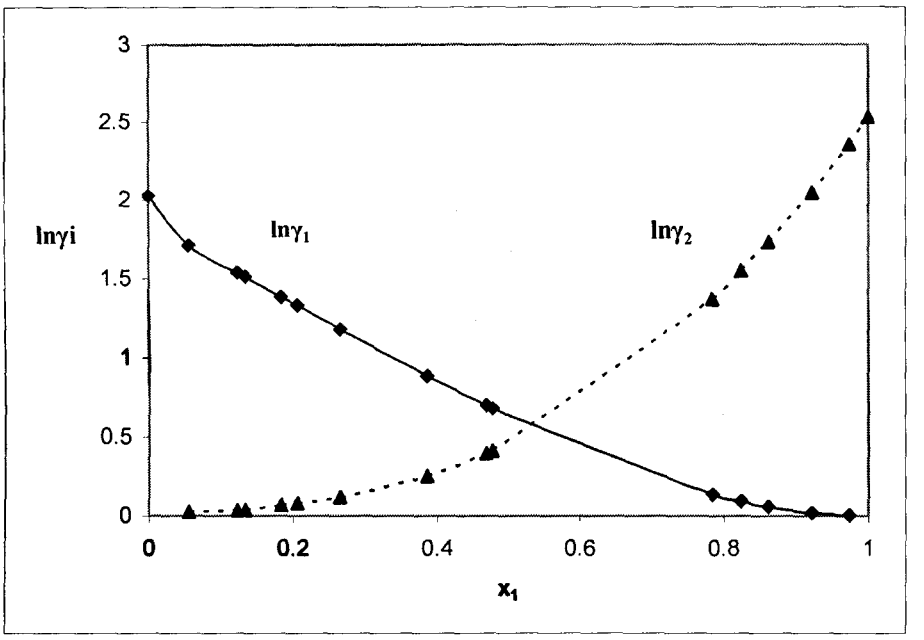

Figure 6-21 Activity coefficients for cyclohexane (1) / ethanol (2) at 308.15 K calculated using NRTL model.

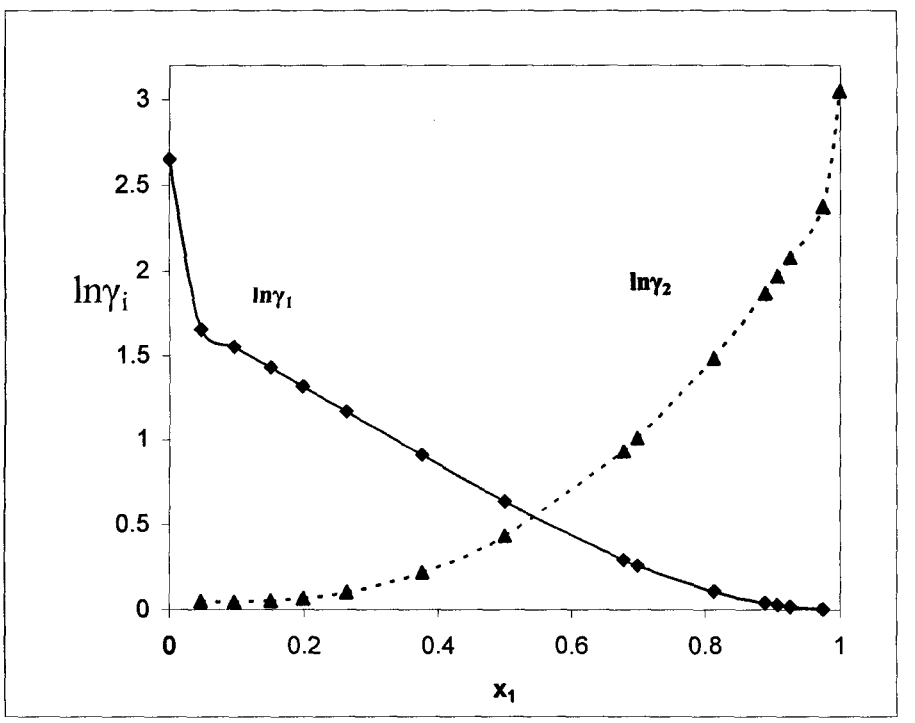

Figure 6-22 Activity coefficients for cyclohexane (1) / ethanol (2) at 323.15 K calculated using NRTL model.

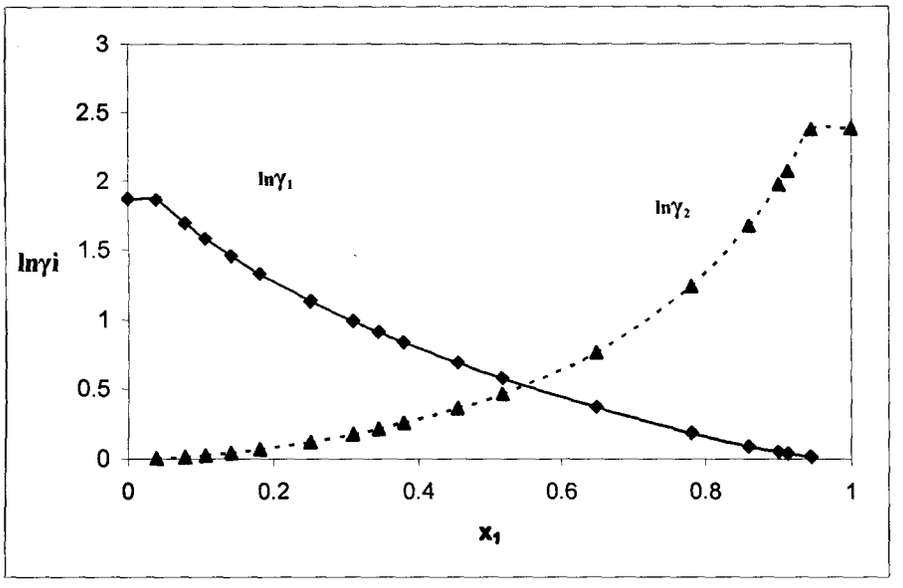

Figure 6-23 Activity coefficients for 1-hexene (1)/NMP (2) at 313.15 K calculated using NRTL model.

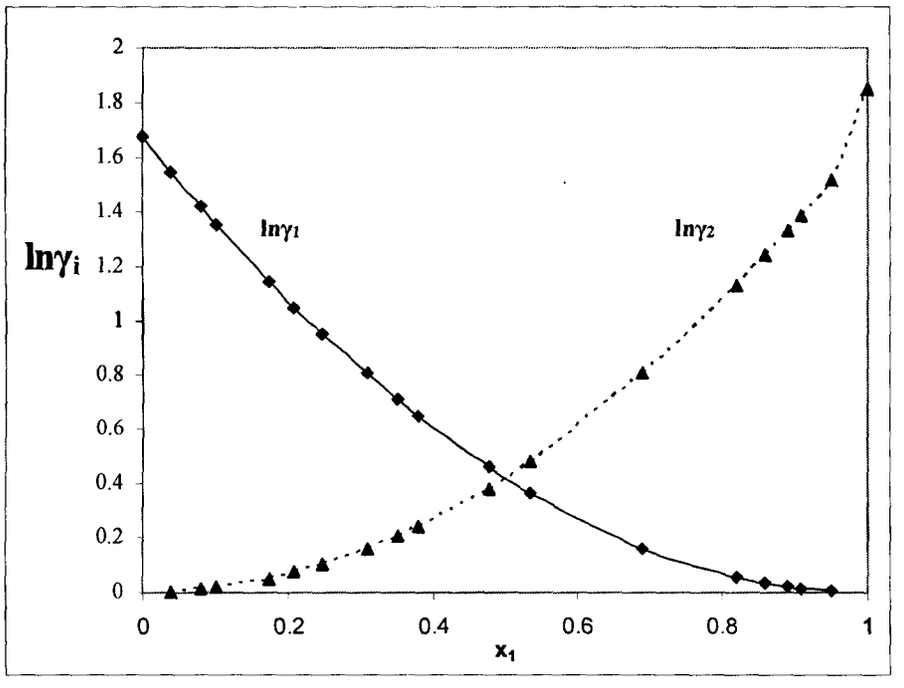

Figure 6-24 Activity coefficients for 1-hexene (1)/NMP (2) at 323.15 K calculated using NRTL model.

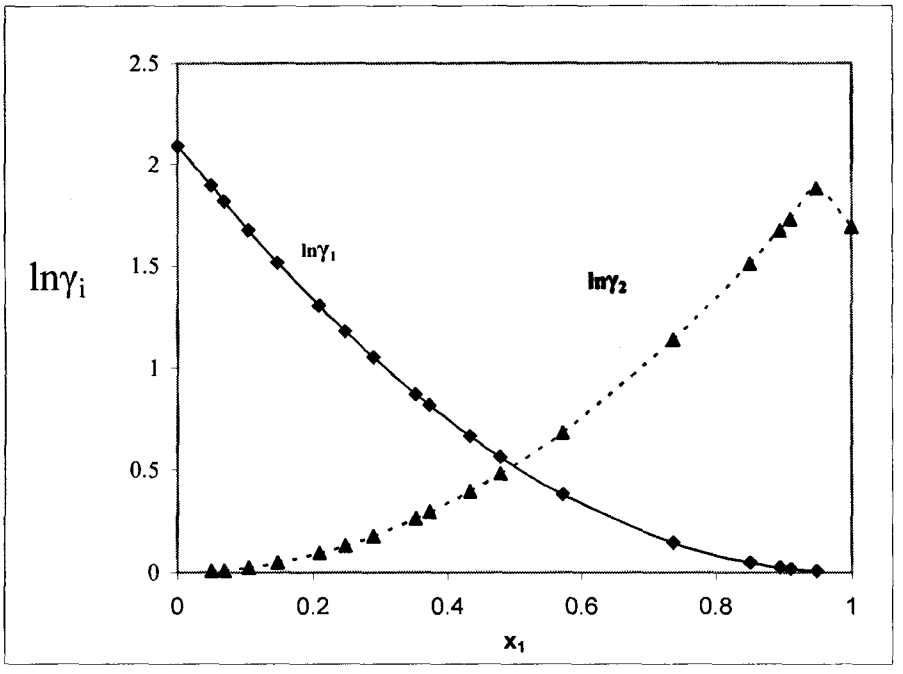

Figure 6-25 Activity coefficients for 1-hexene (1)/NMP (2) at 333.15 K calculated using NRTL model.

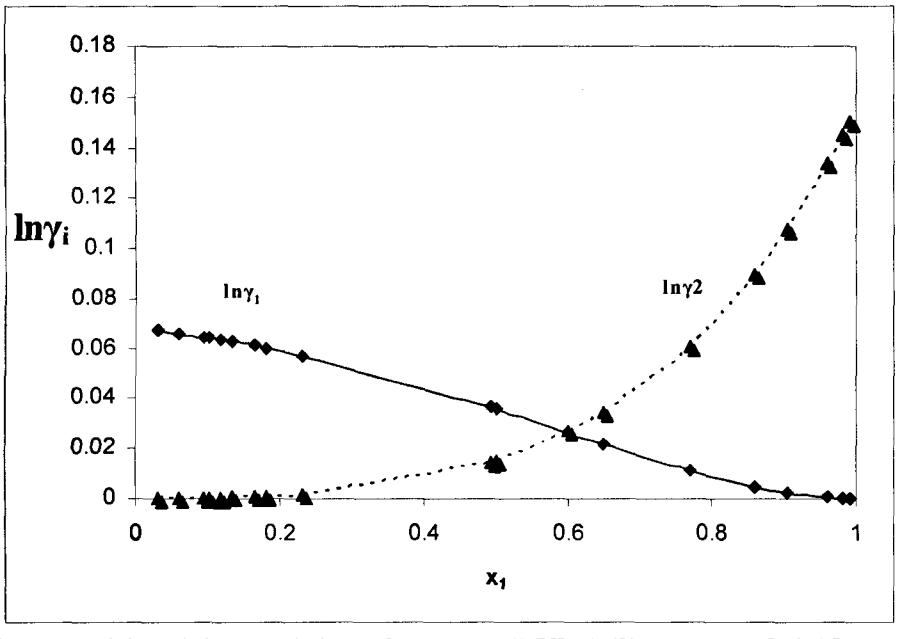

Figure 6-26 Activity coefficients for water (1)/NMP (2) system at 313.15 K calculated using NRTL model.

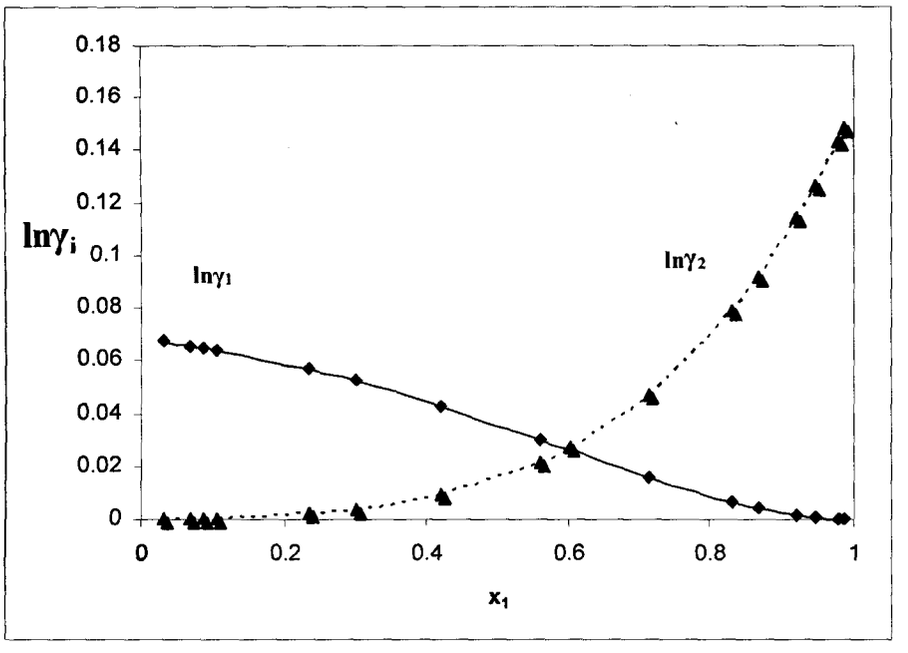

Figure 6-27 Activity coefficients for water (1)/NMP (2) system at 323.15 K calculated using NRTL model.

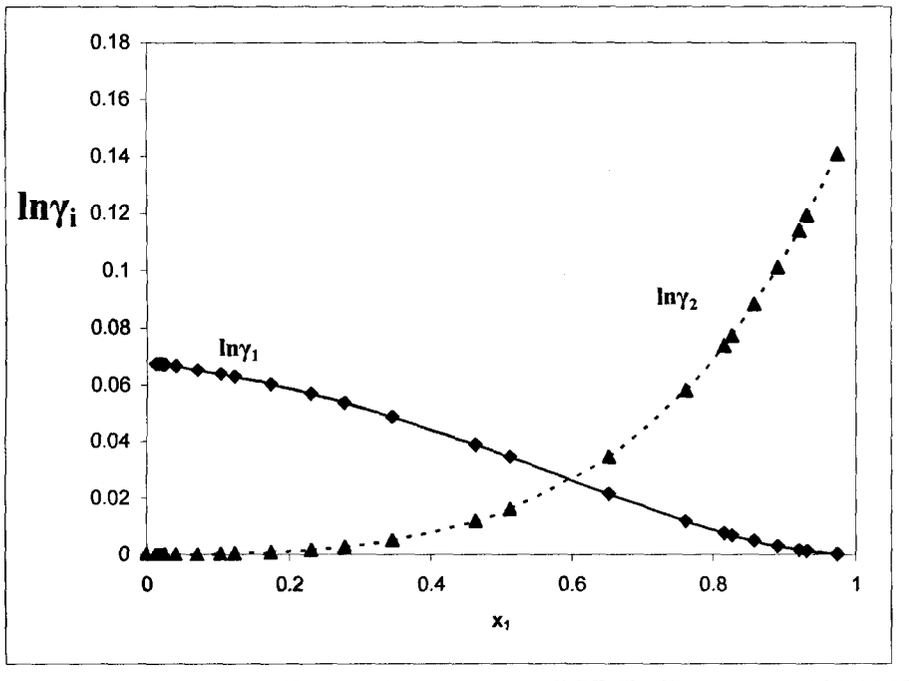

Figure 6-28 Activity coefficients for the water (1)/NMP (2) system at 333.15 K calculated using NRTL model.

CHAPTER 7

CONCLUSIONS AND RECOMMENDATIONS

7.1 CONCLUSIONS

The initial phase of this work involved the re-design of a new static cell cluster (Chapter four); thereafter vapour-liquid equilibrium data were measured for binary mixtures of the following three systems: cyclohexane + ethanol, 1-hexene + N-methyl-2-pyrrolidone (NMP) and water + N-methyl -2- pyrrolidone (NMP) at 313.15 K, 323.15 K and 333.15 K at sub-atmospheric pressures.

The measurements of vapour pressures for the cyclohexane+ ethanol system were used for testing the operating procedure and measuring capacity of the new static cell cluster and its data show a reasonable agreement with the published data [Joseph et al. (2001)]. However a certain degree of scatter is noted. This could be due to the leaks and difficulties to maintain the bath temperature constant during the experimental runs. Incomplete degassing can be another source of errors as there is no general test for completeness of degassing available. The rest of the binaries are the new data, as they have not been found in the literature yet at the isotherms measured.
The Barker's Method used for predicting vapour compositions performed well and these calculations by this method agree well with the literature values.

P-x_1 data measured were modeled; firstly for calculating vapour composition using Barker's Method; these predictions agree well with the published values. Secondly the NRTL and Wilson equations were utilized for fitting the data. In these modelings, the Virial correlation of Hayden and O'Connell (1975) was used to describe the vapour phase deviations from ideality. 1-hexene +NMP and water + NMP shown a non-ideal behaviour i.e. they deviate from Raoult's law and they present positive deviation. Their (x_1, y_1) curves are largely separated from the 45° diagonal and furthermore they do not form azeotropes. This means that they present high relative volatility and can be easily separated by distillation. The NRTL model provides the best fit for all systems.

Infinite Dilution Activity Coefficient Values from total pressure VLE data have been calculated using the equation of Ellis and Jonah (1962) as presented by Maher

and Smith (1979). Unfortunately the plots of $(x_1x_2/P_{D)}$ vs x_1 or (P_D/x_1x_2) vs x_1 of some isotherms for these 3 systems in dilute region are not straight lines, hence γ^{∞} is not accurate. This failure is due to the very dilute solutions being very sensitive, making it very difficult to obtain accurate and reliable measurements.

The majority of the static cells at low pressure published up to date have employed the technique of submersion of the equilibrium cell in the water bath for getting constant temperature in previous designs. This causes corrosion inside the circular base (by the penetration of water) on which the apparatus stands. The new design described in this work eliminated this weakness and the overall innovation has shown good results.

Advantages of new design over prior designs:
As described earlier in chapter four, the new design of the static cell with a water jacket around the equilibrium cell for circulation of hot water has significantly reduced the experimental time taken for the degassing to half an hour for each cell .(Tests conducted in this work showed that degassing was complete in this time). The previous normal degassing method (which was applied to various static cells) was lengthy freezing-evacuation-thawing cycles. Seven to nine cycles were required, with about 1 hour per cycle [Maher and Smith (1979)]. In a word, the objectives of this work were achieved as the new design gave improved performance over the older designs.
This design would have given large quantities of reliable binary data if the manifold and Bellows valves had not experienced leaks.

7.2 RECOMMENDATIONS

It is recommended that when the apparatus is used again, the manifold and all the Bellows valves should be replaced in order to avoid leaks. An accurate temperature sensor should also be used in each individual cell.
The number of the cells could also be increased to six in order to produce more data in a shorter time.

REFERENCES

Abbot, M M, 1986," Low-Pressure Phase Equilibria: Measurement of VLE". *Fluid Phase Equilibria, Vol. 29,p.193-207.*

Abrahams, D S & Prausnitz, J M, (1975), Statistical Thermodynamics of Liquid Mixtures: A New Expression for the Excess Bibbs Energy of Partly or Completely Miscible Systems", *American Institute of Chemical Engineers, Journal, Vol.21, p 116-128.*

Armando del Rio, Coto,B, Pando,C, Renuncio,J A R, (2001),"Vapor-Liquid Equilibria for the Binary Systems Decane + 1,1-Dimethyl Methyl Ether (MTBE)
And Decane + 1,1-Dimethylpropyl methyl Ether (TAME) at 308.15, 318.15 and 328.15 K, *Fluid Phase Equilibria, Vol.187-188, p.299-310.*

Barker, C, (1953), "Determination of Activity Coefficients from Total Pressure Measurements", *Australian Journal of Chemistry, Vol. 6, p. 207-210.*

Brown, I, (1952) "Liquid-Vapor Equilibria.III. The Systems Benzene-n-Heptane, n-Hexane-Chlorobenzene and Cyclobenzene and Cyclohezane-Nitrobenzene", *Australian Journal of Scientific Research, Vol.5, p. 530-540.*

Chen, G, Hou, Y and Knapp, H, (1995),"Diffusion Coefficients, Kinematic Viscosities, and Refractive Indices for Heptane + Ethylbenzene, Sulfolane + 1-Methylnaphthalene, Water + N,N-Dimethylbenzene, Water + Methanol, Water + N-Formylmorpholine, and water + N-Methylpyrrolidone", *Journal of chemical Engineering Data,Vol.40,p.1005-1010.*

Christensen, S P, (1998),"Measurement of Dilute Mixture Vapor –Liquid Equilibrium Data for Aqueous Solutions of Methanol and Ethanol with a Recirculating Still", *Fluid Phase Equilibria, Vol.150, p.763-773.*

Comelli, B & Francesconi, R, (1995),"Excess Molar Enthalpies of Dimethyl Carbonate or Diethyl Carbonate +Cyclic Ethers at 298.15 K". Journal of Chemical Engineering Data. Vol.40,p.28-30.

Clifford, S L, (2004), " Low-Pressure Vapour-Liquid Equilibrium and Molecular Simulation of Carboxylic Acids". Msc. Thesis, University of Kwazulu-Natal.

Davison,R R, Smith, W H J R & Chun, J W,(1967),"A Static Vapor Pressure Apparatus for Mixtures",*American Institute for Chemical Ingineering Journal, Vol.13,No.3,p.590-593.*

Davison,R R,(1968),"Vapor-Liquid Equilibria of Water –Diisopropylamine and Water-Di-N-Propylamine", *Journal of Chemical and Engineering Data, Vol.13,No,p.348-351.*

Davison,R R, & Smith, W H, (1969),"Vapor –Liquid Equilibrium of N-Ethyl-N-Butylamine-Water and N-Ethyl-sec-Butylamine-Water", *Journal of Chemical and Engineering Data,Vol.14,No. 3,p.296-298.*

Davison, R R & Smith, W H, (1969),"Phase Equilibria in the System N,N, Dimethyl-Tert.-Butylamine-Water by the Total Pressure Method", *Chemical Engineering Science, Vol.24,p.*1589-*1597.*

Dortmund Data Bank (DBR) Software (1998).

Duran, J L & Kaliaguine, S, (1971),"Application de l'Equation de Wilson à l'Estimation des Enthalpies de Melange", *The Canadian Journal of Chemical Engineering, Vol.49, p.278-281.*

Dymond, J H& Smith, E B, (1980), "The Virial Coefficients of Gases and Gaseous Mixtures", Clarendon Press, Oxford.

Ellis, S R M. & Jonah, D A, (1962),"Prediction of activity coefficients at infinite dilution", *Chemical Engineering Science, Vol.17, p.971-976.*

Eubank, P T, Lamonte, B G, & Alvarado, J F J, (2000), "Consistency Tests for Binary VLE Data". *Journal of Chemical Engineering Data, Vol.45, p.1040-1048.*

Fabries, J F & Renon, H,(1975),"Method of Evaluation and Reduction of Vapor-Liquid Equilibrium Data of Binary Mixtures", *American Institute of Chemical Engineering Journal, Vol.21,No. 4,p.735-1975.*

Fischer, K & Gmehling, J, (1994),"P-x and γ^{α} Data for the Different Binary Butanol-Water Systems at 50oC", *Journal of Chemical Engineering Data, Vol.39.p.309-315.*

Fischer, K & Gmehling, J, (1996),"Vapor-Liquid Equilibria, Activity Coefficients at Infinite Dilution and Heats of Mixing of N-methyl pyrrolidone-2 with C5 or C6 Hydrocarbons and for Hydrocarbon Mixtures", *Fluid Phase Equilibria, Vol.119, p.113-130.*

Fischer,K & Gmehling, J, (2004),"Influence of Water on the Vapor-liquid Equilibria, Activity Coefficients at Infinite Dilution and Enthalpies ofMixing for mixtures of N-methyl-2-pyrrolidone with C5 or C6 Hydrocarbons", Fluid Phase Equilibria, Vol.218,p.69-76.

Gautreaux, M F & Coates, J, (1955),"Activity Coefficients at Infinite Dilution", American Institute of Chemical Engineers. Journal, Vol. 1,p.496-500.

Gibbs, R E & Van Ness, H C, (1972), "Vapour-Liquid Equilibria from Total Pressure Measurements. A New Apparatus", *Industrial and Engineering Chemistry Fundamentals, Vol.11, p.410-413.*

Gieycz, P ,Rogalski,M & Malanowski, S, (1985),"Vapor-Liquid Equilibria in Binary Systems Formed by N-Methyl pyrrolidone with Hydrocarbons and Hydroxyl Derivatives", *Fluid Phase Equilibria,Vol.22.p107-122.*

Gillespie,D T C, (1946), Vapour Liquid Equilibrium Still for Miscible Liquids', Industrial and Engineering Chemistry, Analytical Edition, Vol. 18,p.575-577.

Gmehling, J & Onken, U, (1977), "Vapor-Liquid Equilibrium Data Collection, Organic Hydroxy Compounds: Alcohols", Vol.1, Parts 2a, p.438, DECHEMA, Frankfurt/Main.

Harris, R A (2004)," Robust Equipment for the Measurement of Vapour-Liquid Equilibrium at High Temperatures and High Pressures", Ph. Thesis, University of KwaZulu-Natal.

Hayden, J G & O'Connel, J P, (1975), "A Generalized Method for Predicting Second Virial Coefficients", *Industrial and Engineering Chemistry, Process Design and Development, Vol.14, p.209-216.*

Heertjies, P M (1960), "Determination of Vapour Liquid Equilibria of Binary Mixtures", *Chemical and Process Engineering, Vol.41,p.385-386.*

Hendriks, E M & Van Bergen, A R D, (1992),"Application of Reduction Method to Phase Equilibria Calculations", *Fluid Phase Equilibria, Vol.74, p.17-34.*

Herington E F G, (1947),"A Thermodynamic Consistency Test for the Internal Consistency of Experimental Data of Volatility Ratios", *Nature, Vol.160, p.610-611.*

Hermsen, R W & Prausnitz,J M,(1963),"Thermodynamic Properties of the Benzene and Cyclopentane System", *Chemical Engineering Science, Vol.18,p.485-494.*

Himmelblau, D M, (1982),"Basic Principles and Calculations in Chemical Engineering", Fifth Edition, Prentice-Hall International, Inc,Englewood C.

Howell, J R & Buckius,R O, (1992),"Fundamentals of Engineering Thermodynamics", Second Edition,McGraw-Hill, Highstow, NJ.

Inoue, M, Azumi, K & Suzuki, N (1975), "A New Vapour Pressure Assembly for Static Vapour Liquid Equilibrium", *Industrial and Engineering Chemistry Fundamentals, Vol.14, p.312-314.*

Joseph, M A, (2001), Computer-Aided Measurement of Vapour-Liquid Equilibria in a Dynamic Still at Sub-Atmospheric Pressures", MSc. Eng. Thesis, University of Natal.

Joseph, M A, Ramjugernath, D and Raal,J D, (2001),"Phase Equilibrium Properties for Binary Systems with Diacetyl from a Computer Contrilled Vapor –Liquid Equilibium Still," *Fluid Phase Equilibria, Vol.182,p.157-176.*

Joseph, M A, Ramjugernath, D and Raal, J D, (2002), "Computer-Aided Measurement of Vapor –Liquid Equilibria in Dynamic Still at Sub-Atmospheric Pressures, *"Developments in Chemical Engineering and Mineral Processing, Vol.10, No. 5-6, p.615-638.*

Kojima, J Moon, H M & Ochi, K, (1990), "Thermodynamic Consistency Test of Vapour Liquid Equilibrium Data-Methanol-Water, Benzene-Cyclohexane and Ethyl methyl ketone-Water", *Fluid Phase Equilibria, Vol.56, p.269-284.*

Kolbe,B & Gmehling, J, (1985),"Thermodynamic Properties of Ethanol + Water. I. Vapor –Liquid Equilibria Measurements from 90 to 150oC by the Static Method, *Fluid Phase Equilibria, Vol.23, p.213-226.*

Kolbe,B & Gmehling, J, (1985),"Thermodynamic Properties of Ethanol + Water. II. Potentials and Limits of G^E Models", *Fluid Phase Equilibria, Vol.23, p.227-242.*

Krummen,M, Gruber, D & Gmehling, J, (2000),"Measurement of Activity Coefficients at Infinite Dilution in Solvent Mixtures Using the Dilutor Technique", *Industrial Engineering Chemistry Fundamentals, Vol.39, p.2114-2123.*

Krumar, R.K & Rao,M V, (1991),"Vapor-Liquid Equilibria in the Binary Systems formed by 1-propanol with 1,2-dichloroethane,1,1,1-trichloroethane and 1,1,2,2-tetrachloroethane at 96.7 kPa", *Fluid Phase Equilibria, Vol.70,p.19-32.*

Krummen, M & Gmehling, J, (2004),"Measurement of Activity Coefficients at Infinite Dilution in N-methyl-2-pyrrolidone and N-formylmorpholine and their Mixtures with Water using the Dilutor Technique", *Fluid Phase Equilibria, Vol.215, p.283-294.*

Letcher,T M, Damanska, U, & Mwenesongole, E, (1998),"The Excess Molar Volumes of (N-methyl –2-pyrrolydone + an Alkanol or a Hydrocarbon) at 298.15 K and the Application of the Flory-Benon-Treszczanowicz and the Extended Real Associated Solution Theories", *Fluid Phase Equilibria, Vol.149,p.323-337.*

Linek,J, Wichterle,I & Marsh,K N, (1996), "Vapor –Liquid Equilibria for N-Methyl-2-pyrrolidone + Benzene, +Toluene, +Heptane, and +Methylcyclohexane", *Journal of Chemical Engineering Data, Vol.41,p.1212-1218.*

Ljunglin,J J & Van Ness, H C, (1962), "Calculation of Vapour Liquid Equilibria from Vapour Pressure Data", *Chemical Engineering Science, Vol.17,p.531-539.*

Macdonald, D D, Dunay, Hanlon, G & Hyne,J B, (1971),"Properties of the N-Methyl-2-Pyrrolidone- Water system", *The Canadian Journal of Chemical Engineering, Vol.49,p.420-424.*

Maher, P J & Smith, B D, (1979), "A New Total Pressure Vapor-Liquid Equilibrium Apparatus. The Ethanol + Aniline System at 313.15, 350.81, and 386.67 K", *Journal of Chemical and Engineering Data, Vol.24, p.16-22.*

Maher, P J & Smith, B D, (1979), "Infinite Dilution Activity Coefficient Values from Total Pressure VLE data. Effect of equation of State used ", *Industrial and Engineering Chemistry Fundamentals, Vol.18, p.354-357.*

Maher, P J & Smith B D, (1997), A New Total Pressure Vapor–Liquid Equilibrium Apparatus. The Ethanol + Aniline System at 313.15K, 350.81K and 386.67K", *Journal of Chemical and Engineering Data, Vol.24, p.16-22.*

Malanowski, S, (1982a), "Experimental Methods for Vapor-Liquid Equilibria. Part I. Circulation Methods", *Fluid Phase Equilibria, Vol.8, p.197-219.*

Malonowski, S, (1982b), "Experimental Methods for Vapor-Liquid Equilibria. Part II. Dew and Bubble-point Method", *Fluid Phase Equilibria, Vol.9, p.311-317.*

Martin, J J & Yu-Chun Hou,(1955),"Development of an Equation of State for Gases", *American Institute of Chemical Engineering Data, Vol.1,No. 2,p.142-146.*

Mixon,F O,Gumowski, B & Carpenter, B H (1965), "Computation of Vapor- Liquid Equilibrium Data from Solution Vapour Prossure Measurements", *Industrial and Engineering Chemistry Fundamentals,Vol.4,p.455-459.*

Nagahama, K, Suzuki, I & Hirata, M, (1971),"Estimation of Wilson Parameters", *Journal of Chemical Engineering of Japan, Vol.4, No.1,p.1-5.*

Nakano, K, sarashina, E, Uemura,Y & Hatate, Y, (1996),"Vapor-Liquid Equilibria of Minute Amounts of N-Methylsuccinimide and Water in N-Methyl-2-pyrrolidone", *Journal of Chemical Engineering of Japan, Vol.29,p.371-372.*

Noll, O, Fischer, K & Gmehling, J, (1996),"Vapor-Liquid Equilibria and Entalpies of Mixing for the Binary System Water + N-Methyl-pyrrolidone in the Temperature Range 80-140oC", *Journal of Chemical Engineering Data, Vol. 41,p.1434-1438.*

O'Connell, J P & Prausnitz, J M,(1967), "Empirical Correlation of Second Virial Coefficients for Vapor –Liquid Equilibrium Calculations, "*Industrial and Engineering Chemistry: Process Design Development," Vol.6,No.2,p.245-250.*

Palmer, D A, (1987),"Handbook of Applied Thermodynamics", Boca Roton, Florida.

Pividal, K A, Britigh, A & Sandler, S I, (1992), "Infinite Dilution Activity Coefficients for Oxygenate Systems Determined Using a Differential Static Cell", *Journal of Chemical and Engineering Data, Vol.37, p.484-487.*

Perry, R H & Green, D W, (1997)," Perr's Chemical Engineers'Handbook", 7th ed.,McGraw-Hill, New York.

Prausnitz, J M, Anderson, T F, Grens, E A, Eckert, C A, Hseih, R, O'Connell,J P,(1980),"Computer Calculations for Multicomponent Vapor-Liquid Equilibria", Prentice-Hall, Englewood Cliffs, NJ.

Prausnitz, J M, Lichtenthaler, R N, Gomes de Azevedo, E, (1986), "Molecular Thermodynamics of Fluid Phase Equilibriua", Prentice-Hall, Englewood Cliffs, NJ.

Raal, J D, Brouckaert, C J, (1992), Vapor-Liquid and Liquid –Liquid Equilibria in the system Methyl Butenol_Water", Fluid Phase Equilibria, Vol.74,p.253-270.

Raal, J D & Mühlbauer, A L, (1998), "Phase Equilibria: Measurement and Comtutation", Taylor and Francis , Bristol PA.

Raal, J D, (2000), "Characterization of Differential Ebulliometers for Measuring Activity Coefficients", *American Institute of Chemical Engineers Journal, Vol.46p. 210-220.*

Raal, J D & Rumjugernath, D, (2001),"Rigourous Characterization of Static and Dynamic Apparatus for Measuring Limiting Activity Coefficients", *Fluid Phase Equilibria, Vol.187-188,p.473-487.*

Rackett, H G, (1970), "Equation of State for Saturated Liquids", *Journal of Chemical and Engineering Data, Vol.15, p.514-517.*

Ramjugernath, D, 2000, " High Pressure Phase Equilibrium Studies ", Ph. D. Thesis, University of Natal, South Africa.

Redlish,O & Kister, A T, (1948), "Algebraic Representation of Thermodynamic Properties and the Classification of Solutions", *Industrial Engineering Chemistry, Vol,p.345-348.*

Reid, R C, Prausnitz, J M & Polling, B E, (1988), "The Properties of Gases and Liquids", McGraw-Hill, New York.

Renon, H & Prausnitz, J M, (1968),"Local Composition in Thermodynamic Excess Functions for Liquid Mixtures". *American Institute of Chemical Engineers Journal. Vol.14, No. 1,p.135-144.*

Sayegh, S G & Vera, J H, (1980), "Model-Free Methods for Vapor-Liquid Equilibria Calculations. Binary Systems", *Chemical Engineering Science, Vol.35,p.2247-2256.*

Scatchard, G, (1949), Equilibrium in Non-Electrolyte Mixtures", *Chemical Reviews, Vol.44, P.7-35.*

Scatchard,G, Wilson,G,M & Satkiewicz, F G,(1963),"Vapor-Liquid Equilibrium. X. An Apparatus for Static Equilibrium Measurements", *Journal of The American Chemical Society, Vol.86.No.2,p.125-127.*

Scatchard, G & Satkiewicz, F G, (1964), "Vapor-Liquid Equilibrium. XII. The System Ethanol-Cyclohexane from 5-65oC", *Journal of the American Chemical Society, Vol.87, p.130-133.*

Schult,C J, Neely, B J, Robinson,R L J, Gasem, K A M & Todd, B A, (2001)," Infinite Dilution Activity Coefficients for Several Solutes in Hexadecane and in N-methyl-2-

pyrrolidone (NMP): Experimental Measurements and UNIFAC predictions", *Fluid Phase Equilibriua, Vol.179,p.117-129.*

Smith, J M & Van Ness, H C, (1987), "Introduction to Chemical Engineering Thermodynamics", 4th ed, McGraw-hill, Singapore.

Soni,M, (2003),"Vapor-Liquid Equilibria and Infinite Dilution Activity Coefficient Measurements of Systems Involving Diketones", Msc. Thesis, University of KwaZulu-Natal.

Teeruth,V ,(1995),"Low Pressure Phase Equilibrium Studies Using A Static Cell Cluster".University of Natal.

Tsonopoulos, C, (1974),"An Empirical Correlation of Second Virial Coefficients", *American Institute of Chemical Engineers Journal, Vol.20, p. 263-272).*
Tsonopoulos, C,(1975),"Second Virial Coefficients of Polar Haloalkanes", *American Institute of chemical Engineers. Journal, Vol.21, No.4, p. 827-829.*

Van Ness, H C, (1995), "Thermodynamics in the Treatment of Vapour /Liquid Equilibrium (VLE) Data", *Pure and Applied Chemistry, Vol.67, No. 6,p.859-872.*

Van Ness, H C & Abbott, M M, (1982), "Classical Thermodynamics of Nonelectrolyte Solutions: With Application to Phase Equilibria", McGraw-Hill, New York.

Van Ness , H C, Byer, S M & Bibbs, R E, (1973), "Vapour Liquid Equilibrium:
Part I. An Appraisol of Data Reduction Methods", *American Institute of chemical Engineers Journal, Vol.19, No.2, p.238-244.*

Van Ness, H C, Pederson, F & Rumussen, P, (1978), "Part V. Data Reduction by Maximum Likelihood", *American Institute of Chemical Engineers Journal, Vol.24, p.1055-1063.*

Walas, S M, (1985), "Phase Equilibrium in Chemical Engineering", Butterworth, Boston.

Wehe,A H & Coates, J, (1955),"Vapor-Liquid Equilibrium Relations Predicted by Thermodynamic Examination of Activity Coefficients". *American Institute of Chemical Engineers Journal, Vol.1, No.2, p.241-246.*

Wilson, G M, (1964), "Vapor-Liquid Equilibrium.XI: A New Expression for the Excess Free Energy of Mixing ", *Journal of the American Chemical Society, Vol. 86,p. 127-130.*

Zhang, S, Hiaki, T & Kojima, K, (1988),"Prediction of Infinite Dilution Activity Coefficients for Systems including Water based on the group contribution model with Mixture-type groups 1.Alkane-Water and Alkanol-Water Mixtures, *Fluid Phase Equilibri,. Vol.149, p.27-40.*

APPENDIX A

A.1 Infinite dilution activity coefficients plots

As discussed in Chapter three and six, the endpoint slopes method of Ellis and Jonah (1962), latter modified by Maher and Smith (1979) was used in the calculation of infinite dilution activity coefficients. (P_D/x_1x_2) or (x_1x_2/P_D) is plotted versus x_1 with objective of getting linearity.

A.1.1 Cyclohexane/Ethanol

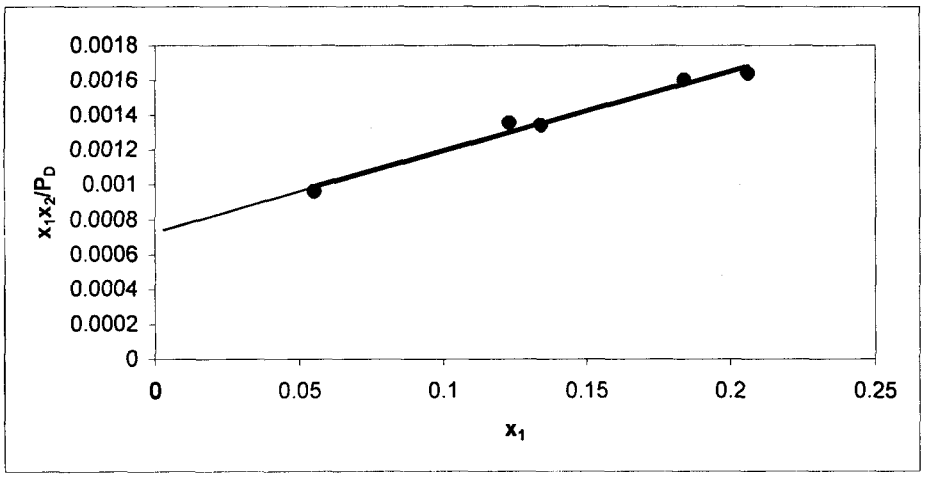

Figure A-1: $\frac{x_1x_2}{P_D}$ **vs.** x_1 **as** $x_1 \rightarrow 0$ **for Cyclohexane (1) + Ethanol (2) at 308.15 K**

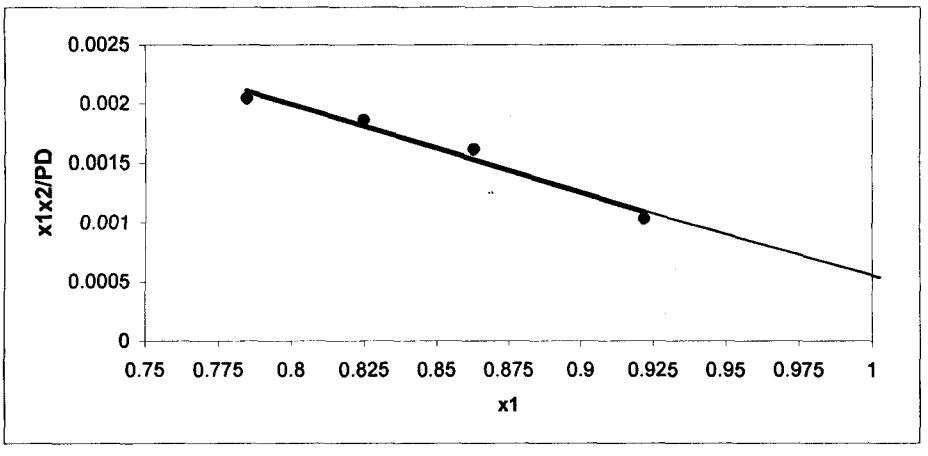

Figure A-2: $\frac{x_1x_2}{P_D}$ **vs.** x_1 **as** $x_1 \rightarrow 1$ **for Cyclohexane (1) + Ethanol (2) at 308.15 K**

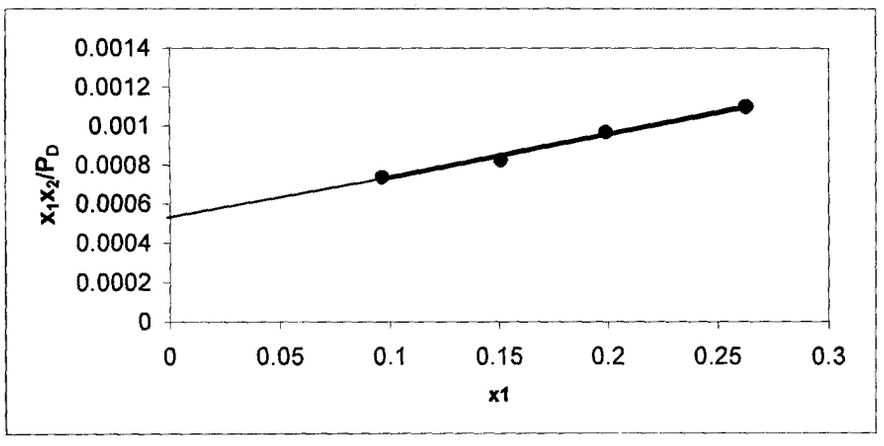

Figure A-3: $\frac{x_1x_2}{P_D}$ **vs.** x_1 **as** $x_1 \to 0$ **for Cyclohexane (1) + Ethanol (2) at 323.15 K**

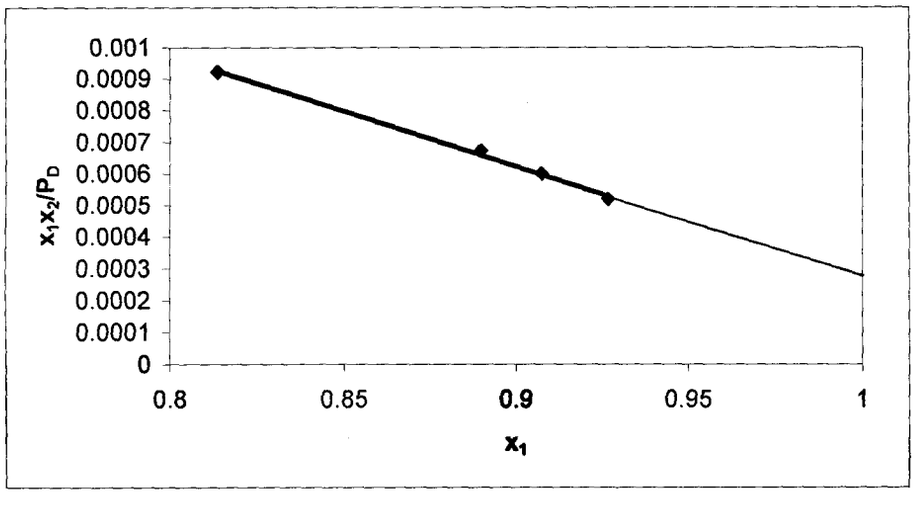

Figure A-4: $\frac{x_1x_2}{P_D}$ **vs.** x_1 **as** $x_1 \to 1$ **for Cyclohexane (1) + Ethanol (2) at 323.15 K**

A.1.2 1-hexene/NMP system

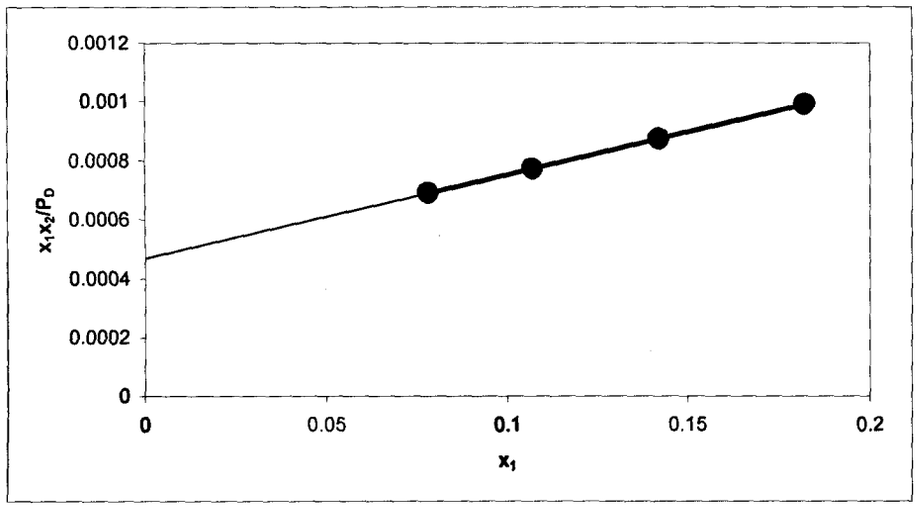

Figure A-5: $\frac{x_1 x_2}{P_D}$ **vs.** x_1 **as** $x_1 \to 0$ **for 1-hexene (1) + NMP (2) at 313.15 K**

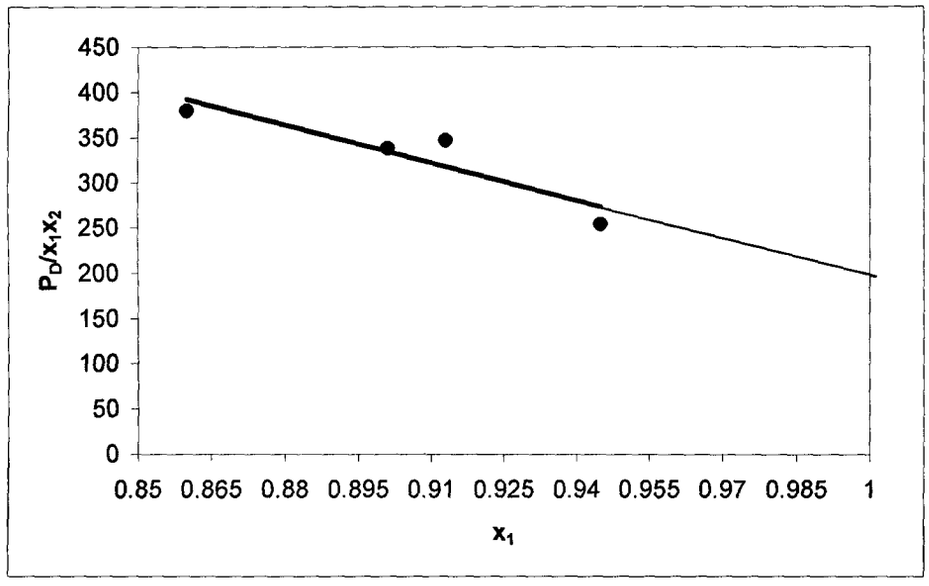

Figure A-6: $\frac{P_D}{x_1 x_2}$ **vs.** x_1 **as** $x_1 \to 1$ **for 1-hexene (1) + NMP (2) at 313.15 K**

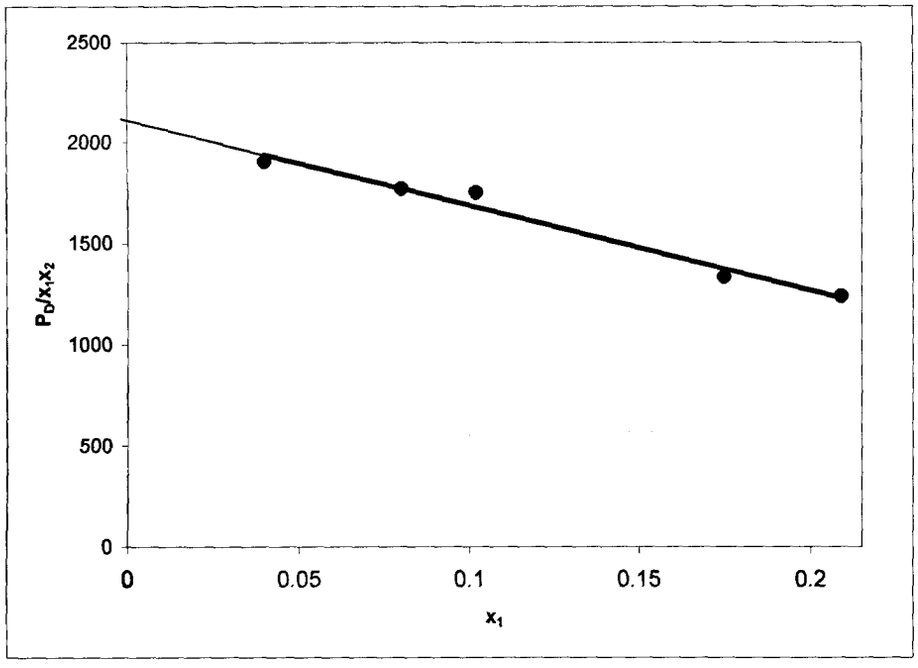

Figure A-7: $\frac{P_D}{x_1 x_2}$ **vs.** x_1 **as** $x_1 \rightarrow 0$ **for 1-hexene (1) + NMP (2) at 323.15 K**

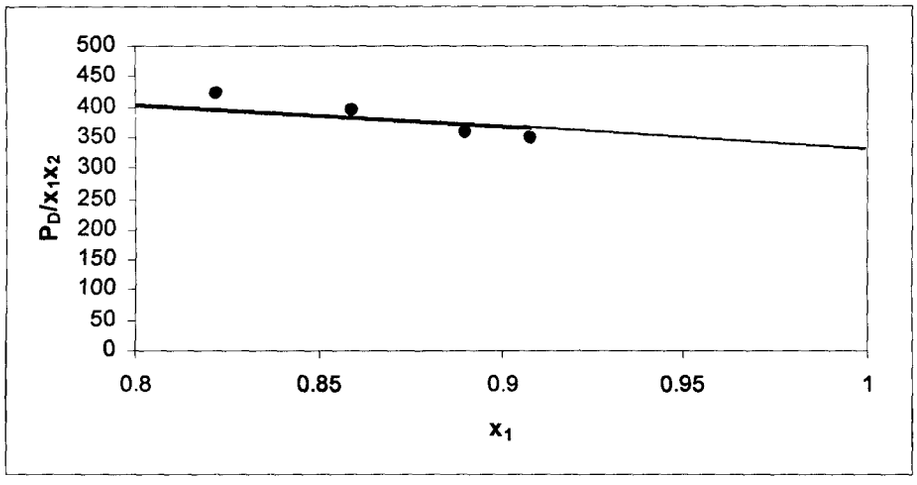

Figure A-8: $\frac{P_D}{x_1 x_2}$ **vs.** x_1 **as** $x_1 \rightarrow 1$ **for 1-hexene (1) + NMP (2) at 323.15 K**

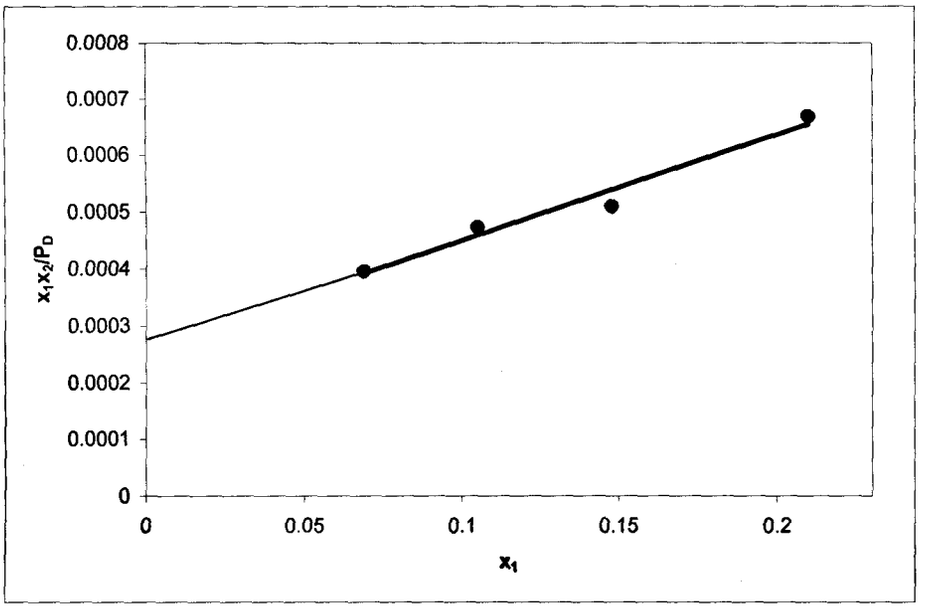

Figure A-9: $\frac{x_1x_2}{P_D}$ **vs** x_1 **as** $x_1 \rightarrow 0$ **for 1-hexene (1) + NMP (2) at 333.15 K**

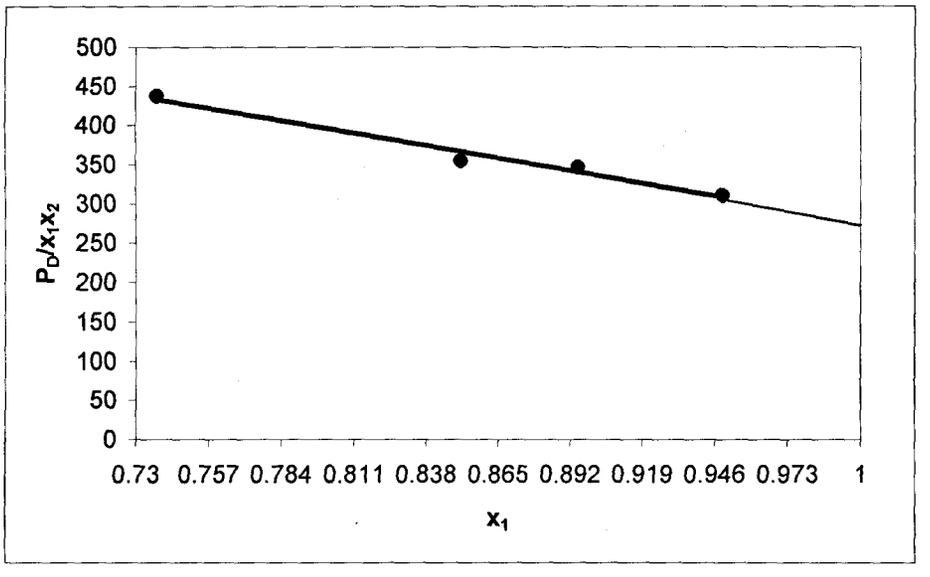

Figure A-10: $\frac{P_D}{x_1x_2}$ **vs.** x_1 **as** $x_1 \rightarrow 1$ **for 1-hexene (1) + NMP (2) at 333.15 K**

A.1.3 Water/NMP system

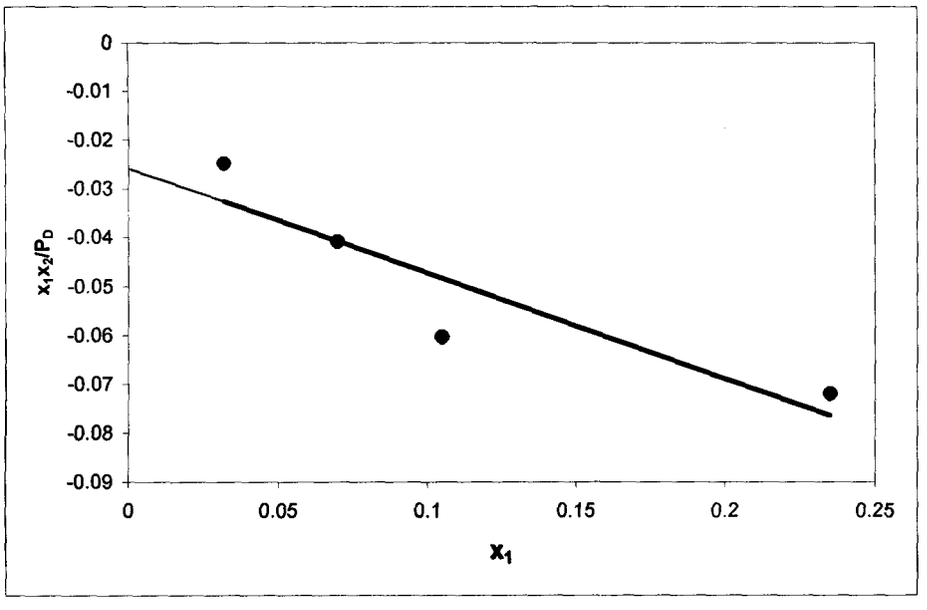

Figure A-11: $\frac{x_1 x_2}{P_D}$ **vs.** x_1 **as** $x_1 \rightarrow 0$ **for Water (1) + NMP (2) at 323.15 K**

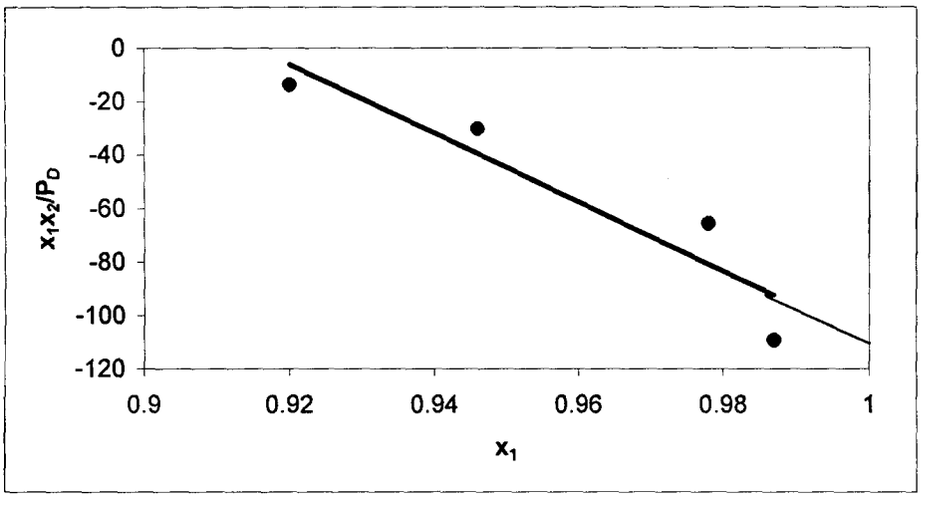

Figure A-12: $\frac{x_1 x_2}{P_D}$ **vs.** x_1 **as** $x_1 \rightarrow 1$ **for Water (1) + NMP (2) at 323.15 K**

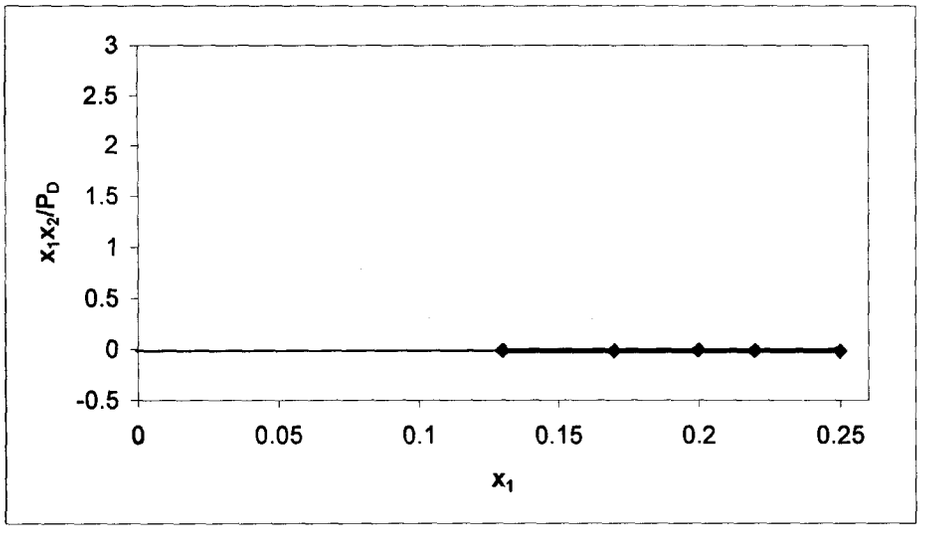

Figure A-13: $\frac{x_1x_2}{P_D}$ **vs.** x_1 **as** $x_1 \rightarrow 0$ **for Water (1) + NMP (2) at 333.15 K**

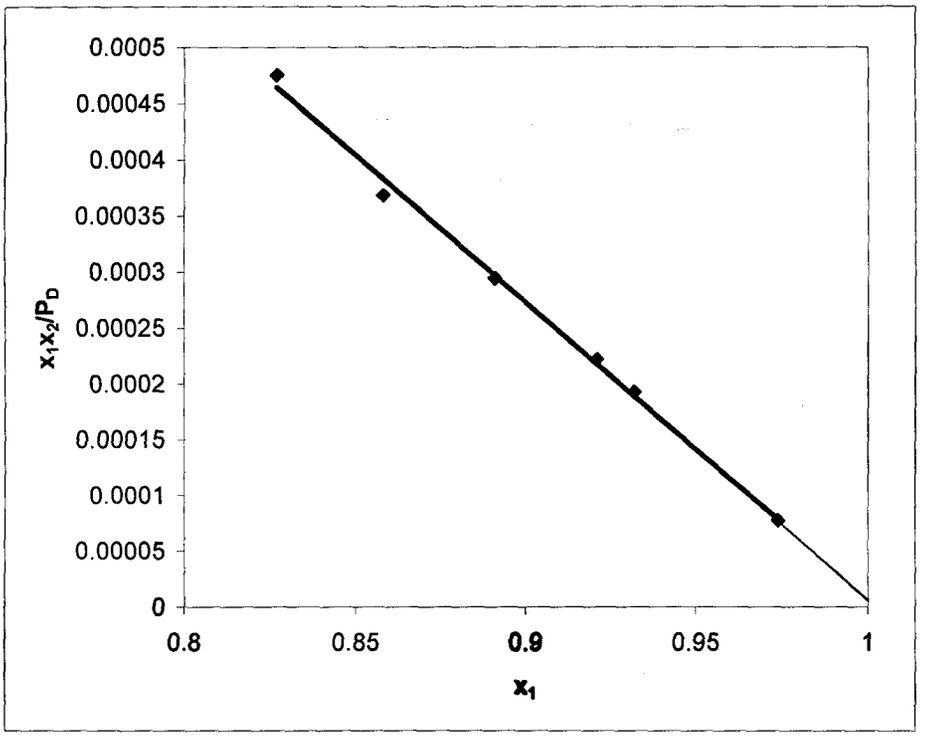

Figure A-14: $\frac{x_1x_2}{P_D}$ **vs.** x_1 **as** $x_1 \rightarrow 1$ **for Water (1) + NMP (2) at 333.15 K**

APPENDIX B

Gas chromatograph calibration

Gas chromatograph procedure is discussed in Chapter 4.

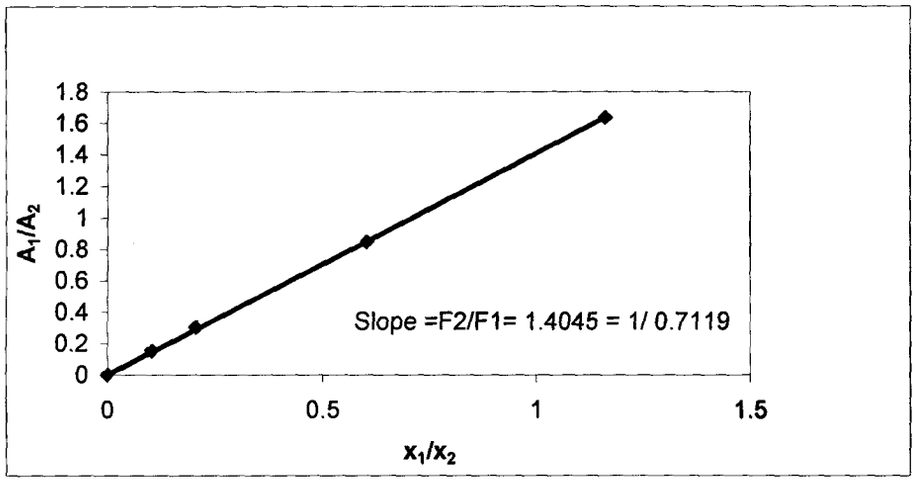

Figure B-1: Gas chromatograph calibration for 1-hexene (1)/NMP (2)

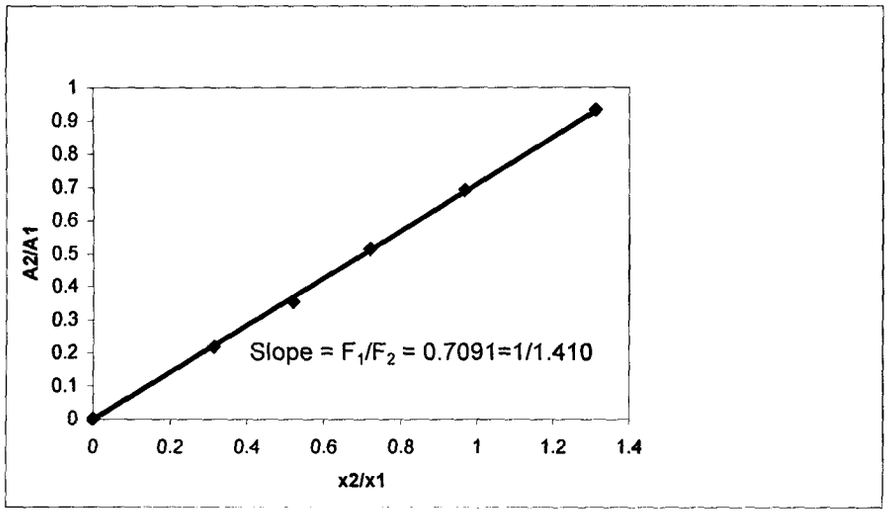

Figure B-2: Gas chromatograph calibration for 1-hexene (1)/NMP (2)

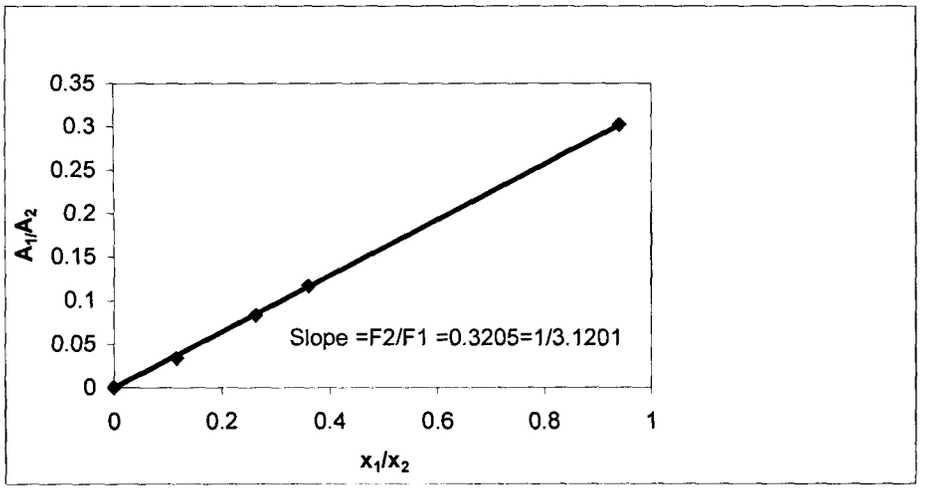

Figure B-3: Gas chromatograph calibration for water (1)/NMP (2)

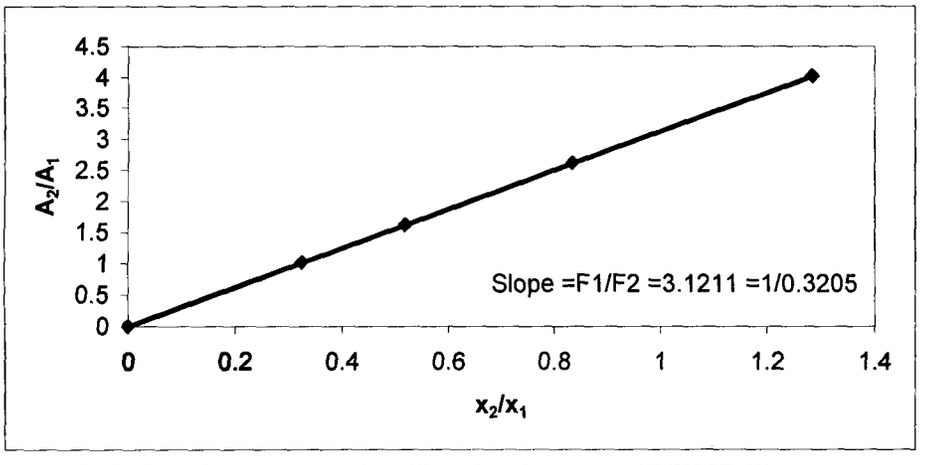

Figure B-4: Gas chromatograph calibration for water (1)/NMP (2)

APPENDIX C

The critical properties of chemicals used in this project were found in Dortmund Data Bank (DBR) and in Prausnitz et al. (1980) and Reid et al.(1988). The Hayden and O'Connell correlation in which these properties were applied is discussed in sections 3.5.4.1 and 6.3.2.

C.1 Pure components properties

Properties	Compounds				
	Cyclohexane	Ethanol	1-hexene	Water	NMP
Tc (K)	516.2000	553.8000	504.000	647.3000	721.700
Pc (atm)	63.0000	40.2700	31.3603	217.6000	44.6000
Vc (cm^3/mol)	167.000	308.0000	350.00	56.0000	310.800
ω (debye)	1.6900	0.3000	0.4000	1.8500	4.0900
Acentric factor	0.6350	0.2130	0.2850	0.3440	0.3577

C.2 Values for the second virial coefficients and liquid molar volumes of cyclohexane/ethanol for each isothermal measurement

Component	T(K)	V(cm^3/mol)	B_{11}(cm^3/mol)	B_{22}(cm^3/mol)	B_{12}(cm^3/mol)
Cyclohexane (1)	308.15	110.5	-1724		-764.2
	323.15	112.1	-1375		-715.8
Ethanol (2)	308.15	57.8		-1645	
	323.15	59.1		-1372	

C.3 Values for the second virial coefficients and liquid molar volumes of 1-hexene/NMP for each isothermal measurement

Component	T(K)	V(cm^3/mol)	B_{11}(cm^3/mol)	B_{22}(cm^3/mol)	B_{12}(cm^3/mol)
1-hexene (1)	313.15	127.2	-1493		- 568.1
	323.15	128.4	-1340		- 509.7
	333.15	129.8	-1262		-475.3
NMP (2)	313.15	98.1		-8471	
	323.15	98.8		- 7138	
	333.15	99.2		-5904	

C.4 Values for the second virial coefficients and liquid molar volumes of water/NMP for each isothermal measurement

Component	T(K)	V(cm^3/mol)	B_{11} (cm^3/mol)	B_{22} (cm^3/mol)	B_{12} (cm^3/mol)
Water (1)	313.15	18.7	- 886.3		-1137
	323.15	19.1	-812.2		-963
	333.15	19.6	-581.3		-628
NMP (2)	313.15	97.8		- 8529	
	323.15	98.1		-7341	
	333.15	99.5		-5539	